

ABSTRACT

Title: **INVESTIGATION OF POXVIRUS HOST-RANGE AND GENE EXPRESSION IN MAMMALIAN CELLS.**

Jorge David Méndez Ríos, Doctor of Philosophy, 2014.

Directed By: **Dr. Bernard Moss, Chief, Laboratory of Viral Diseases, NIAID, NIH; Adjunct Professor Department of Cell Biology and Molecular Genetics, University of Maryland;**

Members of the Poxviridae family have been known as human pathogens for centuries. Their impact in society included several epidemics that decimated the population. In the last few centuries, Smallpox was of great concern that led to the development of our modern vaccines. The systematic study of Poxvirus host-range and immunogenicity provided the knowledge to translate those observations into practice. After the global vaccination campaign by the World Health Organization, Smallpox was the first infectious disease to be eradicated. Nevertheless, diseases such as Monkeypox, Molluscum contagiosum, new bioterrorist threats, and the use of poxviruses as vaccines or vectors provided the necessity to further understand the host-range from a molecular level. Here, we take advantage of the newly developed technologies such as 454 pyrosequencing and RNA-Seq to address previously unresolved questions for the field. First, we were able to identify the Erythromelalgia-related poxvirus (ERPV) 25 years after its isolation in Hubei, China. Whole-genome sequencing and bioinformatics identified ERPV as an Ectromelia strain closely related to the Ectromelia Naval strain. Second, by using RNA-Seq, the first MOCV *in vivo* and *in vitro* transcriptome was generated. New tools have been developed to support future research and for this human pathogen.

Finally, deep-sequencing and comparative genomes of several recombinant MVAs (rMVAs) in conjunction with classical virology allowed us to confirm several genes (O1, F5, C17, F11) association to plaque formation in mammalian cell lines. We also provided additional evidence that plaque formation and virus replication can be independent. More importantly, we identified vgf as the first gene outside MVA's deletion that explains its host-restriction. Replacement of this region with a vgf cassette derived from a replication-competent virus demonstrated to be sufficient to increase viral yield in all mammalian cell lines tested. Several research and clinical applications can be envisioned derived from this work.

INVESTIGATION OF POXVIRUS HOST-RANGE AND GENE EXPRESSION IN
MAMMALIAN CELLS.

By

Jorge David Méndez Ríos

Dissertation submitted to the Faculty of the Graduate School of the
University of Maryland, College Park, in partial fulfillment
of the requirements for the degree of
Doctor of Philosophy
2014

Advisory Committee:

Dr. Jeffrey DeStefano, Chair

Dr. Bernard Moss, Vice-chair

Dr. James Culver, Dean's Representative

Dr. Kim Green

Dr. Alison McBride

Dr. Donald Nuss

© Copyright by
Jorge David Mendez Rios
2014

Dedication

To my wife, parents, grandparents and mentors which all contributed as the building blocks for my success. To the All Mighty, who keeps bringing new surprises to my life. Aby and Ann, study hard.

Acknowledgment

I want to acknowledge my mentor Dr. Bernard Moss for sharing his knowledge and experience in science and virology. Wisdom and ingenious are two things worth imitating from him. I thank Linda Wyatt for teaching me the basic assays in virology. I also want to acknowledge technical support by Zhilong Yang for the plasmids provided; and Karl Erlandson and Andrea Weisberg for the Electron microscopy done for this work. Thanks also to all the post-docs in the lab from 2009 to 2014 for sharing with me all the little tricks that only experience provides. Thanks to my country, Panama, for all the support provided through SENACYT & IFARHU.

Table of Contents

Dedication	ii
Acknowledgment	iii
List of Tables	viii
List of Figures	ix
List of Abbreviations	xi
Chapter 1: Review of Literature	1
The Poxviridae.....	1
History and epidemiology	1
Virion structure and morphologies.....	4
Genome structure	4
Viral entry	7
Gene expression	7
DNA replication	11
Morphogenesis and egress	14
Host-range determinants for VACV.....	14
Plaque formation phenotype and its determinants.....	20
Chapter 2: Whole-genome sequencing and identification of the Erythromelalgia-related poxvirus.....	23
Summary.....	23
Introduction	23
Materials and Methods	24
Cells and virus growth.....	24
Virus purification and DNA extraction	24
Library preparation and pyrosequencing.....	25
Assembly and completion of the genome sequence.....	25
Genome annotation and ORF comparison	28
Genome alignment and comparison of ERPV to closest sequences.	28
Phylogenetic tree of ERPV and other poxviruses.	29

Results	29
ERPV genome sequence	29
Comparison of ERPV with ECTV genomes	30
Phylogeny of ERPV and other orthopoxviruses.....	35
Discussion.....	36
Conclusions	37
Chapter 3: Generation of MOCV transcriptome profile from <i>in vitro</i> and <i>in vivo</i> samples.	38
Summary.....	38
Introduction	38
Materials and Methods	39
Virus stock preparation	39
Cell culturing and infection.....	40
Electron microscopy evaluation	40
Cytopathic effect evaluation.....	41
Plasmids and expression constructs	41
RNA extraction and RNASeq library preparation.....	42
Sequencing and quality control	42
qRTPCR and primers	43
Functional gene expression assays	43
Transcriptome analysis.....	43
Results	45
Initial characterization of MOCV preparations.....	45
MOCV gene expression in multiple cell lines.....	50
MOCV transcriptome from <i>in vitro</i> experiments	50
MOCV gene profiling in MRC5 cells	52
Detection of PR genes explained by read-through mechanism.....	52
Functional assay	61
MOCV transcriptome from human infected tissues	65

Host transcriptome and absence of shutdown	66
Discussion.....	72
Conclusions	79
Chapter 4: Identification of host-range genes responsible for MVA's attenuated phenotype.....	81
Summary.....	81
Introduction	81
Materials and Methods	84
Plaque formation assay and clonal purification.....	84
Evaluation rMVAs by EM	85
DNA extraction and electrophoresis of digested genome fragments	85
Library preparation and pyrosequencing.....	86
Genome assembly and gap closure	86
Multiple genome alignment and genome annotation	90
Selection of candidate genes	90
Generation of GFP constructs and 44/47.1 rMVA deletion mutants	91
Plaque formation assay for the 44/47.1 rMVA deletion mutants.....	91
Virus yields of deletion mutants in mammalian cell lines	94
Trans complementation assay of MVA.....	94
Simplified method to generate replicative-competent MVA for mammalian cell lines.....	95
Results	96
Confirmation of rMVA plaque formation ability.....	96
Evaluation of rMVA morphogenesis by EM	97
Identification of major recombination events on the left portion of the genome	100
Genome annotation and comparison	100
Replication and spreading are distinguishable phenomena.....	101
Selection and deletion of candidate genes.....	102
Testing the screening strategy.....	103
Plaque formation is regulated in a modular and cumulative fashion.....	103

Measuring virus yield for 44/47.1 rMVA deletion mutants	104
C11 is selected to evaluate its role as host-range gene.....	111
C11 expression in trans increases MVA’s yield in VERO and BS-C-1 cells	112
Conceptualization and development of a one-tier recombination method and generation of MVA-C11.....	116
MVA-C11 as a novel host-range gene without affecting plaque size	118
Evaluation of wild-type vgf and other poxvirus sequences.....	118
Discussion.....	123
Conclusions	133
Chapter 5: Significance of our findings from a clinical point of view.	135
Erythromelalgia-related poxvirus and future research	135
Molluscum contagiosum transcriptome and new tools to study the virus.	136
MVA and improvements to current vaccines and vectors.....	138
Final words	142
Appendices.....	143
Bibliography	149

List of Tables

Table 1. Comparison of ERPV's genome with close related strains.	31
Table 2. Amino acid changes relative to Ectromelia Naval.....	32
Table 3. Detection of MOCV's early and PR gene expression in different cell lines by qRT-PCR.	49
Table 4. Summary of read counts for the MOCV transcriptome from the <i>in vitro</i> assay. 56	
Table 5. Summary of post-replicative genes detected <i>in vitro</i>	60
Table 6. MOCV was unable to initiate PR gene expression in trans-.....	67
Table 7. Summary of other findings from <i>in vitro</i> and <i>in vivo</i> experiments.	70
Table 8. Quantification of mature and dense particles for the rMVAs in HeLa cells.	99
Table 9.1. Results of plaque assay for 44/47.1 deletion mutants.	109
Table 9.2. Results of plaque assay for 44/47.1 deletion mutants organized by the impact in plaque size.	110
Table 10. Sequence differences in vgf gene and flanking sequences between the replication-competent MVA-C11 (Ank) and MVA	121
Table 11. Amino acid identity of the vgf ORF of 51.2 rMVA is closest to that of ACAM2000	125
Supplementary table 1. Comparative table of all predicted proteins on the left side of the genome for all rMVAs and other relevant Vaccinia viruses.	143

List of Figures

Figure 1. Schematic representation of poxvirus replication cycle.....	3
Figure 2. Common features for all poxvirus genomes.....	6
Figure 3. Summary of clone isolation and virus amplification process.	26
Figure 4. Bioinformatics workflow, genome assembly and genome annotation.....	27
Figure 5. Phylogenetic relationship of ERPV relative to other poxviruses.	33
Figure 6. ERPV genome map and mutations relative to Ectromelia Naval strain.	34
Figure 7. Evaluation of Molluscum contagiosum virus by electron-microscopy.....	46
Figure 8. MOCV induces CPE in MRC5 cells and it is inhibited with UV light.	47
Figure 9. MOCV-induced CPE in MRC5 cells was inhibited with CHX.....	48
Figure 10. Experimental design for MOCV's transcriptome profiling.	54
Figure 11. Workflow for RNA extraction and generation of Illumina-compatible libraries.	55
Figure 12. Principal component analysis for all RNA-Seq samples.....	57
Figure 13. MOCV's RNA expression patterns depict early gene expression <i>in vitro</i>	58
Figure 14. Promoter-based classification confirms enrichment of early genes <i>in vitro</i> ...	59
Figure 15. Composite of transcription tiles for the PR transcripts detected.....	62
Figure 16. Experimental design to evaluate PR gene expression from a functional perspective.....	63
Figure 17. Promoter pMC095 is cross-compatible with VACV transcription machinery and is specific for post-replicative gene expression.	64
Figure 18. Global transcriptome expression map from an infected human tissue.	68
Figure 19. Complete MOCV transcriptome map using <i>in vitro</i> and <i>in vivo</i> derived RNA.	69
Figure 20. Host's transcriptome shows no evidence of a transcription shut-down.	71
Figure 21. Schematic representation of MVA's deletions and overview of marker-rescue experiments.	83
Figure 22. Initial characterization of plaques formed by MVA and the rMVAs in mammalian cells.	88

Figure 23. Restriction analysis of the rMVA genomic DNA demonstrated migratory shift of band “C”	89
Figure 24. Alignment of the left-termini for all rMVAs and location of the selected candidate genes.	92
Figure 25. Schematic representation of the gfp-cassettes used to generate the 44/47.1 rMVA deletion mutants.	93
Figure 26. Evaluation of virus morphologies in HeLa cells at 24 hpi.	98
Figure 27. Plaque formation assay using one deletion mutant (vdO1-gfp) to test the strategy. Human, primate and mouse cell lines were infected with vdO1-gfp and plaques	105
Figure 28. Deletion of gene O1 from 44/47.1 rMVA reduced plaque size significantly in several mammalian cell lines	106
Figure 29. Plaque assay for all 44/47.1 rMVA deletion mutants revealed that plaque size is determined in a modular fashion.....	107
Figure 30. Statistical analysis of plaque sizes for 44/47.1 rMVA deletion mutants.	108
Figure 31. Workflow for high-throughput method to measure virus yield by flow-cytometry.....	113
Figure 32. Virus yields were significantly reduced for several 44/47.1 rMVA deletion mutants revealing the contribution of each gene to viral replication.	114
Figure 33. Trans-complementation experiment provides initial evidence for C11 as a host-range determinant.....	115
.....	120
Figure 34. Repair of endogenous vgf with a homologous sequence derived from a replication-competent virus was sufficient to recover MVA’s host-range in mammalian cells.	120
Figure 35. Multi-sequence alignment of C11 for several orthopoxviruses.	122
Supplementary figure 2. Replication of MVA and 51.2 rMVA in BS-C-1 cells 24 hpi.	146
Supplementary figure 3. Additional deletion mutants generated.	147
Supplementary figure 4. Sequence inserted into MVA responsible for the host-range extension.....	148

List of Abbreviations

Acam2000	Vaccinia strain; FDA licensed Smallpox vaccine
Acam3000	Vaccinia strain; Acambis Modified Vaccinia Ankara
AraC	Cytarabine or cytosine arabinoside
BAF	barrier of auto integration
bp	base pairs
cos	cosmid.
CRS	concatemer resolution sequence
dpi	days post infection
DR	direct repeats
dsRNA	double-stranded ribonucleic acid
ECTV	Ectromelia virus
ECTV-Mos	Ectromelia virus Moscow strain
ECTV-Nav	Ectromelia virus Naval strain
EM	electronmicroscopy
ERPV	Erythromelalgia-related poxvirus
EV	extracellular virus
G	magnitudes of gravitational force
GFP	green fluorescent protein
gfp	green fluorescent protein gene
HCl	hydrochloride
hpi	hours post-infection
IFN	Interferon
IMV	intracellular mature virus
ITR	inverted terminal repeats

IV	immature virus
LUC	luciferase gene
MOCV	Molluscum contagiosum
MOI	measure of infectivity
MV	mature virus
MVA	Modified Vaccinia Ankara virus
ORF	open reading frame
PAMP	pathogen-associated molecular pattern
PAS	polyadenylation sites
PCA	Principal component analysis
PR	post-replicative
PRR	pathogen recognition receptor
rMVA	recombinant mutant derived from MVA
rpm	revolutions per minute
SDS	sodium dodecyl sulfate
TF	transcription factors
TLR	toll-like receptors
Tris	Tris (hydroxymethyl) aminomethane
TSS	transcription start sites
VETF	viral early transcription factor
VITF	viral intermediate transcription factor
VLTF	viral late transcription factor
vp	viral particles
WV	wrapped virus
Y2H	yeast 2 hybrid assay

Chapter 1: Review of Literature

The Poxviridae

The Poxviridae is a large, family of enveloped viruses with linear, double-stranded DNA genomes. Members of the family have a broad host-range capable of infecting animals from insects to mammals. It is divided in two subfamilies, Chordopoxvirinae and Entomopoxvirinae, with additional unclassified strains. The Chordopoxvirinae subfamily is divided into nine genera (Avipoxvirus, Capripoxvirus, Cervidpoxvirus, Leporipoxvirus, Molluscipoxvirus, Orthopox-virus, Parapoxvirus, Suipoxvirus, and Yatapoxvirus) capable of infecting vertebrates [1-3]. Orthopoxviruses have been a major concern for centuries for their ability to infect a broad range of vertebrates including humans. In fact, Variola virus, the causative agent of smallpox, was responsible for pandemics decimating the human population several times in the last 12,000 years [4, 5].

History and epidemiology

As mentioned before, Variola virus distinguishes itself from the other Orthopoxviruses by being the causative agent of the deadly smallpox. The history of this disease has been comprehensively reviewed extensively [5, 6]. It has been suggested that smallpox was present before the Egyptian dynasties. Facial lesions found in Pharaoh Ramses V were compatible in morphology to the lesions caused by smallpox; nevertheless, virus was never isolated. In other latitudes, immunization using smallpox lesions from patients were documented as early as 1122 B.C. This practice was later named variolation, by association to ancient Greek chronicles. The practice of variolation became common in Asia and Africa, and was later brought to Britain in 1721 by Lady Mary Wortley

Montagu, who was personally affected by the disease [7]. Later on, in 1796, Edward Jenner identified the safety and cross protection against smallpox when milkmaids were exposed to a cowpox strain. In the following years, this new method called vaccination was widely implemented, reducing the mortality by smallpox in Europe and North America. Nevertheless, smallpox continued to be a major health problem for its high mortality ranging from 10 to 40% in non-vaccinated populations. Because of this, by 1969 the World Health Organization (WHO) initiated a global program to eradicate smallpox [8]. Several years of systematic vaccination allowed the first eradication of an infectious disease [9]. Before and after eradication, ground-breaking discoveries in this field provided knowledge and new tools to understand this virus and interaction with its host. Although vaccination was a success, the vaccine had important but uncommon adverse effects that includes encephalitis, myocarditis, and other systemic infections [10]. This highlighted the need to develop a safer vaccine. For this reason, an attenuated virus was generated, incapable of replicating in most mammalian cell and proving to be safer in humans [11]. Serial passage of a replication-competent virus resulted in the attenuated virus called Modified Ankara Virus (MVA) which is currently used as a safe smallpox vaccine and a potential vaccine vector against several infectious diseases [12-15].

Other poxviruses also affect humans with a relatively milder impact. Molluscum contagiosum (MOCV) is another human pathogen that causes infection mainly in children and immunosuppressed patients [16]. Although it is similar in structure to other poxviruses, it significantly differs in sequence [17]. Currently, there is no specific anti-viral for this infection, making it very difficult to treat severe cases. The conventional treatment is the removal of the lesions which produce significant scars and pain in

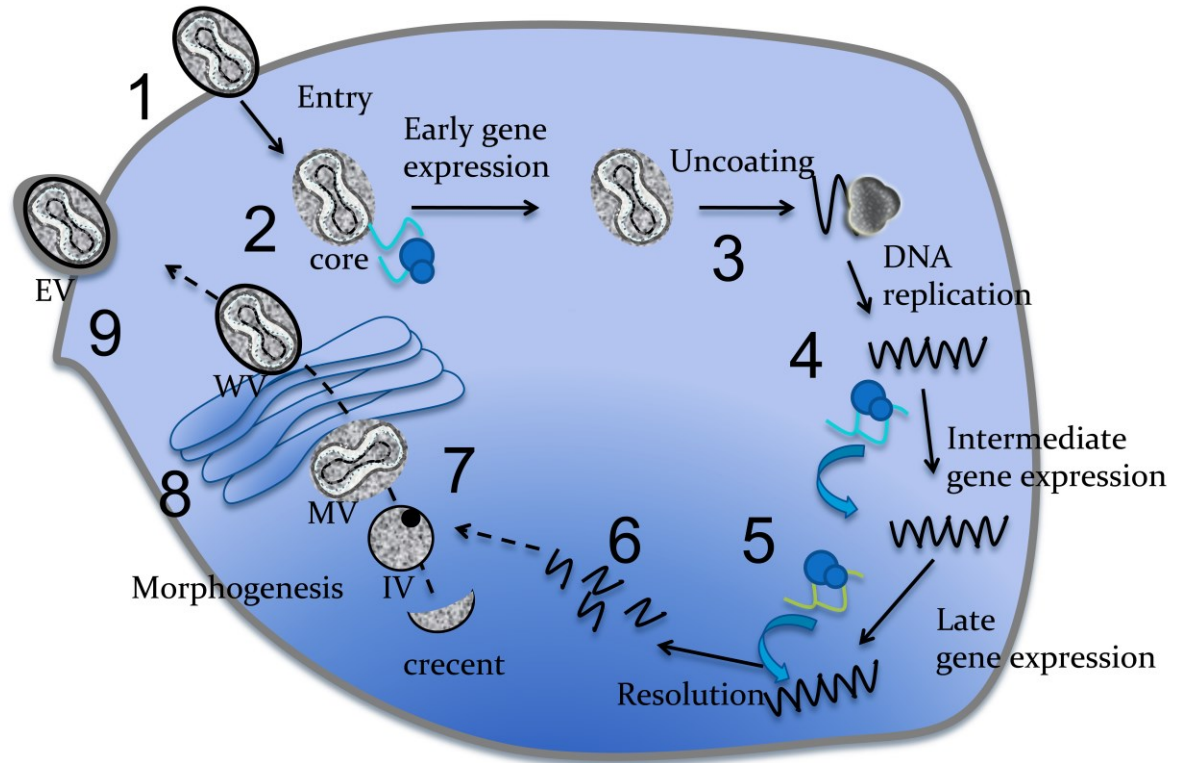


Figure 1. Schematic representation of poxvirus replication cycle. Poxvirus viral cycle starts with (1) attachment of the virus followed by fusion of the lipidic membranes to the cellular membrane. (2) The core is released into the cytoplasm, which allows the factors within the virion to start early gene expression. (3) A less understood process of genome uncoating allows DNA replication to occur followed by intermediate transcription through the transcription factors synthesized in the previous stage. This occurs in perinuclear structures denominated viral factories. (4) Transitory DNA concatemers are formed and resolved with late gene expression. (5) Intermediate and late gene expression occurs using transcription factors expressed on each previous stage, allowing the virus to proceed into morphogenesis. (6) Concatemers are resolved into single genomes using a viral protein. (7) Formation of crescent-like structures occurs and shaped into IVs in which newly synthesized DNA and other proteins are packaged. Proteolytic cleavage allows the immature spherical virus to acquire a brick-shaped morphology and internal dumb-bell structure. (8) Additional lipidic membranes are acquired by the virus from Golgi and Trans-Golgi to form the enveloped virus (EV). (9) Egress occurs by fusion of the external lipidic membrane to the cytoplasmic membrane allowing the extracellular enveloped virus to the exterior of the cell.

patients [18]. Moreover, Monkeypox virus (MPXV), which is endemic in some regions in Africa, is also a concern. The infection is transmitted as a zoonosis, causing similar clinical manifestations to those in smallpox [19]. More recently, bioterrorism threats put poxvirus in the spotlight and identified the need for specific and effective antiviral drugs and vaccines [20]. To put our work in context, identifying the gene or genes that provides poxvirus with the ability to replicate in mammals serves as an important tool from the vaccinology, therapeutic and biodefense perspective.

Virion structure and morphologies

Vaccinia virus (VACV) is the prototype Orthopoxvirus that has been widely used in research. Most of our understanding of poxviruses comes from several decades of research using VACV. In this literature review, I will refer mostly to VACV research except when noted otherwise. The basic infectious particle is the mature virion (MV) or intracellular mature virion (IMV). This particle is a brick-shaped structure with dimensions near 360 x 270 x 250 nm [21, 22]. A lipidic envelope surrounds the viral core. The viral core consists of a protein shell that forms a dumbbell structure with lateral densities of heterogeneous consistency [23]. The inner cavity of the core contains an electron dense material that embeds the viral genome in the form of a nucleoprotein complex. Chemical analysis of the MVs revealed they are mainly composed of protein, with an estimated 3.2% DNA, 5% lipids and 0.1% RNA [24]. Other morphologies can be observed as a byproduct of viral assembly and egress, which will be discussed later.

Genome structure

Poxviruses have a genome that consists of a single linear, double-stranded DNA genome that range from 130,000 up to 380,000 base pairs with similar features throughout all

strains. [17, 25-28]. For most VACV strains, the G+C content ranges from 33-35%, in contrast with other poxvirus that could reach 64% [17, 26, 29]. This linear DNA structure contains a central conserved region of ~80,000 bp that is flanked by two distal variable regions (Figure 2) [30, 31]. The central conserved region encodes most of the essential genes associated with replication and morphogenesis, while the variable regions encode genes related to immune-evasion. Additional features can be identified in these variable regions. Within each variable region, long inverted terminal repetitions (ITR's) can be found [32, 33]. These ITR's are mirror images of each other and they can be as long as 10,000 bp in some strains. Moreover, tandem repeats of variable length, known as direct repeats (DR's), are within each ITR [34, 35]. Both ends of the genome are composed of a polynucleotide hairpin with imperfect base pairing, which loops back and continues as the complementary strand, making the genome a covalently closed structure [36, 37].

The VACV genome contains ~ 200 genes, with a density of 1 ORF every 1 kbp. Advances in genome sequencing and computational analysis allowed intensive comparison among poxvirus genomes. Essential genes involved in replication, transcription and morphogenesis are the highest conserved throughout the family [30]. A set of ~90 gene families were identified in all Chordopoxvirus; whereas 41 of these are present in all members of Poxviridae.

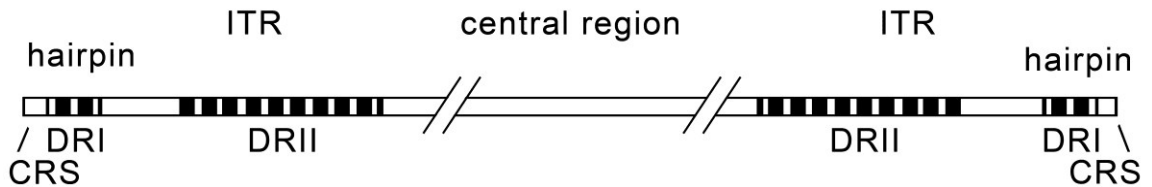


Figure 2. Common features for all poxvirus genomes. All poxvirus share a similar genomic structure and its size ranges from ~100kbp to ~300kbp. Each genome has a central region that codes mostly for the essential genes. The distal terminal portions are complementary sequences called inverted terminal repetitions. Smaller regions with tandem repeats could be found within the ITRs. Each end is composed of a hairpin loop that produces a covalently closed genome. ITR: inverted terminal repeat; DR: direct repeats; CRS: concatamer resolution sequence.

Viral entry

Cell entry starts with attachment of the virus to the cellular membrane followed by fusion of the membranes, allowing the viral core to be released into the cytoplasm [38, 39]. Entry and the viral cycle are depicted in Fig. 1. Fusion of the membranes is initiated by 12 viral proteins, some of which are known to form the entry fusion complex (EFC) [39-53]. Fusion can occur at the plasma membrane or following macropinocytosis or fluid-phase uptake [54-60].

Gene expression

Poxvirus transcription occurs in a multi-stage fashion divided into three temporally defined and promoter-dependent events [61-63]. For each stage, a different subset of genes is expressed through the interaction of several viral and host factors [64-68]. The three stages have been identified as early, intermediate and late gene expression, and each one of them depends on the successful expression of the previous stage. This cascade-like interdependence occurs by the sequential expression of the transcription factors, which provides strict regulation of the transcriptional events [69]. Experiments limiting gene expression to this stage have revealed 118 early, 53 intermediate and 38 late genes respectively [70]. The two last stages are collectively known as post-replicative (PR) gene expression because both requires DNA replication in order to occur [67].

Early gene expression occurs as soon as the viral core is released into the cytoplasm. This early stage is unique relative to the other two stages in that all the transcriptional enzymes and factors were previously packed into the viral core. [71-74]. Components of the early transcription system includes the viral DNA-dependent RNA polymerase (RPO), RPO-associated protein of 94 kDa (RAP94), VACV early transcription factor (VETF), the

capping and methylation enzyme, the poly(A) polymerase, nucleic-acid dependent ATPase, and the topoisomerase. The specificity for early promoters and transcription termination depend on the RAP94 (H4) [64, 75-77]. Additional functions such as poly(A) polymerase-stimulatory, methyl-transferase and transcription elongation functions are provided by the viral J3 protein [78-80]. All these factors seem to be tightly bound through the viral protein H4 forming the RPO complex [81]. Interestingly, RAP94 has an exclusive role in early transcription, and is also required for the packaging of several RPO subunits into the virion [82-84].

For intermediate gene expression, a different set of transcription factors is required. Similar to early transcription, the RNA polymerase is required for intermediate gene expression. Nevertheless, it has been suggested that newly synthesized RNA polymerase is required for intermediate and late gene expression [85]. Partial purification of the intermediate transcriptional components identified three factors (VITF-A, VITF-B and the RNA polymerase) as sufficient for transcription [86, 87]. Further purification of these components permitted the reclassification of these factors as VITF-1 and VITF-2. VITF-1 was identified as a 30kDa (RPO30 or E4L) subunit of the RNA polymerase with homology to the human TFII transcription factor [88, 89]. Another factor functions as a cap methyl-transferase, a Poly(A) polymerase processivity factor and an elongation factor [78, 90]. VITF-2 is another intermediate transcription factor, which turned out to be a nuclear host factor involved in poxvirus gene expression. A third factor named VITF-3 was also identified as an heterodimer composed of two viral proteins, A8 and A28 [91]. Finally, protein B1 is a serine/threonine kinase packaged within the virion [92, 93]. It has been shown that expression of B1 is required for intermediate gene expression [94]. More

recently, it was demonstrated that B1 is necessary to inhibit the antiviral activity of the host's barrier of autointegration (BAF), suggesting an immune-evasion role that supports viral DNA replication [95].

Late gene expression has its own set of transcription factors as well. Three late transcription factors (G8, A1L and A2L) were demonstrated to be sufficient for late gene expression in conjunction with the RNA polymerase using naked DNA templates [67, 96-98]. G8, A1L and A2L have been historically known as VLTF-1, VLTF-2 and VLTF-3 respectively. A host transcription factor named YY1 has also been shown to have negative regulatory functions for late VACV transcription [99, 100]. Another host's derived factor, VLTF-X, has been suggested as a late expression stimulator for VACV. Purification of this factor revealed a complex of two host proteins, hnRNP A2 and RBM3 [101]. Interestingly, the use of yeast-two-hybrid (Y2H) has also depicted a more complex late gene regulation demonstrating that most of these transcription factors interact between each other. The Y2H assay also revealed interaction of these viral and host factors with the viral H5 protein [102]. Viral protein H5 has also been implicated in post-replicative gene expression with a less clear role [103].

Viral protein NHP-I (nucleoside triphosphatasephosphohydrolase-I) , also known as D11, is a DNA-dependent ATPase with a dual role in facilitating release of nascent RNAs from the elongation complex, and works as a polymerase elongation factor to avoid pause sites [104]. As mentioned previously, J3 has been shown to have methyl-transferase, processivity factor activity, and capability of stimulating post-replicative gene expression [105]. The role as elongation factor for viral protein G2 has been demonstrated when deletion mutants of the gene showed shorter transcripts [106].

Promoter motifs for each temporal class have been determined by computational and transcriptional analysis [62, 63, 107, 108]. For example, evaluation of early promoters revealed a core motif that consists of a stretch of A's interrupted by TG between position -13 and -29 of the coding strand, with an increased amount of T's upstream the transcription start site (TSS), and a AT-rich spacer. These two features were defined as essential for a functional TSS [62, 108]. On the other hand, intermediate promoters contain the sequence TAAA immediately upstream of the ORF, with no T in position -10, an AT rich region 15-19 nucleotides upstream of the TSS and a predominant T. Most late promoters contain the sequence TAAAT upstream of the ORF and a predominant T in position -18. Dual activity (intermediate and late) have also been observed, and later identified in a whole-genome scale [70]. By using a virus lacking intermediate and late transcription factors and a complementing cell line expressing only late viral transcription factors (TF), promoters with dual intermediate and late activity were identified.

Viral transcripts have several common features. For example, they have a methylated cap at the 5'-UTR [109, 110] catalyzed by a viral encoded proteins [111-113] and a poly(A) tail at the 3'-UTR [114, 115] produced by the viral RNA polymerase and associated factors [116]. Additionally, poly-adenylation signals (PAS's) have been associated with the location of poly(A) tails for each nascent transcript [108, 117]. Nevertheless, transcripts lacking PAS also occur, providing some variability in the transcription products [108, 117-122].

The function of each gene and its temporal expression is consistent with the requirements of the virus throughout the infection. Grouping genes with the temporal classification revealed that early genes are mostly associated with DNA replication, transcription, host

evasion and core-associated enzymes [70]. The intermediate genes are enriched in DNA binding and packaging proteins and core-associated non-enzymatic proteins. Also, late genes are associated with redox disulfide bond enzymes, morphogenesis, crescent formation, virion membrane proteins, and components of the entry-complex fusion. This provides some insight to the complexity and modularity acquired by poxvirus through evolution.

DNA replication

Poxviruses are large enveloped, double stranded DNA viruses with an exclusive cytoplasmic viral cycle. Factors and enzymes required for the viral DNA replication are encoded as early genes, and the new synthesized DNA serves as the template for further gene expression [70]. Discrete perinuclear structures called viral factories can be identified early in infection where DNA replication, transcription and viral assembly also occur [123-126].

Poxviruses are very independent in that they provide their own DNA synthesis machinery. VACV encodes at least eight genes directly associated with DNA replication [127]. E9 is a 117-kDa protein with primer and template dependent polymerase and 3' to 5' proofreading exonuclease activity [128-130]. Additionally, it allows branching and recombination during DNA synthesis [131-133]. D5 is a multifunctional enzyme with helicase and primase function with a mass of 90-kDa [134]. Its ribonucleotide diphosphatase and desoxyribonucleotide dephosphatase activities seem to depend on its multimeric conformation [135]. Because of non-specific DNA primase activity, a role in lagging strand synthesis has been suggested [136]. D4 also has an essential role in DNA synthesis. It encodes a uracil DNA glycosylase (UDG), capable to excise and repair

misincorporated dUMP's or deaminated cytosine [137]. Recovery of viruses with mutated D4 [138], and further characterization of deletion mutants demonstrated that D4 is essential for virus growth in several cell lines [139]. Other experiments have suggested additional function yet unknown for this protein [140]. A20 is one of the replication-associated proteins with indirect evidence of its function. It is considered a processivity factor that cooperates during DNA replication because of its ability to bind to other replication related proteins such as D4, D5 and H5 [141]. Furthermore, conditional lethal virus with mutations that map to this gene shows a defect in the DNA polymerase processivity [142]. B1R ORF encodes a 35-kDa protein with serine/threonine kinase activity [92, 93, 143]. This protein, packed within the virion, is released early in infection and blocks the antiviral effect of the protein Barrier of Autointegration (BAF) [95, 144, 145]. BAF in its dimeric form binds viral DNA preventing viral replication. B1 also has a less clear function in replication since it also interacts with and phosphorylates viral protein H5 [141, 146-149]. A50 is a single-stranded DNA binding protein with ATP-dependent DNA ligase activity [150]. Regardless of its important function, it is not present in all chordopoxviruses. Another VACV protein involved in DNA replication is A50, which is able to repair nicked DNA from a 5'-phosphate end to a 3'-hydroxyl strand when both are bridged by a template [151]. Interestingly deletion mutants for this gene were able to replicate but with a restricted host-range and lower pathogenicity (Colinas et al. 1990; Kerr and Smith 1991; Parks et al. 1998; Kerr et al. 1991). Recent findings show that a virus lacking this gene can use the cell's DNA ligase I (Paran et al. 2009), which explains why A50 is not an essential gene and its absence in several chordopoxviruses.

As mentioned before, formation of genomic concatemers is an intermediate byproduct of the replication process [152]. Specific sequences near the hairpin loop are required for the resolution of the concatemers into individual genomes [153]. These concatemers resolution sequences (CRS) when inserted into plasmids, show a cruciform structure similar to Holiday Junctions (HJ) [32]. A22, a viral protein expressed late in the viral cycle has nuclease activity and was found to be capable of binding to these HJ structures [154-156]. Deletion mutants of A22 are incapable of resolving the genome concatemers [157]. A 32-kDa viral polypeptide (H7 in VACV genome) has been identified as a topoisomerase with homology and functions similar to the eukaryotes enzyme [158, 159].

Two main models have been suggested for poxvirus genome replication. The first one is similar to the parvovirus self-priming and rolling-cycle model, which uses its hairpins for strand displacement [160]. This model is compatible with findings in VACV in which a nick in one of the strands may provide an 3' hydroxyl group available for extension of the sequence and formation of DNA concatemers [35, 37, 161]. The second model is the semi-discontinuous DNA replication model, which includes DNA synthesis in a lagging strand [162, 163]. This is further supported by the discovery of the viral primase and ligases that are required in a replication fork [136, 164]. The existence of an origin for replication is still unknown. Early research showed that poxviruses are able to replicate circular DNA molecules in an origin-independent manner [32, 165]. Nevertheless, viral sequences located at the telomeres have been associated with an increase in DNA replication [166], and the origin of replication was suggested to be within the first 150 bases of the genome [167].

Morphogenesis and egress

The first evidence of viral assembly is observed when membrane structures in the form of crescents appear in the cytoplasm. These crescents continue to grow forming a spherical container. The membranes are supported by the formation of a protein scaffold composed of trimers of the viral protein D13 [168]. The membranes were believed to be derived from the ERGIC complex [169] but are now known to be derived from the endoplasmic reticulum [170, 171]. Protein and newly synthesized viral genomes enters into these structures before the crescent closes, forming the immature virus (IV). The IVs suffer structural changes associated with proteolytic cleavages that allow the virion to form the naked or intracellular mature virus (IMV, see virion structure and morphology section) [172, 173]. A fraction of these IMVs go through the trans-golgi system, acquiring an additional lipidic layer and becoming the intracellular enveloped virus (IEV) [47]. Egress of the infectious particle occurs when the lipidic bilayer of the IEV fuses with the cellular membrane, releasing the particle into the extracellular space and leaving behind one of the envelopes. At this point, the virus is identified as the extracellular enveloped virus (EEV) [47, 174].

Host-range determinants for VACV

Right after the virus enters the cell, the transcription machinery packed within its core starts synthesizing early viral mRNAs. Many of these early genes are involved in the initial countermeasures against the host defense. Poxviruses have a large variety of genes that target the immune system; nevertheless, I will be focusing on those present on VACV strains that are relevant to our work.

Global mechanism for immune evasion

Poxviruses are capable of inducing global effects in the cell to avoid cellular defenses. One of these strategies is disrupting the expression of host genes. Poxviruses contain proteins that snatch the methylated cap of the host's mRNA and promotes its degradation. This global targeting to the host's transcripts is mediated by two viral proteins, D9 and D10, both expressed at different times during the infection [175, 176].

Another global strategy acquired by the virus is the targeting of key cellular functions. For example, VACV C16 inhibits the host's hydroxylase PHD2 [177]. This host protein is required for the normal degradation of HIF-1-alpha, which functions as an oxygen sensor. Stable concentrations of HIF-1-alpha have been shown to favor growth of other viruses, for which poxviruses may benefit as well [178].

Blocking external interferon (IFN)

Since the discovery of IFN by Isaacs and Lindenmann [179-181], the mechanisms of cellular defense and virus-host interaction have been intensively studied. Early on, it was observed that viruses were equipped with a probable defense mechanism to avoid the cellular interference effect [182]. Poxviruses were not an exception, for as cells stimulated with IFN were capable of inducing an antiviral that and prevented viral growth [183]. Poxviruses have evolved to target this pathway and counteract its effect at several levels. For example, VACV B18 is a protein capable of directly binding IFN from a broad range of species [184]. It has specificity for INF-alpha [185]. By secreting this viral protein, the virus can protect itself even before IFN reaches its receptor [178]. Another viral protein that targets the IFN pathway is B8. It functions as a decoy IFN receptor,

which prevents IFN-gamma binding to its cellular receptor [186]. Together, these viral proteins (B18 and B8) intercept IFN before it reaches its cellular receptor.

Vaccinia virus targets the IFN's downstream effectors

IFN's signal transduction can also be blocked by VACV immune evasion proteins at different levels. IFN receptors have intracellular domains that play an important role in signal transduction [187]. When IFN and its cellular receptor interact, conformational changes in the receptors allow phosphorylation of both the Janus Kinases and the IFN receptor. This in turn allows activation of various STAT molecules, which continue transduction of the signal. The poxvirus protein VH1 is a phosphatase packaged within the core that is released early after entry [188, 189]. It causes dephosphorylation of STAT1 and STAT2. By targeting these kinases, it is able to block IFN's signal from all IFN receptors. C12, another VACV protein, also diminishes the production of INF-gamma and increases its virulence [190].

PAMPs and PKR

Another primitive immunological system is capable of recognizing foreign pathogen-associated molecular patterns (PAMPs) through specialized receptors [191]. These cellular receptors known as Pathogen Recognition Receptors (PRR) are broadly distributed in the cytoplasm and in the cellular membrane, and have the ability to activate a broad immune response. Several of these PRRs have been recently characterized and include RIG-I, PKR, MDA-5, IPS-1, and the TLR's family of receptors. PKR is an intracellular PRR capable of binding and detecting foreign dsRNA. It is a surprising hub for several antiviral pathways, and at the same time, capable of triggering multiple

downstream effectors to mount a strong antiviral response through its kinase activity [192-194]. Upon binding to dsRNA, PKR is activated and capable of phosphorylating the cellular translation factor eIF-2-alpha [195]. Phosphorylated eIF-2-alpha causes a general inhibition of translation reducing the ability of the virus to express its genes.

To evade this defense mechanism, poxviruses have also acquired a protein capable of sequestering dsRNA, therefore blocking recognition of this PAMP by the host. The E3 protein is a dsRNA binding protein that prevents activation of PKR, and OAS, allowing the virus to proceed efficiently into the post-replicative stages of its cycle [196-200]. E3 is also capable of binding to an important member of the ubiquitin-like proteins, ISG15, preventing its antiviral activity [201]. Moreover, the viral protein K3 is a pseudo substrate for PKR. By competing as a substrate for PKR, it is able to prevent phosphorylation of eIF2-alpha [202], preventing downstream activation of the effectors molecules. The recent expansions in research on this pattern recognition system have increased the potential targets for poxviruses proteins. For example, it has been shown that poxvirus can be detected by TLR2, TLR6, MDA-5 and NALP3, causing up regulation of MDA-5 and IPS-1 followed by secretion of IFN-beta [203]. Interestingly, this is the first demonstration of MDA-5 sensing a DNA virus rather than a RNA virus and these pathways may also be targeted by viral proteins.

VACV host-range genes

Immune evasion genes have also the ability to extend the virus host-range. It has been shown that insertion of gene K1L into the attenuated MVA allows viral replication in RK13 cells [204]. K1 and also C7 proteins have both been associated with antagonizing

the IFN pathway in mammalian cells [205]. It was later shown that K1 was preventing PKR and eIF-2-alpha, allowing translation of viral proteins in HeLa and RK13 cells [206]. Interestingly, both C7L and K1L have been shown to prevent phosphorylation of eIF-2-alpha through a PKR-independent mechanism [207]. Restoration of each gene into an MVA deletion mutant showed a significant decrease in phosphorylated eIF-2-alpha, confirming their role as immune evasion genes. Interestingly, other poxvirus genes have been identified as host-range genes in different cells such as B23 (C18), B24, B13, C17, and B4 [208].

Cytokines are targeted

Cytokines are another group of molecules produced in response of a foreign threat, which are also targeted by poxviruses. Secretion of cytokines that have autocrine or paracrine effect could initiate an antiviral response. For example, interleukin-1 (IL-1) is a highly inflammatory cytokine with receptors present in nearly all cells [209]. It has an important role in amplifying the immune response against an aggressor. IL-1 needs two different signals in order to be active and secreted from the cell that are targeted by viral proteins. The first requirement is an activated NF-kB, which induces expression of pro-IL-1B. VACV peptides target NF-kB activation at multiple levels. Several proteins that belong to this category were discussed above. The second requirement for IL-1 secretion is activation of caspase-1, which occurs through the inflammasome, allowing cleavage of pro-IL-1b to IL-1b. Another viral protein, F1, binds NLRP1, a component of the inflammasome, and prevents cleavage of pro-IL-1 [210]. Furthermore, VACV B13 (also known as SPI-2) and the cytokine response modifier A (CrmA) from cowpox, both can bind to caspase-1, preventing the formation of the active IL-1 [211-213].

VACV B13 and B15 are both associated with IL-1 antagonism, but with different consequences after deletion. Deletion of B13 did not affect virulence [214]; nevertheless a lack of B15R reduced virulence in mice from intracranial inoculation [215], and allowed accelerated weight loss and fever [216]. C10 is another IL-1 antagonist inferred by sequence homology [26].

VACV codes for 6 additional proteins (A46, A49, A52, B14, C4 and N1) that inhibit IL-1 mediated activation of NF-k-b (Reviewed by Smith 2013). It is important to note that even when these proteins are deleted independently, each mutant presents a variety of phenotypes [217-222]. The explanation by Smith is that these proteins have non-redundant functions and possibly multiple binding partners.

IL-18 is another pro-inflammatory cytokine targeted by poxviruses [223]. This cytokine is also produced in an inactive form that requires cleavage by caspase-1 [178]. So, it is inferred that VACV B13 also inhibits cleavage of this product and activation of IL-18.

TNF is targeted

Tumor necrosis factor (TNF) is another host cytokine with important antiviral roles. It promotes an antiviral state in uninfected cells, recruits lymphocytes to the infection site and induces selective cytolysis [178, 224]. VACV has evolved mechanism to target this immune system as well. A53 (CrmC) and CrmE are both viral TNF decoy receptors (vTNFRs) that contain similar extracellular domain to its cellular counterpart; nevertheless, they lack the intracellular signaling domain and are incapable of signal transduction [225]. CrmE has also been shown to inhibit TNF's pro-apoptotic effect for human cells *in vitro*, and has proven to be a virulence factor in a murine model [226].

Several VACV proteins have also been identified that target chemokines. The VACV chemokine-binding protein (vCKBP or vCCI), and protein A41, both are secreted early from infected cells and capable of binding CC-containing chemokines [227-231]. The former directly blocks interaction of the chemokine with its receptor, whereas the later reduces its affinity to the receptor [232]. B7 and B23 are two additional viral proteins with predicted chemokine binding ability based on sequence homology [229].

Targeting apoptosis

The process of apoptosis is also targeted by poxviruses. Poxviruses are capable of inhibiting apoptosis at several levels, including preventing activation of caspase-1 through the inhibitory effect of F1 binding to NLRP-1, which activates this caspase [210]. F1 can also acquire a bcl-2-like conformation (mimics a bcl-2 domain) and bind to the host's apoptosis effector molecule BAK [233-236]. N1 is another viral protein with a bcl-2-like structure capable of binding to several bcl-2 homologs and to the pro-apoptotic bcl-2 proteins BID and BAD [237-239]. Finally, VACV B13 (SPI-2) inhibits bcl-2 activity and inhibit the apoptosis induced by extracellular TNF-alpha or by Fas ligand [213, 240, 241]. The dsRNA binding protein (E3) also shows anti apoptosis effect upon induction with external dsRNA [242, 243].

Plaque formation phenotype and its determinants

Poxvirus ability to form plaques have been widely used to estimate the amount of infectious particles (or plaque-forming particles PFP) a viral preparation contains [244]. It was calculated for VACV that 1 out of 10 virions are able to form such a plaque. Changes in plaque sizes have also been used to identify genes involved in attenuation or

virulence upon deletion or re-insertion into the virus [245, 246]. Other applications of plaque formation include the use of genes as genetic markers to select for recombinant mutant [247, 248].

Plaque size varies depending on the cell lines used or the capacity to infect neighboring cells. Plaque formation have been shown to be dependent on several processes that include cell to cell spread, production of new progeny, efficiency of viral egress or formation of actin-tails, which favors infection of neighboring cells [249, 250]. Also, recent findings have shown that plaque formation is not necessarily correlated with viral replication. For example, repair of gene F5L from the attenuated strain MVA causes an increase in plaque size without affecting replication [251]. Similar observations have been documented showing the independence of plaque formation and the amount of infectious particles for recombinant MVA viruses [252]. This highlights the importance in evaluating plaque formation and replication independently. Plaque reduction for the purpose of identifying neutralizing antibodies has also been used, but does not overlap with the scope of this document [253].

Several VACV genes have been associated with the ability to produce larger plaques. The viral protein B5R affects plaque formation by promoting re-arrangement of actin and formation of the actin tails [250]. F12 is another important protein that if deleted affects both plaque formation and virulence [249]. The ability of F12 to affect plaque size has been associated with the formation of actin tails. O1L is a 78-kDa protein, which is also required for formation of large plaques. It was shown that O1 promotes sustained activation of the Raf/Mek/Erk pathway in human 293A cells, and its deletion reduced plaque size, virulence, and spread in BALB/c mice [254]. Repair of MVA's truncated O1

showed sustain reactivation of the ERK1/2 pathway without contributing to virulence and replication [254], suggesting that these two processes can be independent. F11 is another early protein truncated in the attenuated MVA. It has also been associated with plaque formation *in vitro* and spreading *in vivo*, and is required for efficient release of viruses from infected cells [255-257]. More recently, F5 has also been involved in plaque formation [251]. Moreover, the ability to form plaques seems to be multigenic since repair of both F5 and F11 allowed formation of larger plaque in a replicative-competent virus. Another viral protein, C2, is also associated with plaque formation without affecting virulence or viral replication, and the effect seems to be mediated by modulating cellular projections and adhesion of cells to the extracellular matrix [258].

The immune evasion repertoire presented here represents a fraction of all immune-evasion mechanism acquired by poxviruses. Most of the mechanism of action of these proteins has not been elucidated. Dissecting their mechanism and interaction with the host, may reveal new antiviral targets and the generation of new vaccines and vectors for human and veterinarian purposes.

Chapter 2: Whole-genome sequencing and identification of the Erythromelalgia-related poxvirus

Summary

In 1987, a group of physicians identified an outbreak Erythromelalgia syndrome in the Chinese province of Hubei. Swab samples from the pharynx of the patients were cultured and a poxvirus isolated. Characterization of the virus using EM demonstrated a poxvirus particle. Further characterization of the virus by pathogenicity in mice and antibody neutralization assays turned inconclusive. The virus was deposited in ATCC but its identity was not determined. Since this human isolate could potentially be an interesting finding, we decided to take advantage of the sequencing tools recently developed to evaluate and identify this virus. 454 pyrosequencing and bioinformatics were carried on to performed whole-genome sequencing and compare this virus to the closest strains. We determined that the virus is very closely related to the Naval strain of ectromelia virus.

Introduction

In the mid 1980's, a team of physicians detected an outbreak of the syndrome known as Erythromelalgia in the province of Hubei, China [259]. All patients were young students, that shared similar signs and symptoms that included fever, malaise, headache, sore throats, and edema of the lower limbs. Pharyngeal samples were taken and used to determine the presence of an infectious agent. A virus was isolated and then characterized showing the ability to grow in different cell lines and proved to have virulence for mice [260]. Morphological evaluation suggested a poxvirus; nevertheless, comparison to other poxvirus was inconclusive. Moreover, serological neutralization assays were also unable

to identify this agent for the cross-reactivity between strains. The virus was then deposited in ATCC as Erythromelalgia-related Poxvirus (ERPV).

In collaboration with the researcher who isolated the virus, we decided to take advantage of the newly available sequencing technology to perform whole-genome sequencing of the isolate. A close evaluation of the genome sequence was used to determine if this virus was a novel Orthopoxvirus or a known strain.

Materials and Methods

Cells and virus growth

ERPV was obtained from the American Type Culture Collection (VR-1431) and clonally purified by three successive plaque isolations on BS-C-1 cells (ATCC, CCL-26) and propagated in minimal Essential Medium with Earl's balanced salts (Quality Biological, Gaithersburg, MD) supplemented with 2 mM L-Gln and 10% fetal bovine serum (Fig. 3). All experiments were carried out in a laboratory with no known Ectromelia virus (ECTV) contact.

Virus purification and DNA extraction

Infected BS-C-1 cells from five T-150 flasks were harvested, and the cell pellet was re-suspended in 10 ml of 1 mM Tris-HCl, pH 9.0 and lysed with 40 strokes of a tight pestle Dounce homogenizer. Nuclei and cell debris were removed by centrifugation at 300 x g for 5 minutes at 5°C. The supernatant was sonicated three times and the viral suspension was overlaid on a 17 ml 36% sucrose cushion. The virus was purified as described elsewhere [261]. The virus pellet was suspended in 1 mM Tris-HCl pH 7.8 and incubated for 4 h at 37°C in a solution containing 10% SDS, 60% sucrose and 10 mg/ml of

proteinase K [261]. DNA was extracted with phenol:chloroform:isoamyl alcohol (25:24:1) and then with isopropanol, followed by DNA precipitation using 100% ethanol containing 0.3M sodium chloride [262]. Viral DNA was confirmed by HindIII digestion and gel electrophoresis (Figure 23).

Library preparation and pyrosequencing

Extracted DNA was quantified by light absorbance at 260 nm (A₂₆₀) and a Picogreen assay (Life Technologies, Grand Island, NY). Separate libraries were constructed using Rapid Library Preparation Method Manual (October 2009) GS FLX Titanium Series (Roche, Branford, CT) and Paired End Library Preparation Method Manual – 3kb Span (October 2009) GS FLX Titanium Series. Each library was processed using emPCR Method Manual – Lib-L MV (October 2009) in separate emulsion reactions with the fragment library being combined with like samples. The paired-end sample was loaded on a single lane and the fragment sample was loaded in two lanes of an 8-region 454 GS FLX Titanium sequencing run.

Assembly and completion of the genome sequence

Paired-end and fragment reads were initially assembled using GS Assembler v.2.5 (Roche/454 Life Sciences), using standard assembly parameters (Figure 4). *De novo* assembly resulted in five contigs with an estimated length of 200,971 nt. The five contigs of ERPV were provisionally ordered by comparison with the genome sequence of ECTV-Mos (Accession NC_004105), which had the highest score on a BLAST search of the NCBI genome database, using the bioinformatic tool Mummer [263] and Geneious pro 5.5 [264]. After identification of the ITR, a reverse complementary version of it was generated and concatenated into the genome draft. Primers were designed based on the

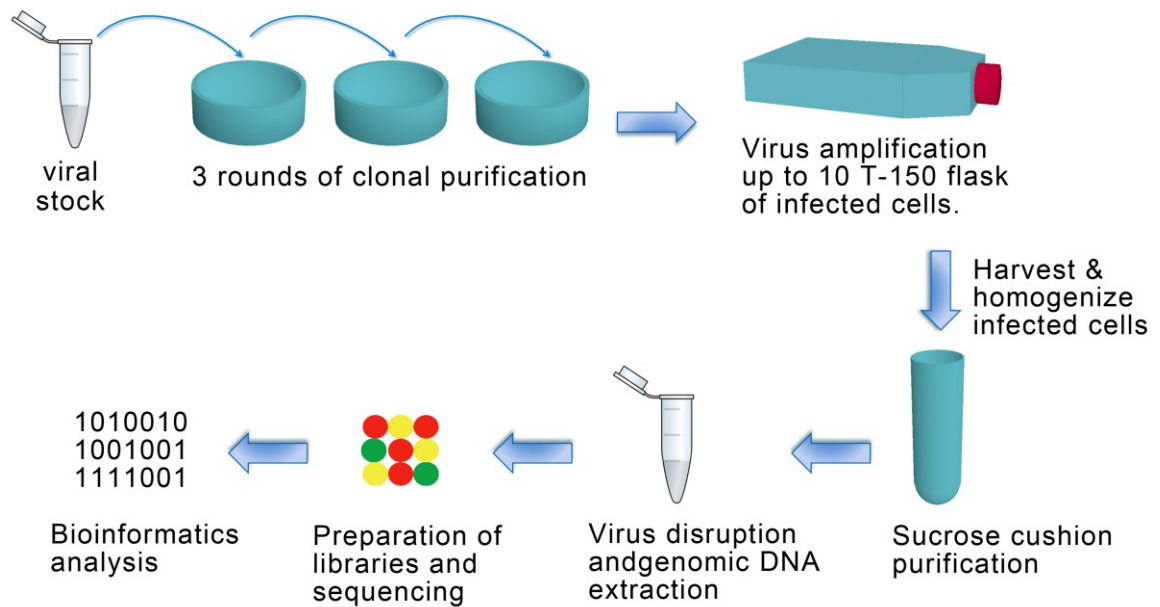


Figure 3. Summary of clone isolation and virus amplification process. The process of clone purification consists of serially diluting a virus preparation and picking a single plaque at the highest dilution possible. This process is repeated several times to eliminate any other virus and isolate the progeny of a single viral particle. Amplification consists of the infection of exponential number of cells until the desired amount of virus is reached. For virus purification, the cell membrane is disrupted to release the intracellular viruses using detergents. The extract is then placed on top of a sucrose cushion that allows pelleting of virus and removal of cell nuclei and lipids. If more purity is needed, a sucrose gradient can also be used in tandem. A solution containing SDS and Tris-HCl is used to disrupt the virus proteins from the genome, followed by ethanol precipitation of the viral DNA. Library generation for sequencing is done as described in the methods.

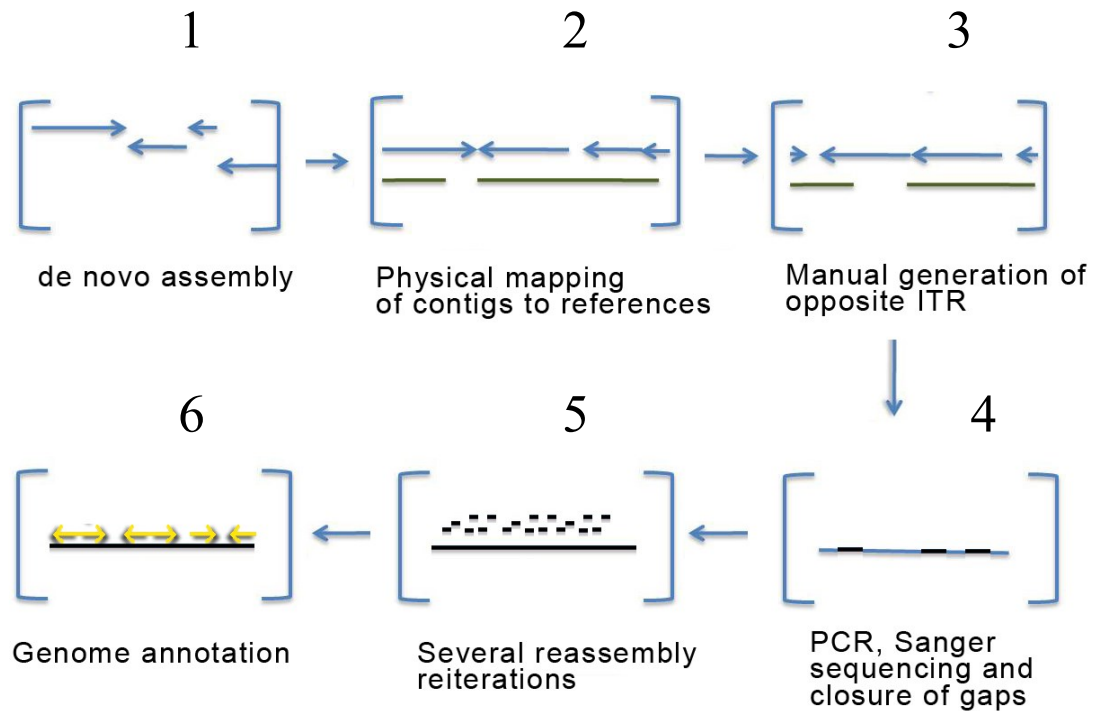


Figure 4. Bioinformatics workflow, genome assembly and genome annotation. After sequencing, (1) *de novo* assembly was used to form contigs of overlapping reads. (2) The order of the contigs was determined by comparing several references with all contigs using a tool called Nucmer. Since the ITR's are homologous sequences, they grouped into the same contig. (3) The opposite ITR was manually assembled using the contig containing the ITR. (4) To fill the gaps (including both ITR junctions) amplification by PCR and Sanger sequencing were done, and inserted into each draft genome. (5) Reassembly of all reads using each draft genome as reference increased the accuracy of the final sequence. (6) Annotation was done using a tool called GATU, which uses translated sequences to determine homology.

physical location and gaps, followed by PCR and dual strand Sanger sequencing. The 5 contigs were assembled using the additional Sanger sequence reads. All single nt polymorphisms located within coding regions were verified by PCR amplification with flanking primers and +/- strand Sanger sequencing.

Genome annotation and ORF comparison

The Genome Annotation Transfer Utility (GATU) [265] was used for annotation of ERPV based on the ECTV-Nav sequence. The criteria for annotation included a cut-off of at least 180 nt, 60% nt similarity score threshold, and less than 50% of overlap to other ORFs. The transferred annotations were back-compared to ECTV-Nav and ECTV-Mos genomes. Every mutation affecting an ORF relative to ECTV-NAV was confirmed by PCR and re-sequencing. ORFs not previously annotated in ECTV-Nav were designated “unassigned ORFs”. All ORFs were translated and compared to the predicted protein sequence from ECTV-Nav, ECTV-Mos (Accession NC_004105), CPXV-BR (Accession NC_003663) and VACV-COP (Accession M35027) using an in-house tool for comparative genomics called MyOrfeome (Mendez-Rios JD, MyOrfeome, Internet: <http://myorfeome.sourceforge.net>). All sequences were obtained from www.poxvirus.org. Protein alignments were visually evaluated and used to curate and correct for alternative start sites.

Genome alignment and comparison of ERPV to closest sequences.

Prior to comparing ERPV and ECTV genomes, regions containing repetitive sequences were masked using the Phobos Software plugin for Geneious Pro 5.5 software and each genome was truncated by removing the right ITR. The genomes were aligned using ClustalW2 [266, 267]. The ends of the alignments were hand edited using Geneious Pro

5.5 Software for optimization purpose. All mutations on coding and non-coding regions were identified.

Phylogenetic tree of ERPV and other poxviruses.

Complete proteomes of representative poxviruses were downloaded from www.poxvirus.org. Using the FASTA description, all proteins were imported and indexed on a MySQL database. 96 conserved ORFs were identified and translated for this analysis. Clustalw2 was used to align all sequences. An unrooted tree was generated by Maximum Likelihood (ML)+ JTT method, with 1,000 boot-strap replications using MEGA Software [268].

Results

ERPV genome sequence

Whole-genome sequencing of ERPV resulted in 54,227 reads initially assembled into 5 different contigs (Fig. 4). Homology search with NCBI Blast tool identified ECTV-Mos as the closest related genome. This genome was then used as a reference for physical mapping of the 5 contigs, followed by completion of the gaps. The gaps were completed by PCR and Sanger sequencing with newly designed primers. The final genome assembly showed a 63X coverage and a total of 206,409 bp counting from the start of the highly conserved 19-bp CRS [32, 152-154] to the end of the distal CRS. The conserved genomic region has a length of 192,365 bp and each ITR 7,022 bp (Fig. 6). Interestingly, 3 direct repeats were identified. These repeats were located at the ends of each contig, preventing the whole genome to be aligned *de novo*. DRI and DRII were located on each end of the genome, with a 69-bp repeat sequence (repeated 2.3 times) and 85-bp repeat sequence (repeated 10.4X times) respectively. They were 316 bp apart with close proximity to the

CRSs. DRIII has a 20-bp repeat sequence (repeated 7.0X times), but located within the VACV F1 ortholog.

Comparison of ERPV with ECTV genomes

In order to select the closest related genomes to ERPV, the contigs were blasted against NCBI's sequence repository. After evidence of its similarity to ECTV Moscow (ECTV-Mos) strain [269] and the ECTV Naval strain (ECTV-Nav), both genomes were used for comparison purposes. The ECTV-Nav genome is publicly available through www.poxvirus.org website [270], but not on NCBI.

Multi-genome alignment of all three strains (ERPV, ECTV-Nav and ECTV-Mos) was used to highlight the differences among them. This comparison showed discrepancies when defining the first nucleotide for each sequence. ECTV-MOS's first nucleotide corresponded to the predicted 10th base pair after the CRS, suggesting that these first nucleotides were not included in the final version of this genome. On the other hand, the ECTV-Nav genome sequence included sequences that correspond to the hairpin region, which were not included in ERPV final genome sequence. Because of this, all lengths were adjusted to account for nucleotides between the first base of the left CRS to the last base of the right CRS. All genomes were compared and features summarized in Table 1. Interestingly, ERPV length is similar to ECTV-Naval, and both are several thousand nucleotides shorter than ECTV-Mos. The differences in sequence length for all three genomes are mainly located within the ITR's. A closer evaluation of the ITR's for ERPV and ECTV-Nav revealed that differences in length are due to deletions and variability of the DR's. Furthermore, all three DR's were masked from all three genomes in order to

Table 1. Comparison of ERPV's genome with close related strains.

	ERPV	ECTV-Nav	ECTV-Mos
Genome length (bp)	206,409	207,516 ^a	209,829 ^a
ITR length (bp)	7,022	7,325	9,442
GC content	33.2%	33.1%	33.0%
Annotated ORFs	183 ^b	183	178
Identical ORFs	-	173	145
Identity to ERPV	-	99.8%	98.4%

ORFs: open reading frames; bp: basepairs; ITR: inverted terminal repetition; ECTV-Nav: Ectromelia Naval strain; ECTV-Mos: Ectromelia Moscow strain. ^a genome sizes are from the first nt of the left CRS to the last nt of the right CRS. ^b the ORF number includes the homolog of O3, which was not originally annotated in ECTV-Nav or ECTV-Mos.

Table 2. Amino acid changes relative to Ectromelia Naval.

ORF	Size (aa)		VACV-COP nomenclature	
	ERPV	Naval		
ERPV_027	282	426	F1L	Contains shorter DRIII within the sequence, shortening the ORF
ERPV_048	332	342	E5R	Deletion of “AT” at TSS of Naval causes truncation at N-terminus
ERPV_066	112	112	G3L	V66A
ERPV_116	892	892	A10L	R236G, V881A
ERPV_152	126	100	A45R	Single “A” deletion in Naval cause a frame shift and earlier termination
ERPV_153	241	241	A46R	S67P
ERPV_160	564	564	A55R	N358D
ERPV_161	282	282	A56R	Y139D
ERPV_177	560	560	A55R	M241V

aa: amino acids; ORF: open reading frame; ERPV: Erythromelalgia-related poxvirus; Naval: Ectromelia Naval strain; VACV-COP: Vaccinia virus Copenhagen strain;

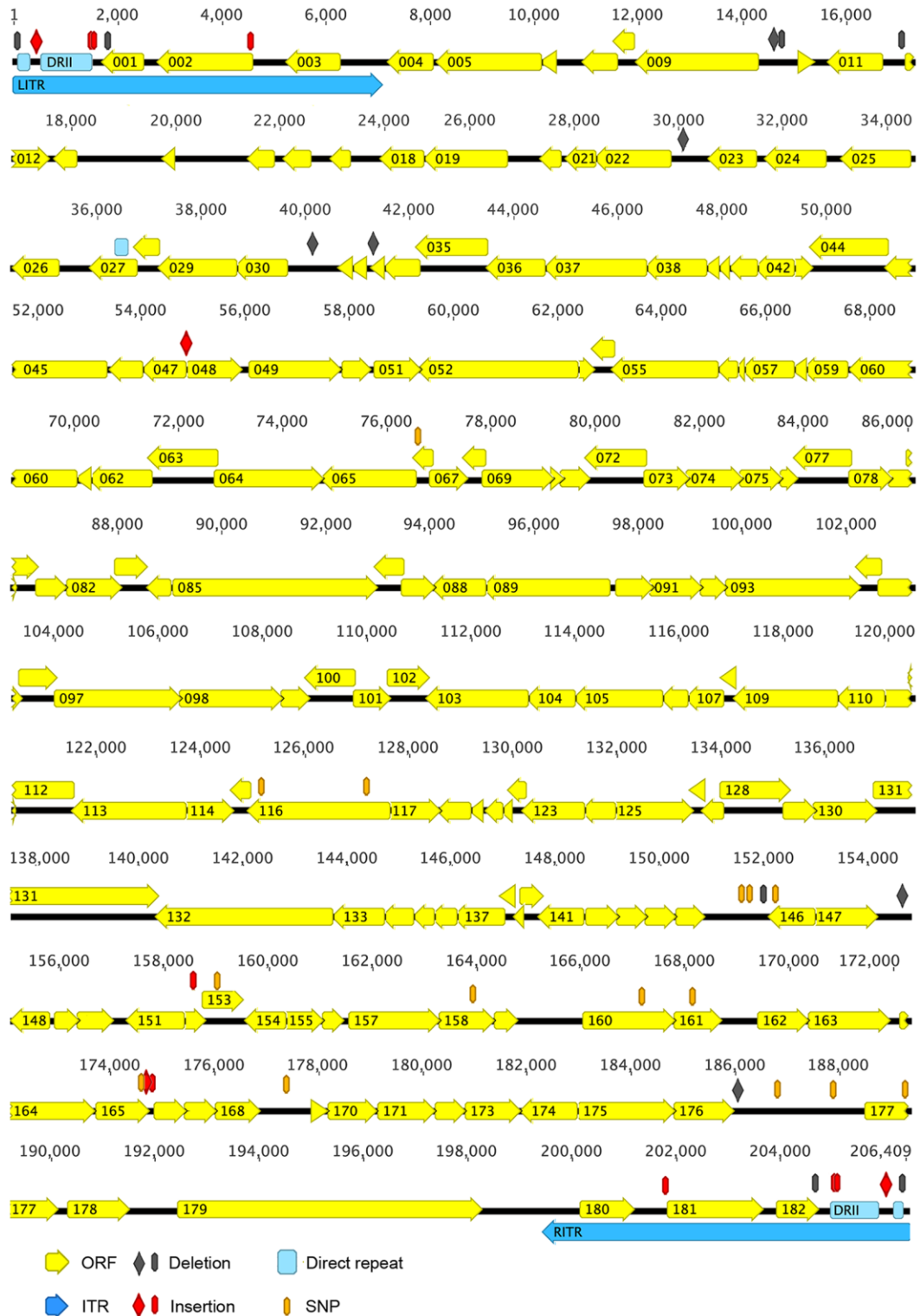


Figure 6. ERPv genome map and mutations relative to Ectromelia Naval strain. ERPv genome was aligned to ECTV-Nav after masking all repeats in both genomes. All ORFs were present in both genomes, and mutations are identified with a symbol over the sequence affected.

compare the global identity. ERPV shows 99.8% sequence similarity to ECTV-Nav, and 98.4% similarity to ECTV-Mos.

The Software GATU (Genome Annotation Transfer Utility) [265] was used to initially annotate and identified ERPV genome. All 183 ORF previously annotated in ECTV-Nav were successfully identified and transferred to ERPV. A total of 173 of these ORFs were identical in ECTV-Nav. All mutations affecting protein coding were verified by PCR and re-sequencing. A summary of these mutations is presented in Table 2. However, essentially all coding mutations found in ERPV relative to ECTV-Nav were identical to ECTV-Mos. Fig. 6 shows the ERPV genome map indicating all differences found relative to ECTV-Nav.

The ERPV genome contains 33 additional ORFs with homology to longer CPXV ORFs not identified in ECTV genomes. Of these, 17 had identical sequences in all ECTV genomes used here; an additional 10 ORFs were identical in ECTV-Nav; and 2 were identical in ECTV-Mos. Nevertheless, these 33 fragments are likely to be non-functional in either ECTV or ERPV.

Phylogeny of ERPV and other orthopoxviruses

A phylogenetic tree was generated using a total of 96 orthologs from several Orthopoxviruses (Fig. 5). Although ECTV-Nav is highly similar to ERPV, it was included to present their relative distance to other poxviruses. The separation of ECTV clade to other poxviruses and their proximity to CPXV is consistent with other analyses [3, 269, 271].

Discussion

Here I was able to sequence and identify ERPV using 454 sequencer technology supplemented with PCR and Sanger sequencing. Sequence homology identifies ERPV as a member of the Ectromelia species, closely related to the Naval strain. The differences between ERPV and ECTV-Nav include deletions in ECTV-Nav, and several mutations throughout the genome. From the 183 ORF previously annotated for ECTV-Nav, a total of 173 ORF were identical in ERPV. These similarities highlight the closest relationship of these two viruses. The presence of multiple deletions in ECTV-Nav's ITR's suggests that ECTV-Nav could not be the immediate progenitor of ERPV.

The origin of ECTV is still controversial. The Hampstead strain was the first ECTV isolated strain from laboratory mice in London [272]. Enzootic cases in breeding stocks of mice in Europe, China and Japan have been reported [273]. Other outbreaks have been reported in mouse colonies in the United States [274]; moreover, there is a single report of ECTV isolation in the wild in Europe [275]. The ECTV-Nav strain was isolated in an outbreak that occurred in the Naval Medical Research Institute in Bethesda, MD, whose source was a contaminated commercial mouse serum [276]. Other outbreaks have also been related to contaminated serum from the United States and China [277-279].

The isolation of ERPV generates an interesting debate on the issue of human infection during the reported Chinese outbreak [259]. Reports of mouse serum as the source suggest contamination as a possibility; nevertheless, isolation of ERPV was done using fetal bovine serum, and not mouse serum. Further evidence that support human infection is the analysis of antibody titers in patient vs non-diseased population that showed significant increase of reactive antibodies [260]. Nevertheless, higher reactive antibody

titers can also be explained by cross-reactivity to ERPV epitopes. [280, 281]. Further efforts to elucidate the serology in these patients are being carried out by other groups.

Conclusions

ERPV is a member of the ECTV species. This report represents the third complete ECTV genome publicly available. Both, ERPV and the Naval strain show striking similarities that suggest a common source. To address the issue of human infection, new serology experiments would have to be designed to rule out vaccinees' cross reactivity against ECTV antigens. The issue of human infection cannot be addressed from sequence analysis, for which further evaluation is being carried out by other groups.

Chapter 3: Generation of MOCV transcriptome profile from *in vitro* and *in vivo* samples.

Summary

Molluscum contagiosum is a human pathogen that infects children and immune-suppressed patients. Our knowledge of the virus is limited for the lack of an *in vitro* and *in vivo* system to grow the virus. Currently, there is no specific treatment or anti-viral agents against the virus, and complicated cases are a real burden for patients and care providers. Here, we evaluate MOCV from the transcriptome point of view using RNA-Seq to determine the genes expressed *in vitro* and from a human specimen (*in vivo*). A complete gene expression map was constructed using the *in vivo* and *in vitro* transcriptome, which confirmed the early nature of 60 predicted genes. Furthermore, new tools and assays were developed to facilitate further research of this virus. Finally, we conclude that MOCV's replication blockage might be in uncoating of the viral core.

Introduction

For more than a century, the Molluscum contagiosum virus (MOCV) has been an intriguing member of the Poxviridae family. Humans are the only natural host known to date, and mostly children and immunosuppressed patients are infected [16, 282-284]. In healthy individuals, the virus causes papular lesions found mostly in the head and neck [16]. Our knowledge of this virus has been limited by the lack of viral growth *in vitro* and the absence of an animal model [285]; nevertheless, some progress has been made with the adoption of new technologies such as sequencing [17] and RNA detection [286, 287]. Bugert and co-workers were able to detect early gene expression by RT-PCR [286], and in-situ hybridization; nevertheless, DNA replication and post-replicative (PR) gene

expression have been controversial [287]. Xenographic models have been attempted with no success [288]. The blockage in MOCV's viral cycle has been proposed to be in the uncoating steps, which is required for DNA replication and intermediate gene expression [289]. This model conflicts with detection of predicted post-replicative transcripts from *in vitro* experiments [287].

Here, RNA-Seq technology was used to generate the first MOCV gene expression profile from *in vitro* and *in vivo* samples; moreover, the temporal classifications of several early genes were confirmed, and the compatibility of MOCV's promoters with VACV and ERPV transcription machinery was demonstrated. The transcriptome map from *in vivo* samples was generated, thus expanding our knowledge and resources to study gene expression of this human pathogen.

Materials and Methods

Virus stock preparation

Molluscum contagiosum (MOCV) lesions were removed by curettage from infected patients, were kindly provided by Jeffrey Cohen (NIAD/NIH). Infected tissues were frozen, transported in dry ice, and stored at -80°C. The tissue plugs used for direct-RNA sequencing were transported in RNAlater solution (Life technologies Cat. AM7021). Samples were stored at 4°C and processed within 72 h after removal. Virus stocks from infected skin were prepared by pooling two tissue plugs from the same patient, followed by maceration using a tight Dounce homogenizer in 1 ml Tris-HCl pH 9.0. The suspension was frozen and thawed three times, followed by three cycles of sonication. The virus preparation was then cleared by slow-speed centrifugation (300 x Gs for 10 min) to remove cell debris. The cleared supernatant was collected and aliquots prepared

for further use. Virus particles (vp) were estimated using a virus counter (Virocyt LLC, Boulder, CO) [290].

Cell culturing and infection

MRC5 cell lines (ATCC CCL-171) were grown using 10% FBS-EMEM, supplemented with 1% L-glut and 1% Pen/Strep (growth media), in a 6-well plates for each *in vitro* transcriptome sample. Before infection, the medium was replaced with 2% FBS-EMEM, complemented with 1% L-glutamine and 1% Pen/Strep (infection media). A volume of 10 μ l of viral stock (\sim 10 vp/cell) was used to infect cells in infection media. After adsorption for 2 h, the medium was aspirated and replaced with growth medium. Infected cells were incubated at 37⁰C, 5% CO₂ (regular conditions) for the remainder of the assays. For the functional gene expression assays, MRC-5, HFF, HutK, HEK_n, HOS, C32Tg, FL, and HEP2 cells were grown in 48-well plates following ATCC's recommended methods and media.

Electron microscopy evaluation

Dilutions of the viral preparation were used for electron microscopy (EM). 3 μ l of each dilution was loaded into an EM grid followed by negative staining for 5 minutes. For transmission EM analysis, carbon-coated Rh Flashed Copper mesh grids (400 mesh, Ted Pella) with nitrocellulose supporting film were placed on 15 μ L droplets of solution for 5 minutes before negative staining in 1% uranyl acetate. Virus particles were observed and photographed at 120 kV in a Tecnai 12. NIH Image J software was used for measurements. The whole mounting, staining and visualization procedures were kindly done by Karl Erlandson.

Cytopathic effect evaluation

In order to test MOCV ability to induce a cytopathic effect (CPE), approximately 10 vp per cell were used to infect multiple cell lines. Different conditions such as pre-exposure of the inoculum to ultraviolet light or pre-incubation of cells with cycloheximide (CHX) were also used. A concentration of 300 µg/ml of CHX was used for pre-treatment of cells in all cases. For inactivation of the inoculum, 10 µl of virus stock were added to 2 ml of infection medium in a 34.8 mm 2 well (6-well plate). The plate with the inoculum was kept on ice and exposed to UV-light for 3 min.

Plasmids and expression constructs

For the functional assays, six plasmids containing reporter genes (luciferase or gfp) under VACV promoters or deleted promoters were kindly provided by Zhilong Yang. These constructs consisted of a single reporter gene (gfp or luciferase) under the control of intermediate (G8) or late (P11) VACV promoter [61, 85]. The constructs were verified by Sanger sequencing before the assay. Two constructs with no promoter (DP) were included as negative controls. Each construct was generated using a Zero-Blunt-II TOPO backbone (Life Technologies, CA, USA). An additional new plasmid was designed to test back-compatibility of MOCV promoters with VACV transcription machinery. For this, a plasmid containing gfp under the control of MOCV's MC095 promoter was also generated again using a TOPO-Blunt backbone. MC095 promoter is a predicted post-replicative (PR) promoter [17]. The exact promoter sequence CCTTTGGTG-CAGATCTCGCGAATAATAA was chosen based on our current knowledge of VACV's PR promoters. Overlapping primers to anneal the promoter to the gfp construct were designed, followed by PCR of each fragment. Fragments underwent overlapping PCR

and insertion of the final product into a TOPO vector. The plasmids were transduced into chemically-competent *E. coli* (Invitrogen, Cat. C4040-10), grown in LB media (Quality Biologicals Inc, Cat. 340-023-101), and selected in agar plates containing kanamycin. This new construct was also sequence verified.

RNA extraction and RNASeq library preparation

The clinical samples plugs were weighed and RNA extracted using 0.8 ml of Trizol Reagent (Ambion 15596-018) following the manufacturer's protocol (Part 2. Phase Separation). RNA from the tissue plug for direct RNA-Seq was carried out using phenol:chlorophorm:iso-amylethanol (ratio 25:24:1). In all cases, RNA was precipitated with ethanol, and eluted in water or commercial elution buffer. RNA samples were aliquoted and purified using solid-phase selection to purify polyadenylated transcripts (Invitrogen, Dynabeads Oligo dT Cat. 61006, Ca, USA) RNA libraries were prepared using ScriptSeq v2 kit (Epicentre SSV21106) for both *in vitro* and *in vivo* samples.

Sequencing and quality control

Illumina libraries were sequenced using Illumina GA IIx sequencer using 68 base fragment reads, in multiplex across 7 lanes. Reads were processed computationally by removing adaptor sequences using RML program. Poor quality bases were eliminated and mapped to MOCV's genome using TopHat. Default settings were used, except for allowing two alignments per read for the terminal repeats. Gene counts were determined by the number of MOCV reads mapped to an ORF in the corresponding strand. Read counts were normalized to total read counts used for mapping and then further normalized to ORF length. Sequencing and quality control was done by Craig Martens, Daniel Bruno and Stephen Porcella from NIH's Rocky Mountain laboratories.

qRTPCR and primers

Quantification of viral transcripts by qRTPCR was done using SuperScript qRTPCR kit (Invitrogen 12574-030). The following primers were used to quantify early and PR genes: MC104R (Fw, 5'-CTTGACCGTCTGCGGACGCAG-3' & Rev 5'-GTGCTG-GAGCAGGGCTACGAG-3'and), MC005R (Fw 5'-CTCCGAGAGAGGCTGGCTCC-3' & Rev 5'-CGATGCAGTGCGGATGTGCT-3'), and ACTB (Fw 5'-GAGACCTTC-AACACCCCAG-3' & Rev 5'-CGATGCAGTGCGGATGTGCT-3'). Products were run and visualized in agarose gels using ethidium bromide for DNA staining (data not shown).

Functional gene expression assays

MOCV and VACV strain WR were used to infect cells in parallel. In all cases, infection was followed by transfection of 2 µg of plasmid using Opti-MEM medium (GIBCO 31985-062) and Lipofectamine 2000 (Invitrogen 11668-500). Luciferase reactions were prepared using a luciferase detection kit (Promega, Cat. E1500), and measured using a luminometer (Sirius Luminometer). WR samples were diluted 10-fold before luciferase reading. Each luciferase reaction was prepared with 2 parts of sample and 5 parts reaction buffer. Detection of GFP expression was done by fluorescent microscopy and direct visualization.

Transcriptome analysis

MOCV tiling files of mapped viral reads were imported into Mochiview [291] to generate transcriptome maps. Images of each map were generated using the same software. Spreadsheets with the normalized read counts for each transcriptome dataset were imported, merged, and analyzed using GeneSpringGX version 12. (Agilent

Technologies). The dataset was organized by time point and each ORF associated to its predicted expression class. Principal Component Analysis (PCA) was performed and compared to the outlier CHX sample. Expression profiles were plotted and grouped based on each promoter classification [17]. Normalized counts were used to generate a gene expression map using a 10 count per ORF cut-off for all time points as the expression criteria. The results of the *in vitro* and *in vivo* transcriptome were converted into annotation files using an in-house script and imported into Geneious Software 6.0 (Biomatter) to generate the complete transcriptome map (Figure 19). Evaluation of the read-through mechanism was done by direct examination using Mochiview (Figure 15).

Results

Initial characterization of MOCV preparations

Extraction of MOCV virus was done with a simplified version of previous MOCV purification protocols [292] to maximize the amount of virus extracted from the small tissue plugs. In order to evaluate the viability of the virus the virus preparations were characterized and quantified. Viral particles were visualized by EM to confirm the presence of intact particles (Fig. 7). EM visualization showed brick-shaped bodies of approximately 200 nm x 400 nm, consistent with poxvirus morphology [293-295]. The bodies were found as single particles or in clusters, similar to previous descriptions [293].

Infection of MRC5 cells was carried out by inoculating approximately 10 vp per cell. In order to confirm that CPE was directly related to the virus, an aliquot of the preparation was exposed to UV-light to inactivate it (Fig. 8). Infected MRC5 cells with the inactivated inoculum showed no evidence of CPE in any time point. A mock infection was also included using the same solution used to generate the viral preparation. CPE effect was observed as early as 4 hpi with a peak between 8 and 12 hpi. As previously described, recovery of the monolayer was also observed at 72 hpi.

The effect of translation inhibition upon an MOCV infection was also evaluated. MRC5 cells were infected with MOCV with or without pre-treatment with CHX. Infection was followed for 15 h (Fig. 9). Similar to our previous findings, CPE in cells with no CHX was observable as early as 4 hpi. Nevertheless cells pre-treated with CHX did not show CPE even after 15 h. Taken together, inactivation of MOCV with UV light and pre-incubation with CHX suggests that CPE depends on the virus early transcriptional events, and that all cells are infected at this viral dose.

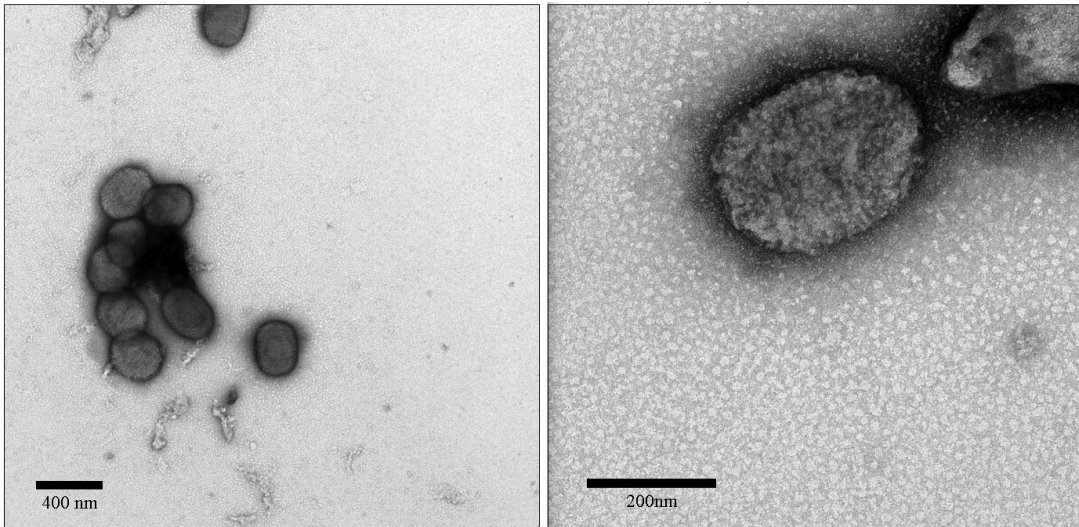


Figure 7. Evaluation of Molluscum contagiosum virus by electron-microscopy. The MOCV stock preparation was evaluated using EM to detect intact viral particles. The morphology and size of viral particles observed was compatible with poxvirus, found singly or in clusters. Scarce cellular debris was observed.

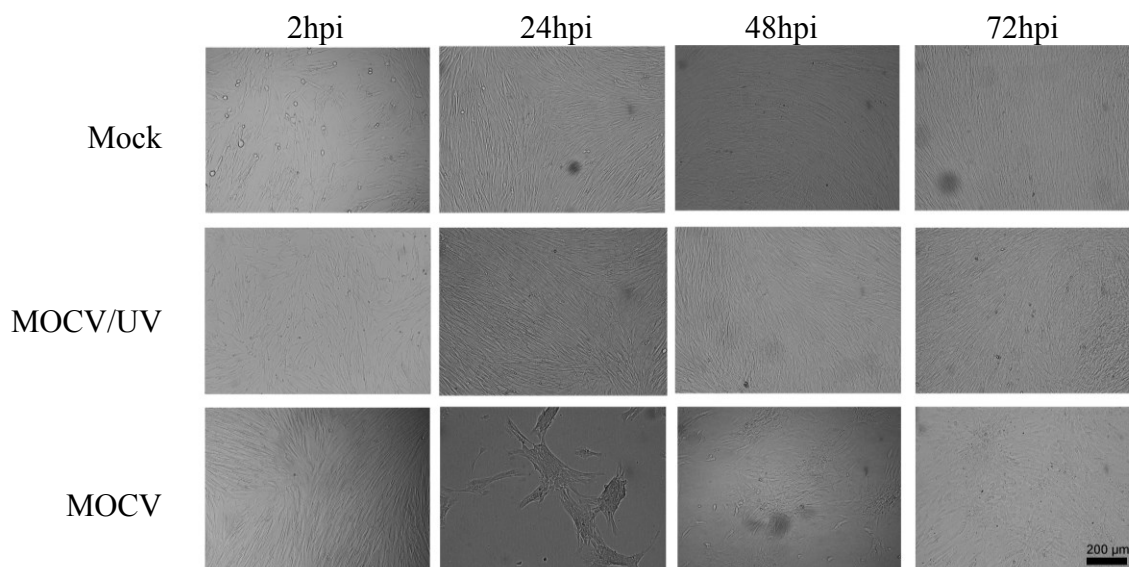


Figure 8. MOCV induces CPE in MRC5 cells and it is inhibited with UV light. MRC5 cells were infected with ~10 vp/cell. An aliquot of the inoculum was pre-exposed for 15 seconds to UV-light before infection (MOCV-UV). At 24 hpi, the whole monolayer showed cytopathic effect, with partial recovery at 48 hpi. At 72 hpi, MRC5 cells were seen again at full confluency. Exposure of the inoculum to UV light before the infection inhibited CPE formation at 72 hpi and later times. The monolayer was completely recovered 72 hpi as shown by others [286, 287].

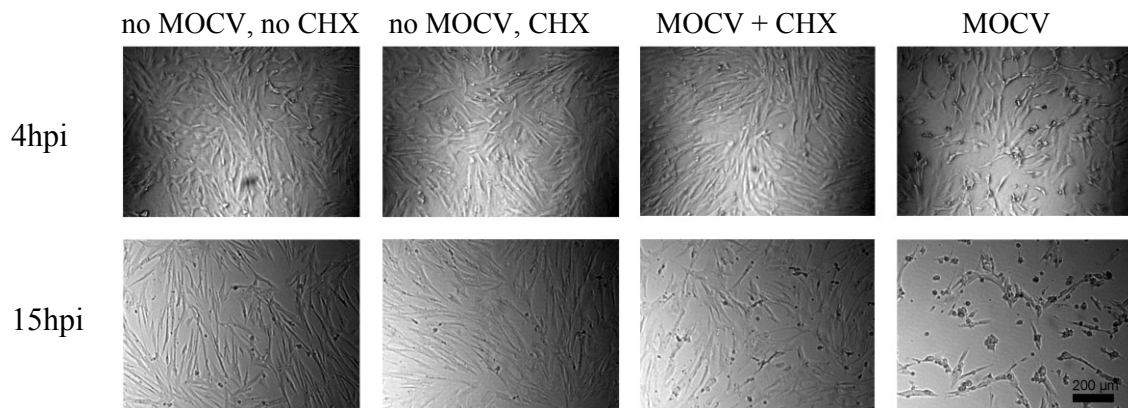


Figure 9. MOCV-induced CPE in MRC5 cells was inhibited with CHX. MRC5 cells were infected with ~10 vp/cell. CPE was documented at 4 hpi and 15 hpi. Pre-treatment of MRC5 cells with CHX shows inhibition of CPE. MOCV: Molluscum contagiosum; CHX: cycloheximide; hpi: hours post-infection; CPE: cytopathic effect.

Table 3. Detection of MOCV's early and PR gene expression in different cell lines by qRT-PCR.

Cell line	Raw dCt values	
	MC005	MC104
MRC5	23.83	25.18
BHK21	23.47	34.69
HFF	24.01	36.9

dCt: raw delta-Ct values which represent the number of cycles needed to detect the transcript.

MOCV gene expression in multiple cell lines

Until now, MRC5 cells have been the most commonly used cell line to study MOCV for the observed CPE when infected. Nevertheless, the identification of a cell line that allows growth of the virus will be valuable to study MOCV's cycle. In order to identify such a cell line, MRC5 cells, BHK21, and HFF cells were compared in their ability to support MOCV's gene expression. All cells were infected with the same dose and viral transcripts measured by q-RT-PCR at different time points. Primers for qRT-PCR were designed to detect expression of MC005 (early gene) and MC104R (PR gene). The results showed similar amounts of early transcripts in all cell lines, and low levels of PR transcripts (Table 3). The data are shown using Ct values that represent logarithmic differences in detection (the lower the value, the less PCR cycles were needed to meet a threshold). MRC5 was the exception, showing similar levels for both targets, early and post-replicative genes. Interestingly, the Ct values in MRC5 were lower, suggesting higher amounts of detected transcripts relative to the other two cell lines. The other cell lines show Ct values for the late transcript (MC104) compatible with background levels. Nevertheless, all cell lines showed similar Ct values for the early transcript. Since there is a much higher amount of PR transcripts in MRC5 cells, they were selected to be used in further assays.

MOCV transcriptome from *in vitro* experiments

RNA-Seq has proven to be a powerful tool to understand poxvirus transcriptional events [108]. In an attempt to address the multiple questions related to MOCV gene expression, a global transcriptome approach was designed to evaluate MOCV's gene expression *in vitro* (Figure 10). MRC5 cells were infected in two different experiments with

overlapping time points. The first experiment evaluated gene expression up to 120 hpi. The second experiment served as an extension for later events up to 14 days pi. RNA was harvested at each time point followed by generation of Illumina libraries (Figure 11). After sequencing, the number of reads mapped to MOCV's genome ranged from ~150,000 to ~216,000 per sample (Table 4). The sample containing CHX had a total of 302,481 sequence reads, the highest count among all samples. Comparison of viral versus host reads showed that no more than 2% of the reads corresponded to MOCV sequences.

Gene counts were determined by mapping reads to each MOCV ORF. Normalization of the gene counts followed, taking into consideration read length and the total number of reads per sample. The Principal Component Analysis (PCA) was used to determine consistency throughout samples (Figure 12). This graphical representation of genes expressed for all samples highlighting the similarities between samples, and their relative difference with the CHX outlier.

In order to have a genome-wide perspective of the gene expression events, expression maps were generated for each time point (Fig. 13). These maps showed incremental amounts of transcripts within the first 8 hpi. Similar findings of incremental amounts of transcripts have been documented [291]. Interestingly, all time points showed similar patterns compatible with early gene expression in which transcripts were located mainly at the ends of the genome, and few a scattered peaks located within the central conserved region. Moreover, no significant increments in the latter time points were observed.

MOCV gene profiling in MRC5 cells

To determine which class or classes of genes are been expressed *in vitro* (early or PR genes), each MOCV gene was associated by its predicted promoter class [17]. The normalized gene counts were associated to each ORF and their promoter classification. The expression profile was then plotted as a time course. Overlapping time points from both experiments were averaged and used in this profile. A total of 60 out of 90 predicted early genes met our gene expression criteria (Fig. 14). Consistent with the observations from the genome expression maps, MOCV transcripts were increasingly detected throughout the first hours. Interestingly, at late time points gene expression seems to follow a steady-state kinetics that continued throughout the assay. Nine PR and eight unknown genes were also detected with this approach.

Detection of PR genes explained by read-through mechanism

In order to address the detection of these nine PR genes (Table 5), the possibility of read-through transcription was considered. This phenomenon is well-known for VACV in which transcription continues further downstream of a gene's 3'UTR, resulting in partial transcription of the downstream CDS into the transcript. If this transcriptional read-through process occurs in MOCV, this could explain detection of PR genes for MOCV. For this reason, the gene context for all nine, PR genes was evaluated using MochiView to browse through the transcriptome tiling. A close-up into the transcriptome tiles revealed that transcriptional read-through is a possible explanation for all PR genes detected (Fig. 15). As expected for a read-through process, transcription starts at a gene classified as early and continues downstream to the PR gene.

Identification of incomplete transcription of the downstream PR gene could be used as a signature for this phenomenon. Only detection of MC014 (Fig. 15 Panel G) cannot be explained by a read-through mechanism. High amounts of transcripts derived from the opposite strand may be contrasted to the scarcity of transcripts found for MC014, suggesting no active expression of this gene.

MOCV infection (~10 vp/cell)

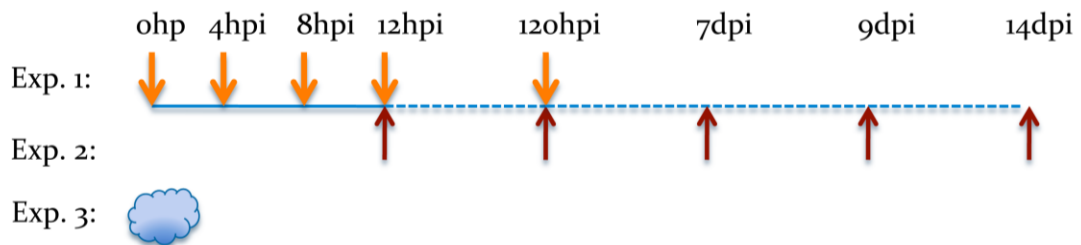


Figure 10. Experimental design for MOCV's transcriptome profiling. RNA extraction for RNA-Seq was carried out at several time points (0h,4h,8h,12h,120h,7d,9d,14d) in experiment 1 and 2 . In this figure, time is represented by the continuous or dashed line. A third experiment required RNA extraction from a non-frozen, recently acquired, MOCV-infected tissue plug (cloud shape). All RNA samples were used for the generation of Illumina-compatible libraries and sequencing. Exp: experiment; hpi: hours post-infection; dpi: days post-infection;

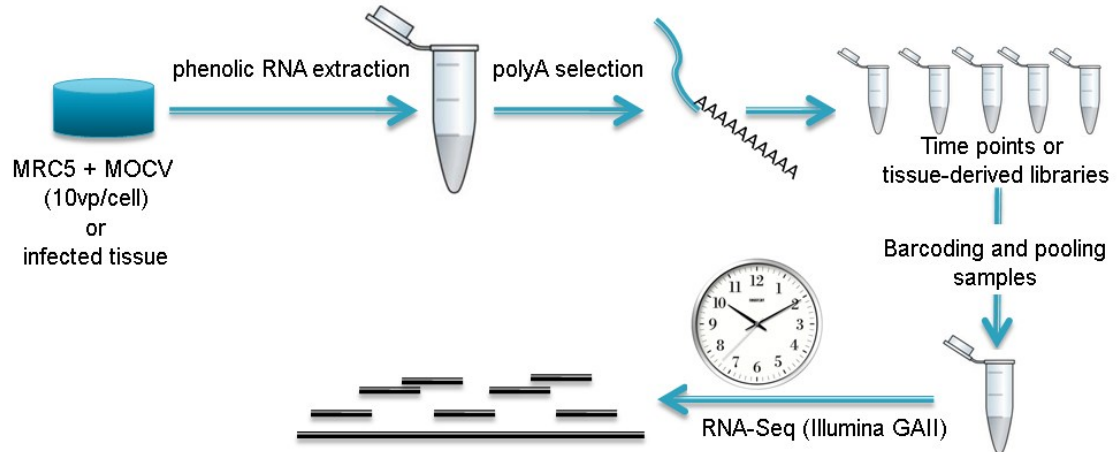


Figure 11. Workflow for RNA extraction and generation of Illumina-compatible libraries. MRC5 cells were infected with MOCV, and RNA extracted at different time points. mRNA was isolated from each sample using a solid-phase method that selecting for transcripts with polyA tails. The enriched mRNA samples were then copied to cDNA and barcoded using Epicenters RNA-Seq kit described in the methods. Libraries were pooled and sequenced using Illumina GAI sequencer. RNA from tissue plug was preserved in RNAlater solution (Invitrogen) and kept in cold (4°C or ice) throughout transportation and processing. Samples were barcoded and pooled for RNA-Seq as described previously.

Table 4. Summary of read counts for the MOCV transcriptome from the *in vitro* assay.

Sample	Total number of MOCV reads
Mock	0
4hpi	170,161
8hpi	216,782
12hpi	216,471
120hpi	176,446
CHX at 12hpi	302,481
12hpi	150,892
120hpi	166,219
7dpi	153,895
9dpi	153,036
14dpi	141,327

dpi: days post infection; hpi: hours post-infection; CHX: RNA samples derived from infected cells pre-incubated with cycloheximide. Mock: RNA derived from mock-infected MRC5 cells.

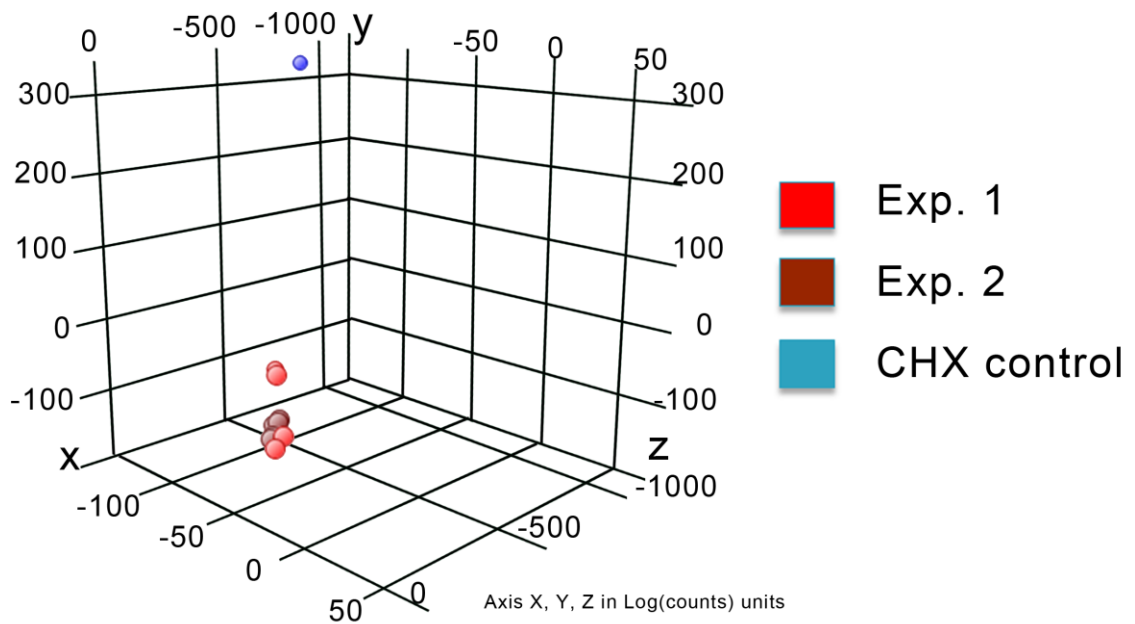


Figure 12. Principal component analysis for all RNA-Seq samples. All *in vitro* samples and CHX control were analyzed and a PCA plot generated using GeneSpring Software. Clustering of all samples provided visual interpretation of similarities in gene expression pattern. Each circle represents a sample, with the axes representing the logarithmic value of the most prominent components expressed. CHX represents the outlier. Exp: experiment; CHX: cycloheximide; red circles: samples from experiment 1; brown circles: samples from experiment 2.

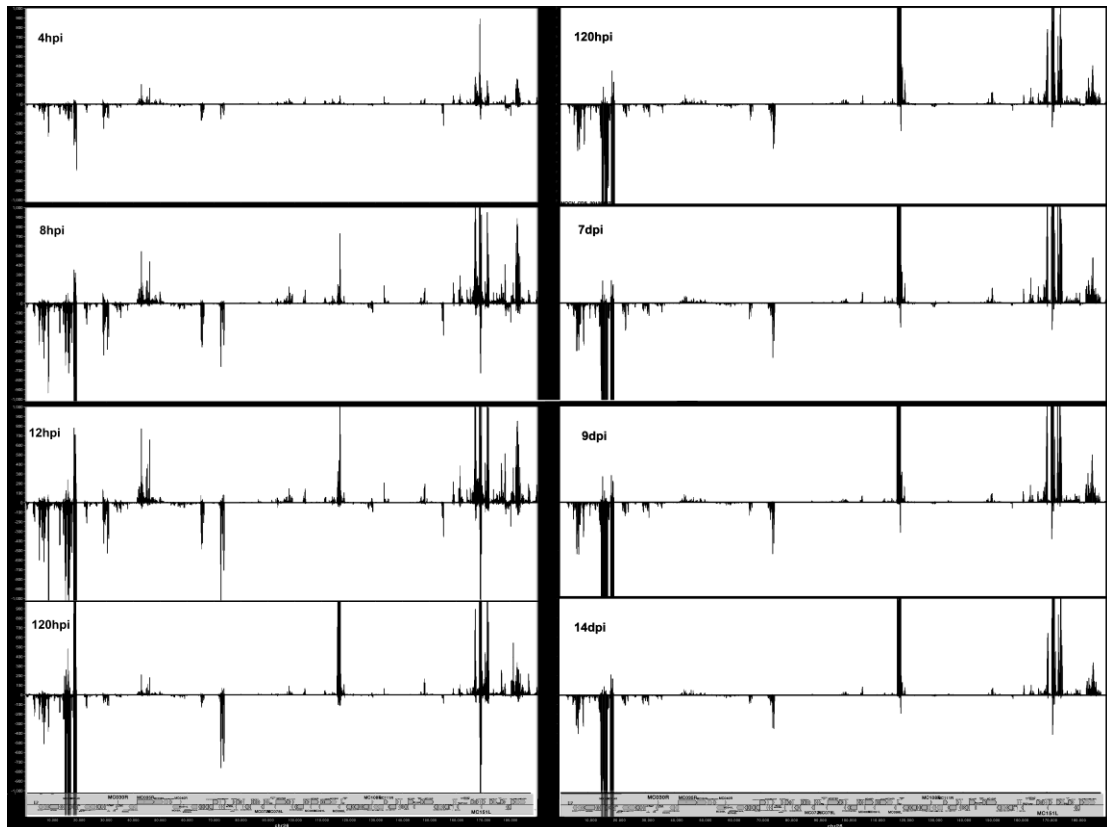


Figure 13. MOCV's RNA expression patterns depict early gene expression *in vitro*. Sequenced reads that mapped to MOCV were imported into MochiView program and visualized as tiles over MOCV genome. The black peaks represent regions in MOCV genome (horizontal line) that were sequenced by RNA-Seq. Both *in vitro* experiments are summarized here. The ordinates display read counts. Reads above and below the horizontal indicate transcription to the right and left, respectively.

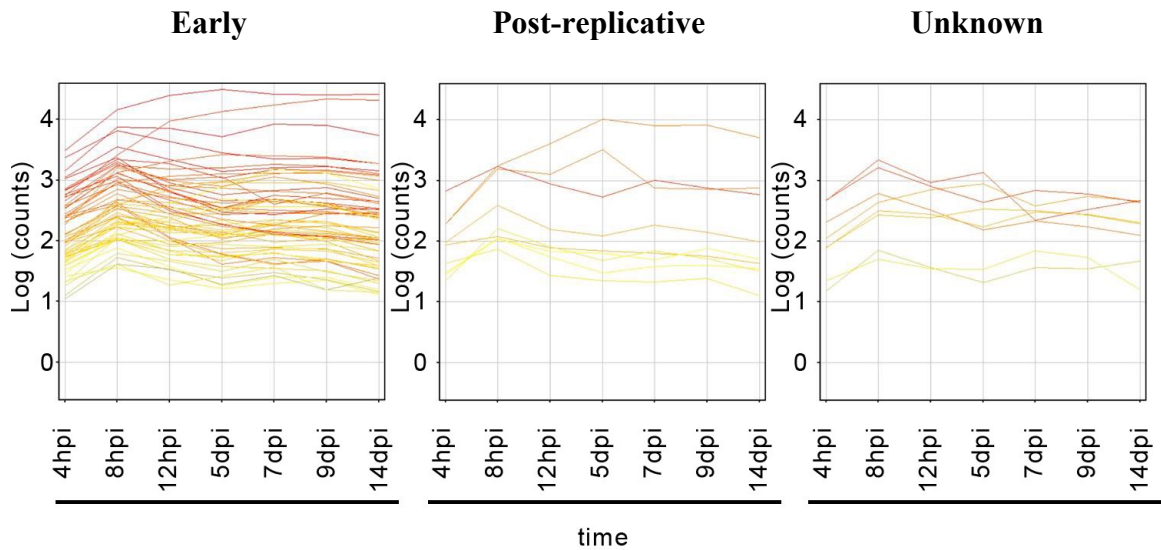


Figure 14. Promoter-based classification confirms enrichment of early genes *in vitro*. Genes were grouped by their promoter classification and gene counts plotted through time. 60 genes were identified as early (shown in the left box), nine PR transcripts were detected (central box), and eight additional genes with unknown promoters were identified. Gene expression profile suggests a steady-state equilibrium of MOCV transcripts. MOCV profile continues to be of early nature 14 dpi.

Table 5. Summary of post-replicative genes detected *in vitro*.

MOCV ORF	VACV-COP nomenclature	Detection explained by read-through
MC013	No VACV homolog	Possible
MC014	No VACV homolog	No /new ORF
MC028	No VACV homolog	Possible
MC031	E1L	Possible
MC041	E11R	Possible
MC044	I1L	Possible
MC045	I2L	Possible
MC107	A4L	Possible

Functional assay

In order to evaluate the presence or absence of PR gene expression from a functional perspective, infection/transfection experiments were carried out by infecting multiple cell lines with MOCV or VACV. This was followed by transfection of plasmids containing reporter genes (GFP or LUC) under the control of intermediate (G8) or late promoters (P11). The experimental design (Fig. 16) included measuring LUC and GFP expression for several days. In order to consider the role of the IFN pathway in MOCV blockage, VERO cells known for defective IFN secretion were used [296]. For all cell lines tested, there was no evidence of GFP expression in the first 72 h. In order to evaluate longer time points, the infection was continued for an extended period up to 14 days. Cells infected with WR showed GFP expression over the entire monolayer. Since compatibility of VACV promoters with MOCV's machinery was a concern, a plasmid was generated with a GFP cassette under the control of MOCV's putative intermediate promoter pMC095 (Figure 17). BS-C-1 cells were infected with VACV and ERPV, followed by transfection of plasmid JM-MC095-gfp 2 hpi. Several controls were added to highlight the specificity of the promoter activity. GFP expression was then captured at 20 hpi, showing that MOCV's PR promoter is compatible with VACV transcription machinery. The assay also showed that AraC inhibits GFP expression. No expression GFP expression was detected in any of the other controls.

A similar experiment was done using a more sensitive detection method. Cells were again infected with MOCV or VACV and then transfected with a LUC-containing plasmid. Chemiluminescence values for all MOCV infections were similar to negative controls (non-

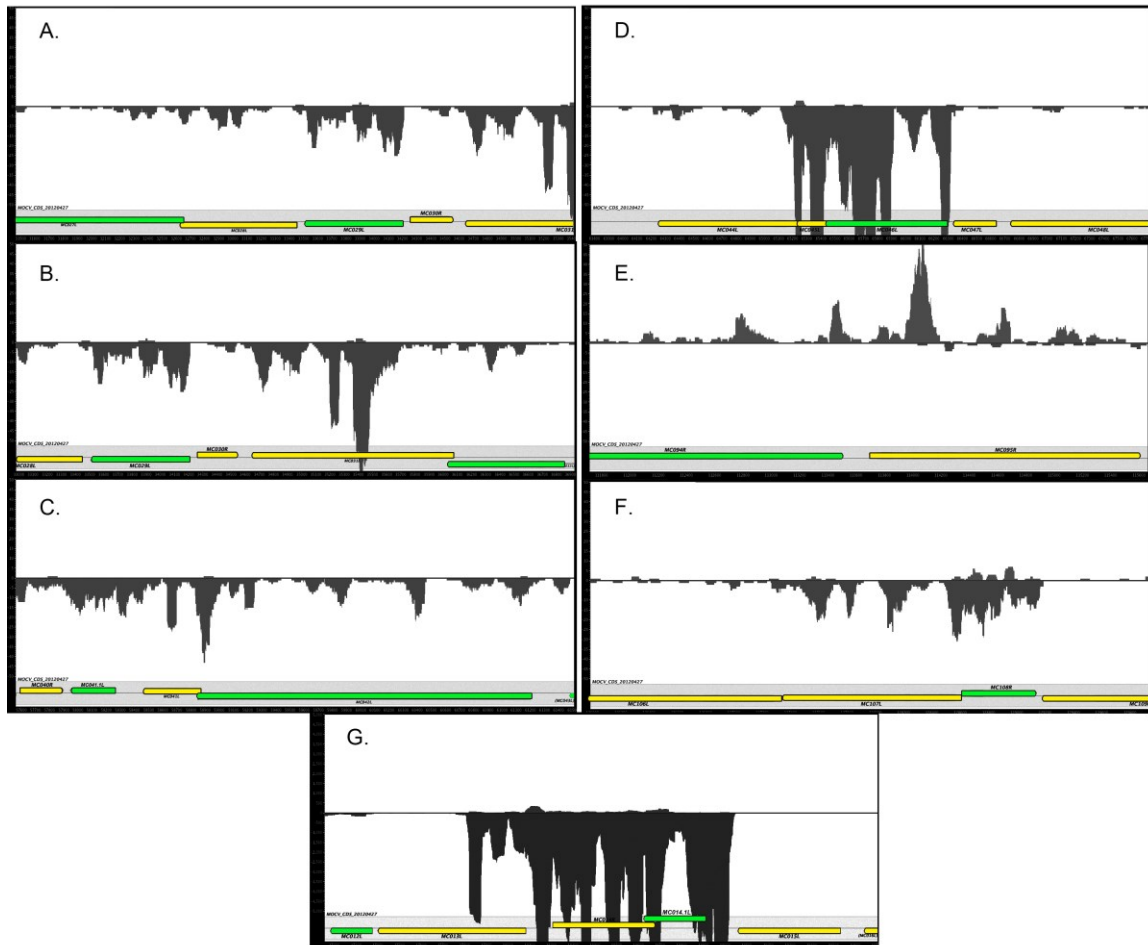


Figure 15. Composite of transcription tiles for the PR transcripts detected. This is a close-up view of the MOCV transcriptome using MochiView. Each PR gene detected is depicted in one of the panels: A) MC028L, B) MC031L, C) MC041L, D) MC044L & MC045L, E) MC095R, F) MC107L, and G) MC013L & MC014R. Sequenced reads (black peaks) were mapped to MOCV genome (horizontal black line). The peaks and valleys represent the accumulative expression level of that region (counts). In most cases, reads from an early gene (green arrow) continues downstream over a PR gene (yellow arrow). Note that some extended reads do not reach the 3'UTR of the PR gene in certain cases.

Viruses: MOCV & WR
(control)

Plasmids: G8-gfp, G8-luc
P11-gfp, P11-luc
DP-gfp, DP-luc

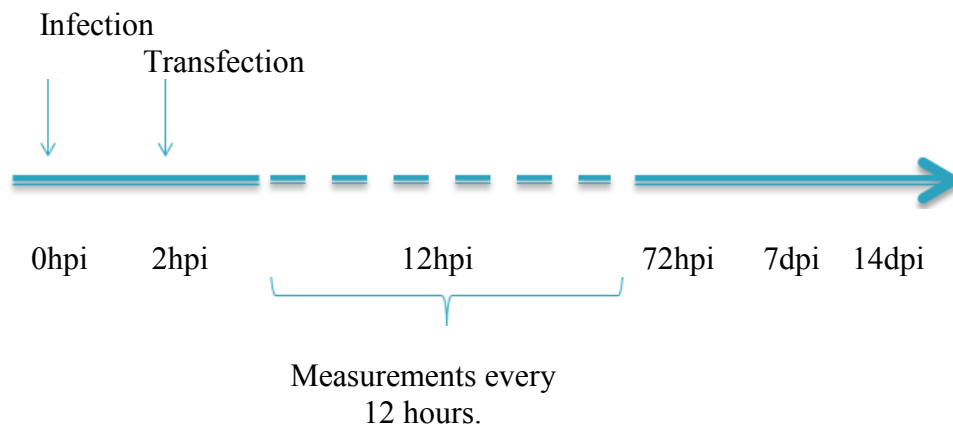


Figure 16. Experimental design to evaluate PR gene expression from a functional perspective. To evaluate PR gene expression from a functional perspective, an assay was used in which luciferase and GFP expression was measured from plasmids under the control of intermediate (G8) or late (P11) promoters. Cell lines were infected and evaluated at multiple time points. GFP was visualized with fluorescent microscopy and luciferase based on a colorimetric reaction and measured with a luminometer. WR: Vaccinia WR; MOCV: Molluscum contagiosum; G8: Vaccinia intermediate promoter; P11: Vaccinia late promoter; GFP: green fluorescent protein gene; luc: luciferase gene; hpi: hours post-infection; DP: deleted promoter.

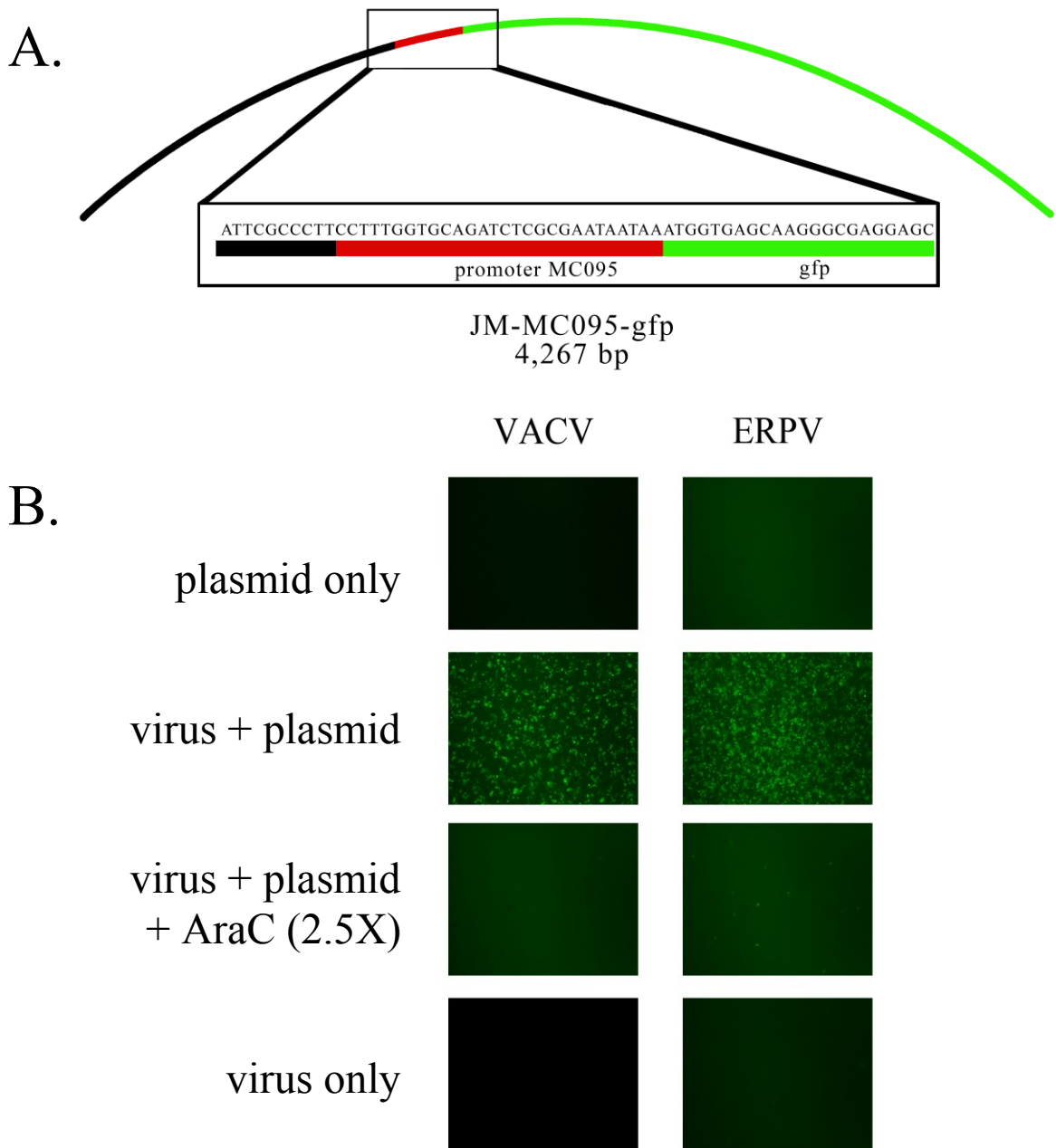


Figure 17. Promoter pMC095 is cross-compatible with VACV transcription machinery and is specific for post-replicative gene expression. To test compatibility of MOCV's promoters with VACV intermediate transcription machinery, the MOCV promoter MC095 was inserted into a plasmid controlling expression of gfp (A). BSC1 cells were infected with VACV-WR or ERPV at an MOI of 5, and transfected with plasmid JM-MC095-gfp two hpi using Lipofectamine 2000. GFP expression was documented at 20 hours post infection (B).

infected cells and plasmids with no promoters) (Table 6 Panel A). Since intermediate gene expression was detected by Bugert and co-workers [287] after five days post infection, a late time point (seven days post infection) was included, and a total of eight cell lines were used (Table 7 Panel B). Failure to detect gene expression in trans- suggested that the minimum requirements for PR gene expression are not met even at seven days post infection for any of the cell lines tested.

MOCV transcriptome from human infected tissues

In order to generate MOCV's transcriptome profile from an infected human tissue, preserving the integrity of the RNA was essential. In coordination with Dr. Jeffrey Cohen, the infected tissue were removed from the skin of patients at NIH Clinical Center and immersed in RNAlater®, which prevents RNA degradation. The samples were maintained at 4°C on ice during transportation until RNA extraction. RNA extraction, library preparation, and RNA-Seq were done as previously described. Read mapping, gene counts and normalization of the data were done following the same criteria described above.

Figure 18 show the gene expression map generated from the tissue plug. In contrast with the *in vitro* dataset (Fig. 13), the transcriptome profile generated from this clinical sample showed a broader expression pattern in which most ORFs are represented by peaks distributed along the whole genome. All 60 genes confirmed as early were detected in the clinical sample transcriptome. Moreover, 97 additional genes were also detected (Table 7). Only six genes did not meet our gene expression criteria (see methods). An expression map was constructed by color-coding each ORF to summarize the findings from the *in vitro* and *in vivo* transcriptome (Fig.19). This *in vivo* transcriptome serves as a reference

for an efficient MOCV infection in a human specimen. Simple subtraction of the 60 confirmed early genes from the whole *in vivo* transcriptome allowed to infer the PR nature of the other 97 identified genes; nevertheless, subcategories of early or PR genes within this group cannot be discarded.

Host transcriptome and absence of shutdown

The MRC5 transcriptome was also detected *in vitro*. Reads were mapped to the human genome and gene counts quantified and normalized. An initial evaluation of the host gene expression was plotted as a heat-map throughout the first time points of the experiment (Fig. 20). Interestingly, the host's gene expression pattern slightly varies, but with no evidence of a shutdown as occurs with other poxviruses. This is in contrast with the significant shut-down reported for VACV's infection in mammalian cells [297].

Table 6. MOCV was unable to initiate PR gene expression in trans-.

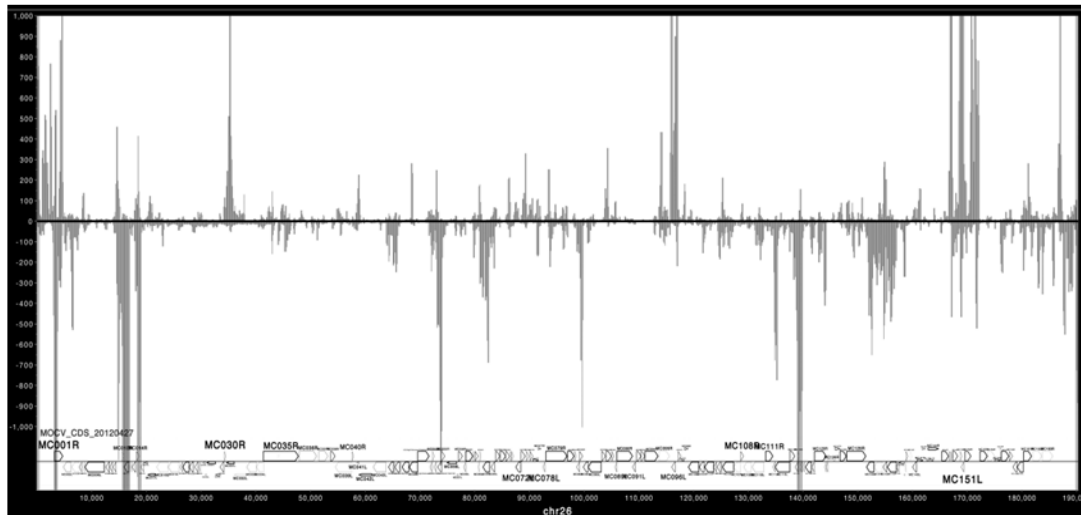
A.

Cell line	VACV promoter	condition	RLU (luciferase)			
			4hpi	8hpi	12hpi	WR (12hpi) 1:10
MRC5	G8	I	66	56	69	6,753,898
		NI	64	85	68	63
	P11	I	56	103	64	905,074
		NI	56	93	73	86
	DP	I	66	73	78	78
		NI	62	88	90	71
VERO	G8	I	90	102	66	45,983
		NI	78	78	69	75
	P11	I	77	90	69	5,817
		NI	96	90	70	81
	DP	I	74	97	67	95
		NI	62	96	71	79

B.

Cell lines	Absolute RLU values		
	12hpi	120hpi	7dpi
HEP	23	213	37
HUTK	36	646	121
A431	9	7	8
C32	11	96	23
FL	271	1108	527
HFF	10	74	51
HOS	14	29	12

A luciferase assay was carried out in MRC5 and VERO cells (Table A). A second luciferase assay included seven other cell lines in an extended time course. All cells were infected (I) with MOCV followed by transfection with a plasmid. Mock-infected cells (NI) were used as a negative control to detect background expression of reporter genes. An additional plasmid with a deleted promoter (DP) was used as an additional negative control. VACV WR was used in a parallel experiment using the same conditions as a positive control.



380,339 reads

Figure 18. Global transcriptome expression map from an infected human tissue. MOCV sequence reads derived from an infected human tissue were mapped to MOCV genome (horizontal line). Regions of expression (peaks) on both strands of the genome were detected. The map shows expression at both ITRs and the central conserved region. The ordinates display read counts. Reads above and below the horizontal indicate transcription to the right and left, respectively.

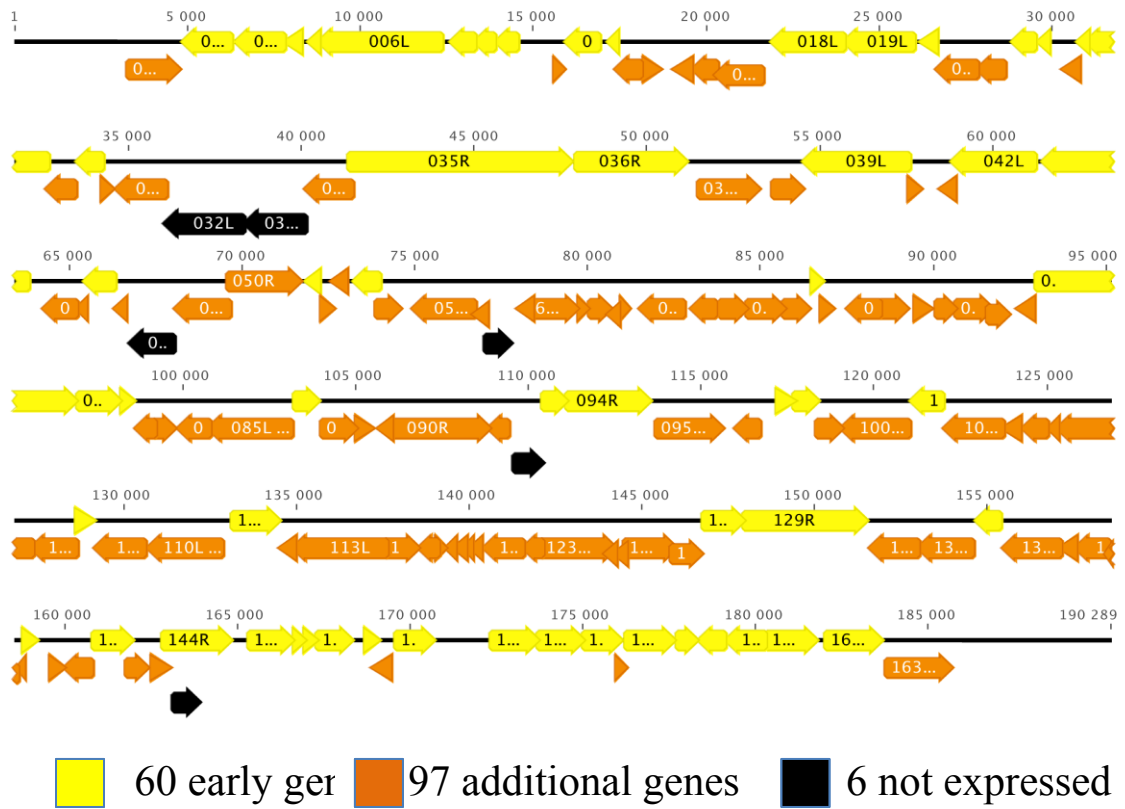


Figure 19. Complete MOCV transcriptome map using *in vitro* and *in vivo* derived RNA. A total of 60 genes were confirmed as early genes by RNA-Seq from the *in vitro* experiments. 97 additional genes detected *in vivo* (tissue plug) were color coded brown. Six genes were not detected as being expressed or did not comply with our gene expression criteria.

Table 7. Summary of other findings from *in vitro* and *in vivo* experiments.

Genes not detected <i>in vivo</i>	Genes with unknown promoters	PR genes detected <i>in vitro</i>	
MC092R,MC058R, MC033L,MC048L, MC032L, MC145R	MC156R,MC071R, MC127R,MC142R, MC151L	MC013L,MC014R, MC028L,MC031L, MC041L,MC044L, MC045L,MC095R, MC107L	
Early genes detected <i>in vivo</i>			
MC002L	MC026L	MC086R	MC147R
MC003L	MC027L	MC093R	MC148R
MC004L	MC029L	MC094R	MC149R
MC005L	MC035R	MC097R	MC150R
MC006L	MC036R	MC098R	MC152R
MC007L	MC039L	MC101L	MC153R
MC008L	MC042L	MC108R	MC154R
MC009L	MC043L	MC111R	MC155R
MC011L	MC046L	MC128R	MC157R
MC012L	MC051L	MC129R	MC158R
MC018L	MC054L	MC132L	MC159L
MC019L	MC070R	MC138R	MC160L
MC020L	MC079R	MC141R	MC161R
MC023L	MC080R	MC144R	MC162R
MC024L	MC081R	MC146R	MOCVgp053

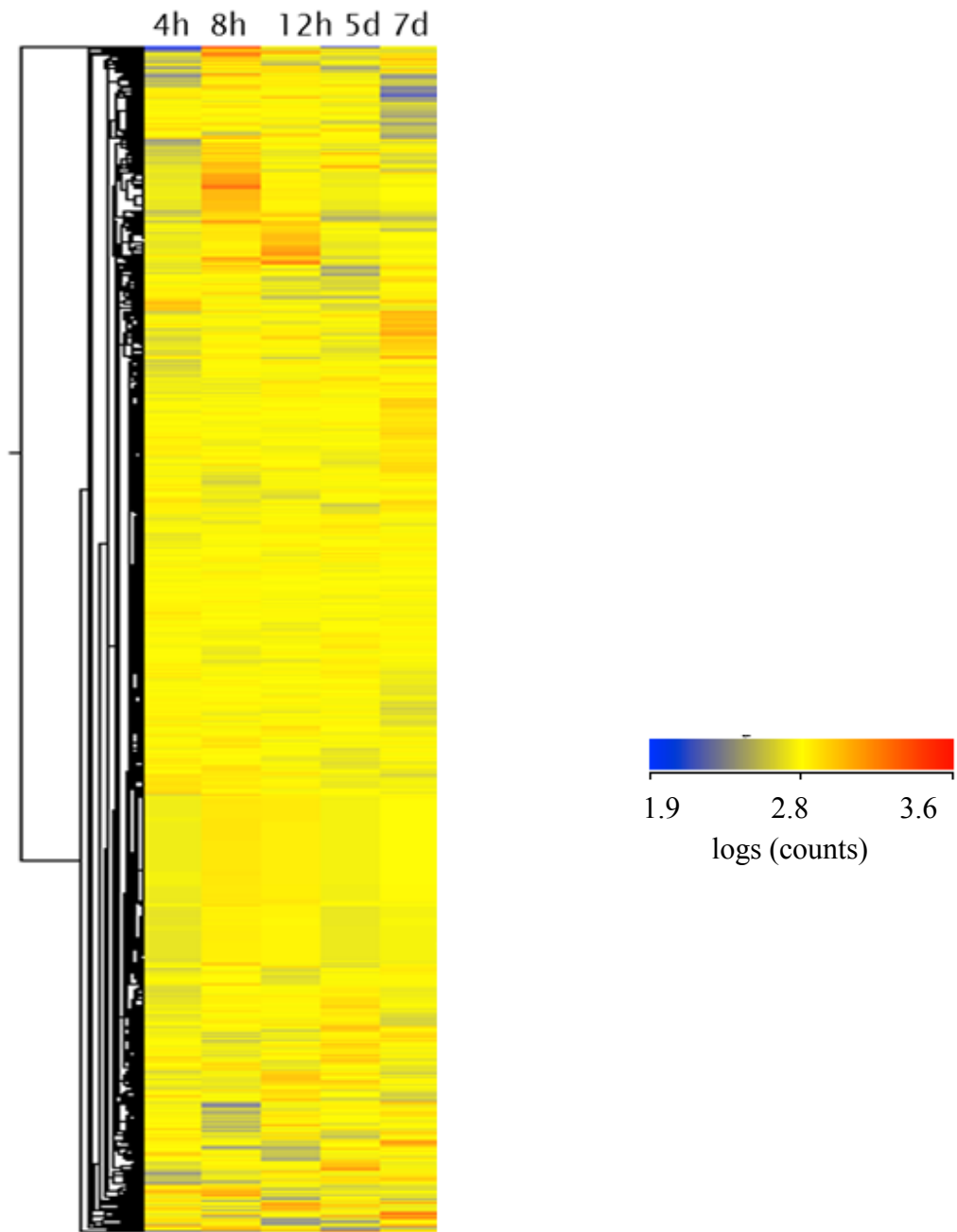


Figure 20. Host's transcriptome shows no evidence of a transcription shut-down. MRC5 transcriptome was also detected and mapped to the human genome. MRC5 gene expression depicted in this heat-map shows no overall reduction (blue areas) of gene expression. Orange areas represent increased gene expression.

Discussion

MOCV is a human-specific pathogen that affects predominantly children and immune-suppressed patients [16]. Our understanding of this virus has been limited for the lack of an *in vitro* system or animal model to grow it [285, 288]. Since infected tissue from patients is the only source of MOCV, a purification protocol [292] was simplified to maximize the amount of virus recovered. The initial EM evaluation of the viral preparation showed morphologically intact poxvirus (Fig. 7). It also confirmed that our simplified extraction method provided a relatively clean virus stock.

UV light prevented CPE formation and confirmed the infectious nature of the preparation (Figure 8) [298]. Experiments using the translational inhibitor CHX provided evidence that gene expression was required for CPE similarly to other poxviruses [299].

The CPE affecting the whole-monolayer also suggested that every cell was infected [300-302]. These aspects are important since they provide evidence of early gene expression that has also been determined elsewhere [289, 303].

Previous reports also showed detection of early and PR gene expression by RT-PCR [286, 287]. MRC5 cells were infected with MOCV and followed through an extended time course. Early and PR gene expression was detected 4 hpi and 120 hpi respectively. Detection of both classes of genes continued up to 14 dpi. Since PR transcripts were detected 5 dpi in MRC5 cells, 3 cell lines were screened for PR transcript with time points that extended for several days (Table 3). Quantification of viral RNA by q-RT-PCR showed similar amount of early transcripts in all cell lines. This suggested that the initial early gene expression occurred in all three cell lines. Similar Ct values for early

and intermediate transcripts in MRC5 cells may be interpreted as a confirmation that both are derived from the same transcripts. In other words, if an early transcript was extended into a downstream PR gene, it would be detected in a similar amount. Interestingly, PR genes were not detected in BHK21 or HFF. This brings an interesting observation that processivity of MOCV's transcription machinery may be impaired in these two cell lines. Without considering the possibility of read-through transcription at this point, MRC5 cells were selected for the RNA-Seq experiments. Further evaluation of MOCV's PR transcripts in MRC5 confirmed Bugert's findings by q-RT-PCR (data not shown) [287].

The sequencing experiments were designed to match the time points from a previous report (Fig. 10) [287]. After RNA extraction and RNA-Seq, MOCV reads were mapped using MOCV genome type I as the reference (Accession number NC_001731). The total number of reads ranged between 150,000 to 400,000 (Table 4). Nevertheless, the cells pre-incubated with CHX showed higher amounts of viral transcripts. Greater expression of early genes in the presence of CHX has been previously described for VACV [108].

Read counts per gene were calculated and normalized based on read length and total number of reads. Normalization of the whole dataset allowed comparison of gene counts across samples. PCA analysis was used to evaluate global gene expression tendencies within the samples (Fig. 12). All samples showed clustering of the principal components, with the exception of the CHX sample. Similarities among the samples demonstrate that genes were expressed in similar proportions in all samples. This analysis provided the initial evidence that the same set of genes were predominantly expressed in all *in vitro* samples.

A total of eight gene expression maps were generated to visualize the expression patterns in a global context (Fig. 13). Similarly to VACV early gene expression [108], MOCV shows expression predominantly within the left and right ends including the ITRs. Mirror images of the peaks on each end depict the complementary nature of the ITR's. The central portion of the genome showed fewer peaks and suggested limited expression of genes in this region. Moreover, the extended assay, which included time points from 12 h up to 14 dpi, showed essentially no difference with the first assay. Taken together, all results indicated that MOCV's gene expression is limited to early genes.

In order to further evaluate MOCV's transcriptome quantitatively, gene counts on each time point were associated to the predicted expression class. MOCV's promoters have been carefully evaluated and classified based on homology information and computational predictions [17]. An arbitrary value of 10 counts per gene throughout the time course was used as the cut-off for gene expression. The incremental amount of transcripts in the first hours of infection was compatible with the expected kinetics of gene expression, and previous description of MOCV early events. Nevertheless, detection of transcripts as a plateau in later time points represents an interesting but unclear finding.

The gene expression profile confirmed the early nature of 60 predicted genes (Fig. 14). It also showed quantitatively the overwhelming amounts of early transcripts compared to the PR genes; nevertheless, detection of nine PR genes complicated the interpretation of our results. In order to reach a more definitive conclusion, a careful examination of these nine PR genes was required. The process known as transcriptional read-through identified in several organisms and viruses is one possibility that could explain PR detection by RT-

PCR and deep-sequencing [304-306]. In fact, this process have been shown for VACV [297], and is prevalent due to the overlap and closeness of most genes. In order to evaluate this possibility, a closer look into the context of each of the PR genes detected was needed. MochiView was again used to visualize and evaluate the tiling of reads and their distribution over those nine PR genes in the 120 hpi sample. This dataset was selected because it matches the time PR genes were detected. Evaluation of the upstream region for all PR genes detected showed the presence of an early gene and the possibility of overlapping transcripts for all, except one gene (Table 5 and Fig. 15). The exception was gene MC014R, which was annotated with a right orientation. The vast majority of transcripts of these regions belong to the opposite strand. Nevertheless, by focusing on this region, the expression of the putative gene MC014.1L was confirmed. As depicted from the expression pattern transcription of this gene occur from the negative strand. Identification and expression of MC014.1L may also explain detection of the predicted late gene MC013L, another PR gene detected in our assay. In summary, the results shown here provide additional evidence that transcriptional read-through may be responsible for false-positive detection of gene expression by traditional methods.

Functional assay addressing PR gene expression

In order to rule out PR gene expression from a functional perspective, plasmids expressing reporter genes under VACV promoters were used. For this experiment, compatibility of VACV promoters with MOCV transcription machinery was a concern. The compatibility of early VACV promoters with MOCV machinery has been recently demonstrated using early-late (synthetic) promoters [307], but not for authentic PR promoters. To address this, a construct containing *gfp* under the control of MOCV's PR

promoter was used and tested for its compatibility with VACV's transcription machinery (Fig. 17). This compatibility has been previously suggested due to sequence similarities between MOCV's and VACV's promoters, and the homology found for several transcription-related enzymes [17, 289]. To select MOCV's promoter for this reporter plasmid, three criteria were used: a) the promoter should be a predicted PR, b) must have been detected by q-RT-PCR, and c) with no evidence expression in our RNA-Seq experiment. The MC095 promoter was selected using these criteria, and cloned to express GFP. The infection and transfection experiment using this novel plasmid confirmed that MOCV's promoter is indeed functional and compatible with VACV and ERPV transcription machinery. This implies that PR promoters might all be compatible through poxviruses, or at least in several Orthopoxviruses. More importantly, pre-incubation of cells before and during infection with a DNA replication inhibitor (AraC) resulted in complete inhibition of GFP expression. This demonstrated that promoter pMC095 is post-replicative (PR), for which DNA replication is required. This result validated our assays and also showed the compatibility of both VACV and MOCV PR transcriptional machineries for the first time.

The results for the functional assay of intermediate or late gene expression are summarized in Table 6. The data shows no evidence of intermediate or late gene expression in any cell lines tested. All levels of LUC, with the exception of the VACV control, were similar to background levels. Furthermore, VERO cells defective in IFN pathway [296] did not show any increment in luciferase nor expression of *gfp*.

The failure to detect intermediate transcripts, and absence of gene expression in trans should be analyzed separately since they are in different contexts. First, a lack of PR gene

expression in MRC5 cells is better explained by the absence of DNA replication demonstrated elsewhere [287]. The viral genome is packaged as a nucleoprotein complex within the viral core. It is believed that uncoating of the genome is required for both DNA replication and intermediate gene expression. This is supported by *in vitro* experiments showing the requirement of a naked genome for PR gene expression [67]. One model for genome uncoating suggests that viral DNA in the form of desoxynucleoprotein is released from the core and transported into specific loci within the cytoplasm. These loci contain viral proteins, DNA, and newly synthesized viral RNA. Within these viral factories, it has been suggested that a) early viral proteins are able to modify the viral core in a way that exposes the viral DNA for replication and PR gene expression; or b) that viral proteins are able to alter the specificity of the viral polymerase toward PR gene expression [308]. For MOCV, it seems that viral uncoating does not occur and consequently, there is no naked template for intermediate gene expression. Moreover, DNA replication, which is required for PR gene expression, does not occur. Consequently, newly synthesized DNA is unavailable as a naked template for PR gene expression [309].

Studies of VACV replication have revealed several requirements for DNA replication and gene expression. The VACV B1 kinase is a serine/threonine viral kinase packed within the virus [93]. This protein has been associated to an important immune-evasion role by targeting BAF. BAF is a DNA binding protein and inhibits DNA replication for VACV [95]. MOCV has no B1 homolog, and has been suggested as an explanation for MOCV's inability to replicate its DNA *in vitro* [17]. A model in which MOCV compensates using host kinases (VRK1 and VRK2) has been suggested [94].

Nevertheless, this does not explain the absence of intermediate gene expression in trans shown here.

By using plasmids with PR promoters, the requirements for DNA replication are bypassed [67, 94]. The plasmids function as naked templates readily available for the virus transcription machinery. The inability to express the reporter genes in trans suggests that the intermediate translation machinery is incomplete or insufficient. In this scenario, one or more transcription components might be insufficient to initiate intermediate gene expression. Our finding that less than 2% of the total extracted RNA corresponded to viral transcripts is compatible with this model specially when contrasted with the 25-50% of viral RNA found for an VACV infection [297]. This is further supported by the absence of a host's shut-down and the recovery of the whole monolayer. The components of the intermediate transcription machinery include the RNA polymerase-capping enzyme complex, VITF-1 (E4) VITF-3 (A8/A23) viral transcription factors, and several host factors (See literature review). Nevertheless, the requirement for a functional B1 kinase for intermediate gene expression is highlighted again for gene expression in trans [94].

Transcriptome snapshot from tissue and generation of expression map

The gene expression map derived from tissue provides a holistic view of an efficient viral cycle. In contrast with the *in vitro* transcriptome, gene expression is not restricted to the ends of the genome, and spans into the central genomic region, which contains most essential and morphogenesis-related genes (Figure 18).

The *in vitro* and *in vivo* transcriptome datasets were used to generate an MOCV gene expression map (Figure 19). By subtracting the early genes identified *in vitro* from those made *in vivo*, additional expressed genes were identified. A total of six genes did not meet our gene expression criteria. Failure to detect these six genes can be explained by the annotation strategy used for MOCV, in which stringency was reduced in order to produce the most complete annotation set [17]. This gene expression map will be a useful as a reference to expand our current knowledge and understanding of MOCV transcription.

Conclusions

MOCV is one of the poxviruses with clinical relevance, affecting mainly children and immunosuppressed patients. Our understanding of this virus has been limited for a lack of an *in vitro* system or animal model to do research. Here, new insights into MOCV gene expression are provided from *in vitro* and *in vivo* samples using RNA-Seq. We have confirmed the early nature of 60 MOCV genes *in vitro* and detected expression of 97 additional genes *in vivo*. Detection of the predicted gene MC014.1L has been confirmed, providing evidence that this method is useful to confirm gene expression.

The identification of the read-through mechanism for MOCV has significant repercussions for research. Detection of PR gene expression should be evaluated by taking into account this mechanism. Strategies such as paired-end sequencing and functional gene expression could prove useful in this scenario.

The location of the MOCV block should be re-evaluated. Identification of the MOCV transcriptome as early in the MRC5 cells suggested that the MOCV block occurs before

DNA replication. Lack of DNA replication for MOCV *in vitro* has been the most supported model. Nevertheless, our data suggest that an insufficient early gene expression might contribute to MOCV's block *in vitro*. Other possibilities that would need to be addressed are: a) the need for host factors, or b) the effect of the host's antiviral mechanisms. A reductionist and systematical evaluation of each one of these possibilities would be useful to determine the cause of MOCV early block.

Finally, the transcriptome generated from infected tissue could be used as a reference for an efficient MOCV expression, thus revealing the virus signature of a successful viral cycle. The host transcriptome also provide insights into the viral and host interaction *in vitro* and *in vivo*.

Chapter 4: Identification of host-range genes responsible for MVA's attenuated phenotype.

Summary

MVA is a strain of VACV used as a smallpox vaccine, as a vector against several infectious diseases, and for viral oncolysis. Its attenuation in chicken embryonic fibroblasts (CEF) was accompanied by several deletions and mutations throughout the genome. To identify the genes responsible for its host-range restriction, whole-genome sequencing and comparative genomics were done on several recombinant MVAs (rMVA) that were generated by introducing long DNA sequences derived from a non-attenuated strain and selected by marker rescue. Several rMVA recovered intermediate phenotypes that ranged from the attenuated parental MVA to the wild type Ankara. The 44/47.1 rMVA acquired similar replication properties as this non-attenuated strain. By comparative genomics, several genes were selected for deletion from 44/47.1 rMVA, and the contribution to plaque formation and replication of the genes were evaluated. O1 was confirmed to be important in plaque formation. Also, C17, F5 and C11 were individually identified as important for plaque formation and replication, whereas C11 was sufficient for extending MVA's host-range into mammalian cells.

Introduction

MVA is an attenuated VACV strain used as a smallpox vaccine [310] and a potential vector against multiple infectious diseases[12-15, 310] and for viral oncotherapy [311, 312]. Re-engineered MVA mutants have been used to induce viral oncolysis while maintaining its safety profile [313-316].

MVA's parental virus was isolated from a horse lesion in Turkey and extensively passaged in chicken embryonic fibroblasts (CEF) causing several deletions and mutations throughout the genome [11, 29, 317]. During this process, its ability to replicate in most mammalian cells was lost, reducing its host-range to a few cell lines which includes CEF cells. MVA's inability to replicate in HeLa cells was demonstrated by EM showing accumulation of IVs and dense spherical particles [318]. The inability to produce progeny efficiently provided the safety profile required for its use in humans. [319, 320]. Whole-genome sequence of MVA's genome and comparison to the parental virus genome demonstrated the changes suffered during the attenuation process. The changes included six major deletions that reduced the genome by ~12% [29, 321]. The six deletions are located in the distal and variable portions of the genome (Figure 21).

Interest in identifying the gene or genes responsible for MVA's attenuation led several groups to address this question in multiple ways. An attempt was carried out by generating multiple overlapping cosmids using a non-attenuated VACV strain and insertion of these long constructs into MVA. [204]. The rMVAs generated with a single cosmid recovered a partial phenotype. Nevertheless, a virus generated with two overlapping cosmids (virus 44/47.1 rMVA) recovered the ability to form large plaques and replication in mammalian cell lines, similarly to the parental, non-attenuated strain. The 44/47.1 rMVA phenotype indicates that all genes responsible for MVA's replication and plaque formation were repaired. This experiment also confirmed that the major host-range determinants were located in the left side of the genome. Other approaches have been attempted by repairing the six major deletions of MVA [322]. Systematic repair of those deletions showed that reinsertion of the deleted sequences was insufficient to rescue

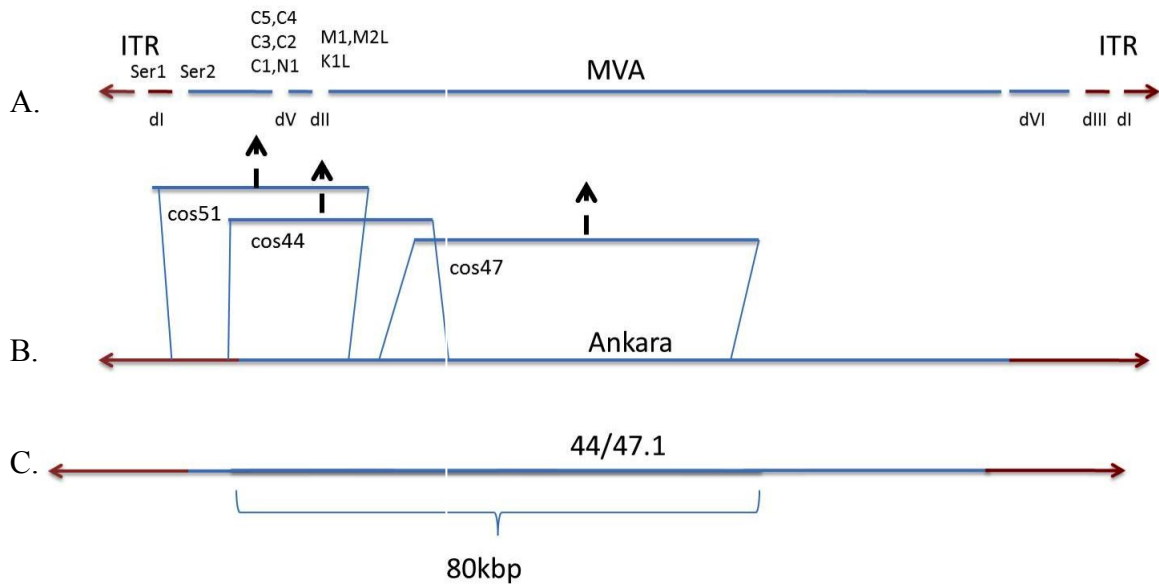


Figure 21. Schematic representation of MVA's deletions and overview of marker-rescue experiments. Panel A depicts MVA six deletions and immune-evasion genes identified within those deletions. Panel B shows the strategy used by Wyatt et al (1998) to rescue MVA's host-range. Cosmids (cos51, cos44, cos47) were generated from a non-attenuated strain (Ankara genome). Arrows point to the regions of homology in MVA where the cosmids were theoretically inserted. Panel C shows how both cos44 and cos47 overlaps an 80 kbp region in 44/47.1 rMVA.

the phenotype [322]. This indicated that mutations outside the deletion also account for MVA's host-restriction.

Here, we took advantage of current sequencing technology to determine the genes repaired in many of the rMVAs generated by Wyatt and co-workers [204], and associated the contribution of these genes to the recovered phenotype in several mammalian cells. A set of genes repaired in the 44/47.1 rMVA were selected as potential host-range determinant and deletion mutants of these genes were generated to evaluate their contribution to plaque formation and replication. By dissecting the contribution of each gene to plaque formation and replication, the number of potential host-determinants was narrow down to a few genes. Moreover, this approach led us to the discovery of the first gene outside of MVA's deletions responsible for its host-range restriction in mammalian cells.

Materials and Methods

Plaque formation assay and clonal purification

Crude preparations of all rMVAs (44/47.1 rMVA, 44.1 rMVA, 44.7 rMVA, 51.1 rMVA and 51.2 rMVA) were kindly provided by Linda Wyatt. Procedures for plaque formation assays, clonal purification, amplification and virus purification were done following Current Protocols Unit 5.12 and 5.13 [261, 323].

Plaque purification of all rMVAs was done in BS-C-1 cells, while plaque purification for the 44/47.1 rMVA deletion mutants was done in CEF cells. Medium was prepared by adding FBS, complemented with 1% L-glutamine and 1% P/S. Before infection, cells were pre-incubated with 2% FBS-EMEM (infection medium), and serial dilutions of each

virus used for the infection. Viral adsorption was allowed for two hours at 37°C, 5% CO₂ (regular incubation conditions), followed by replacement of the medium with an overlay of 0.5% methyl cellulose, +5% FBS (methyl cellulose overlay) or 10% FBS-EMEM (growth medium). Initial confirmation of plaque sizes for all rMVAs was done in BS-C-1 cells using a methyl cellulose overlay (Figure 22). Staining of infected cells was carried out 36 hpi or 48 hpi by fixing cells with a methanol:acetone (1:1) solution and immunostaining using VACV antiserum (provided by Dr. Linda Wyatt) and protein G conjugated with peroxidase (Pierce, Cat. 32400).

For virus amplification, infected CEF cells were incubated for at least 48 h and evaluated for CPE. The infection and harvesting procedure was repeated sequentially until cells from ten T-150 flasks were infected for each rMVA or deletion mutant. Half of the viral crude preparation was used for purification using a single sucrose cushion. The other half of the crude preparation was used for higher-quality viral purification that consisted of one sucrose cushion and two sucrose gradients. Titers of all viruses were determined by plaque assay using immunostaining techniques in CEF cells.

Evaluation rMVAs by EM

EM was used to evaluate the morphologies of each rMVA. HeLa cells were infected with an MOI of 5, and incubated at standard conditions for 24 h. Samples were fixed and prepared for EM. All EM staining and evaluation were kindly done by Andrea Weisberg.

DNA extraction and electrophoresis of digested genome fragments

DNA was released from purified virions using a solution containing 10% SDS, 60% glucose, 50 mM TRIS, pH 7.8, and 10 mg/ml proteinase K [323]. A phenolic extraction

(phenol:chlorophorm:IAA, ratio 25:24:1) was done twice for the removal of proteins. DNA precipitation was carried out with ethanol, and DNA eluted with water or EB Buffer (Quiagen Cat. 19086). Quantification of DNA was done with a NanoDrop device (Thermo Scientific). Aliquots of extracted DNA from each rMVA was digested with restriction enzyme HindIII and run on an 0.8% agarose gel at 10 volts at 4°C overnight (Figure 23) [324]. The gel was stained with ethidium bromide and visualized and recorded using the Carestream Image Station 4000MM.

Library preparation and pyrosequencing

The non-digested genomic DNA for each rMVA was also quantified using Picogreen assay (Life Technologies, Grand Island, NY). Separate libraries were constructed using Rapid Library Preparation Method Manual (October 2009) GS FLX Titanium Series (Roche, Branford, CT) and Paired End Library Preparation Method Manual – 3kb Span (October 2009) GS FLX Titanium Series. Each library was processed using emPCR Method Manual – Lib-L MV (October 2009) in separate emulsion reactions with the fragment library being combined with like samples. The paired-end sample was loaded on a single lane and the fragment sample was loaded in two lanes of an 8-region 454 GS FLX Titanium sequencing run. Library construction and initial *de novo* assembly was done by Rocky Mountain Team: Martens C, Bruno D, Porcella SF.

Genome assembly and gap closure

A *de novo* assembly strategy was used to generate all contigs (Fig. 4). Some genomes were fragmented in up to seven different contigs. Physical mapping was carried out using an in-house script coupled with Nucmer software [325]. Since these rMVAs were generated using an MVA backbone and the inserts were derived from a non-sequenced

virus, several different genomes (MVA, Lister, Copenhagen genome sequence) were used as references to find the consensus order of the contigs. After determining the order of all contigs, assembly of the drafts sequences, generation of the opposite ITR and identification of the gaps were done. Primers flanking each gap were designed for PCR and Sanger sequencing. The sequences derived from each gap were used to complete the drafted genomes. The final genome drafts were used as their own reference to remap all reads into a final most accurate genomic sequence.

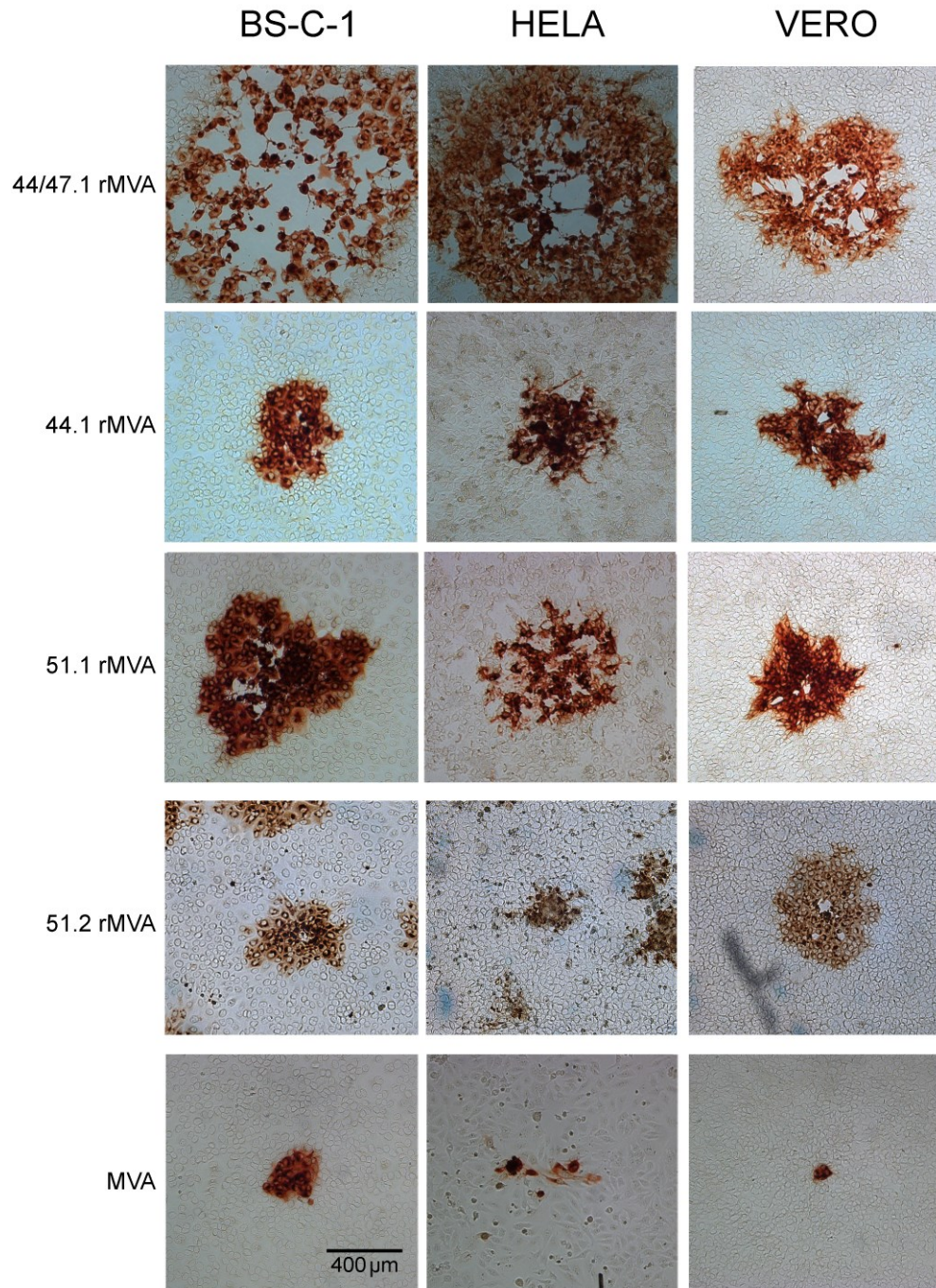


Figure 22. Initial characterization of plaques formed by MVA and the rMVAs in mammalian cells. rMVAs were evaluated for their formation of plaques. The assay was done in three mammalian cell lines (BS-C-1, HeLa and VERO) showing differences in morphology and size at 48 hours post infection.

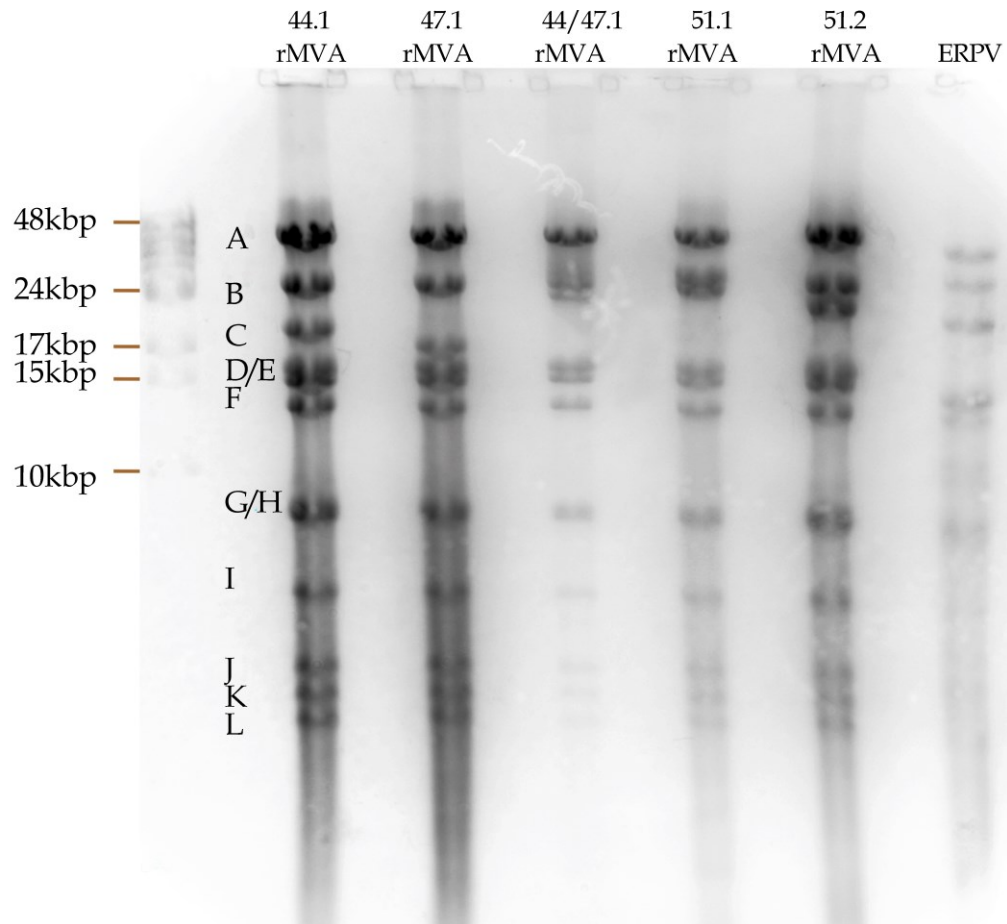


Figure 23. Restriction analysis of the rMVA genomic DNA demonstrated migratory shift of band “C”. The genomic DNA for each rMVA was digested with the restriction enzyme HindIII overnight at 37°C. The digested DNA was then loaded on a 0.8% agarose gel and run at 10V for 24 hours. The gel was stained with ethidium bromide. Changes in migration of the HindIII C fragments were observed. Additionally, the ERPV genome was also run in parallel (see chapter 2).

Multiple genome alignment and genome annotation.

All five rMVAs and the MVA's genome were aligned using ClustalW2 [326] under NIH's Linux High-Performance Computing Cluster. Results were imported into Geneious Software (Biomatters) to visualize the alignment. Additional genome sequences were downloaded from www.poxvirus.org, which included VACV-Lister_107 (Accession number DQ121394), VACV-CVA (Accession number AM501482), Acam2000 (Accession number AY313847), Acam3000 (Accession number AY603355), VACV-Cop (Accession number M35027). All genomes and the rMVA's genome sequences were re-annotated using Acam2000 as the reference. All translated ORFs were compared to the protein sequence of Acam2000 using NCBI's BLAST tool. A table with the ORF's number, VACV-Cop nomenclature and size was produced to compare all viral proteins (Suppl. Table 1).

Selection of candidate genes

The virus 44/47.1 rMVA was determined to have the most number of genes repaired, and was used for the selection of the host-range candidates. Candidate genes from 44/47.1 rMVA were selected using three criteria: a) genes in which truncations were repaired, b) genes re-inserted within MVA's deleted region, or c) mutated genes with a known immune evasion role. From the selected genes, seven were located outside MVA's deletion (C9L, C17L, F11L, F5L, O1L, C11R and C10L). Thirteen other selected genes were inserted within the deletions. Genes C12, C13, C14, C15 were repaired within deletion I, and K1L, M2L, M1L, N1L, C1L, C2L, C3L, C4L, and C5L within deletions V and II. A schematic representation of all rMVAs and mutations is shown in Figure 24.

Generation of GFP constructs and 44/47.1 rMVA deletion mutants

To generate deletion mutants from the 44/47.1 rMVA, flanking regions for each candidate gene or genes were selected. In order to cover a greater extension, some genes were deleted in clusters (two or more genes at a time). A three-fragment cassette was designed per gene, with flanking sequences to facilitate homologous recombination (Figure 25). The distal fragments corresponded to flanking regions homologous to 44/47.1 rMVA sequences; and the central fragment corresponded to the GFP gene under the control of the early/late synthetic VACV promoter [327]. Primers were designed to allow overlapping PCR and annealing of the fragments. CEF cells were infected with 44/47.1 rMVA at an MOI of 0.05. Infected cells were transfected with 2 µg of the construct using Lipofectamine 2000 (Life Technologies, cat. 11668027) following the manufacturer's instruction. After the second round of clonal purification, single plaques showing GFP expression were purified and amplified as described previously. All deletion mutants were verified by PCR and Sanger sequencing.

Plaque formation assay for the 44/47.1 rMVA deletion mutants.

Three mammalian cell lines (HELA, VERO and BS-C-1) were selected for the initial plaque formation screening. Serial dilutions of each deletion mutant were used for the assay. GFP positive plaques were visualized at 24, 36, or 48 hpi using a fluorescent microscope, and images were captured using the same objectives. Brightness of the GFP plaques was adjusted for visualization purposes.

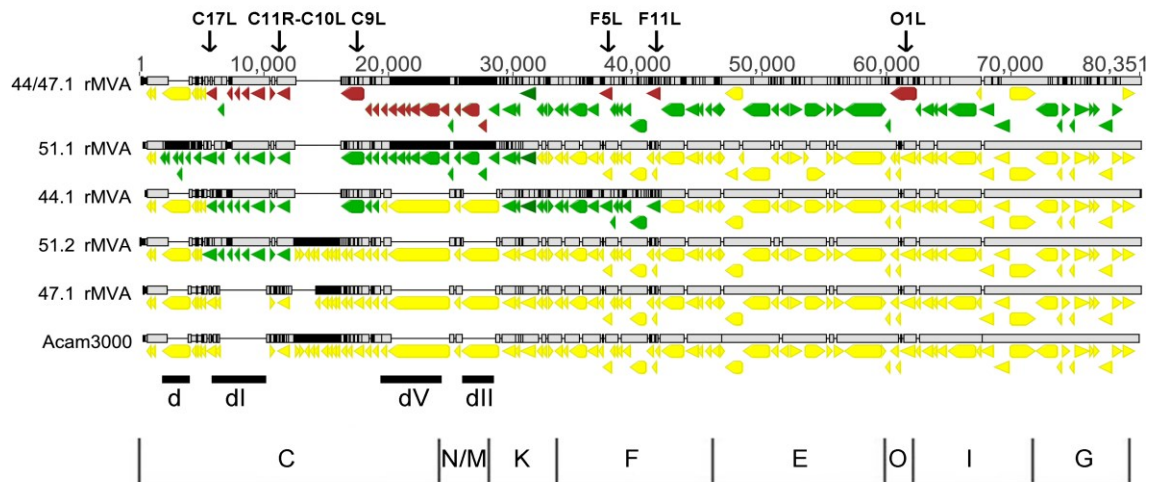


Figure 24. Alignment of the left-termini for all rMVAs and location of the selected candidate genes. All rMVA genomes (black lines) were aligned and visualized with Geneious. Acam3000 genome was included to identify the mutations and insertions in the others rMVA's. Genes that differ to Acam3000 (green arrows). Genes selected for screening were also identified (red arrows). The region indicated with a “d” represents additional genes not present in Acam3000. dI, dV and dII regions indicate the location of MVA's deletions.

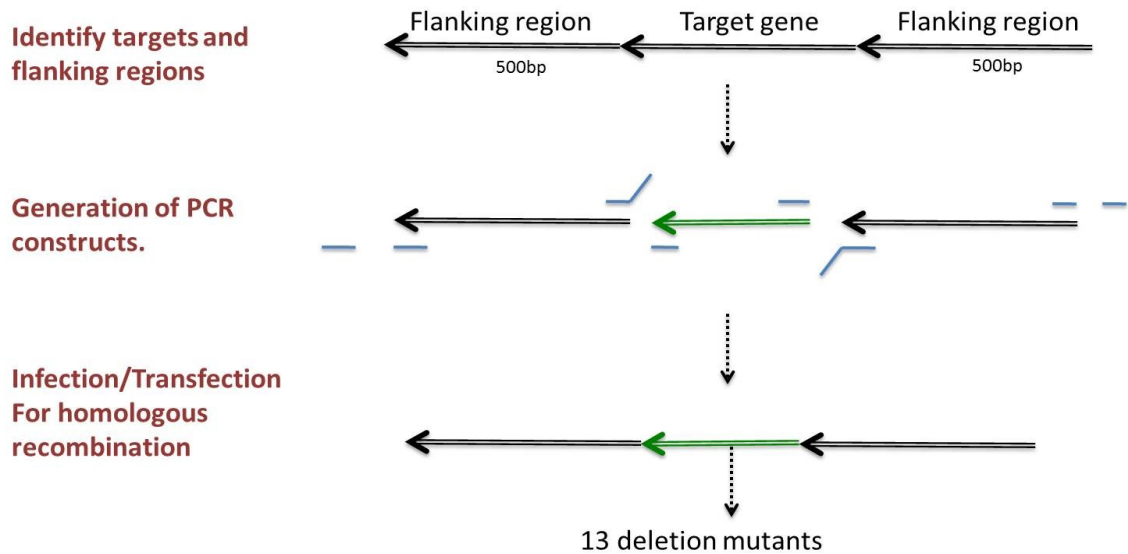


Figure 25. Schematic representation of the gfp-cassettes used to generate the 44/47.1 rMVA deletion mutants. To design the constructs, flanking regions were identified around the target genes. Primers were designed for each flanking region, with internal primers that overlaps with a pre-designed gfp cassette. Additional primers were designed to verify the inserts by PCR and Sanger sequencing. The selected genes were deleted by homologous recombination and isolated through the expression of gfp as a marker. A total of 13 deletion mutants were generated using this approach.

Virus yields of deletion mutants in mammalian cell lines

Virus yields of each deletion mutant were measured by a high-throughput method based on GFP detection using a flow cytometer. This method consists of a three step process in which the first step consists of infecting the cells to evaluate virus growth. To minimize the effect of virus spreading, an MOI of 3 was used, followed by virus adsorption for 2 h. Each well was washed twice with 1X PBS before adding growth medium. Incubation was allowed for 24 h. For harvesting the infected cells, the medium was replaced by infection medium, followed by 3 freeze and thaw cycles and sonication as described in previous methods. The second step consisted of infecting S3-HeLa cells with serial dilutions of each virus in a 96-well configuration. Infection and incubation of S3-HeLa cells was in Spinner media (Quality Biological, Inc. Cat.112-038121), and AraC (80 $\mu\text{g}/\mu\text{l}$) to limit the viral cycle to early gene expression, allowing translation of the encoded GFP gene. Several controls were done before using the technique, and compared to traditional immunostaining techniques (data not published). Medium, incubation time and reagents to design this assay were adopted from a related protocol [328]. The FACSCalibur (Becton-Dickinson) cytometer coupled with a plate-reader module was used to gate for GFP and count all events. FlowJo software (TreeStar, ver. 8.5.3) was used to analyze all output from the flow cytometer. The statistical data was then expressed as fold increase calculated by dividing the GFP-positive counts at 24 hpi by the input measured at 2 hpi.

Trans complementation assay of MVA

PCR products encoding genes C11 and F11 were cloned into TOPO vector under E/L synthetic promoters. An additional plasmid kindly provided by Zhilong Yang with no promoter was used as the negative control. VERO and BS-C-1 cells were infected with

MVA and transfected 2 hpi with the plasmids. Infected cells were incubated at 37°C, 5% CO₂. Infected cells were harvested at 24 hpi, and the virus titer determined by immunostaining using CEF cells.

Simplified method to generate replicative-competent MVA for mammalian cell lines

A simplified, one-tiered method allowed extension of a replication-incompetent virus to grow in mammalian cells. The method was based on our discovery that insertion of a DNA construct containing the vgf gene derived from a replication-competent virus was capable of extending the host-range of MVA into mammalian cells. For this, a ~800 bp region containing the vgf gene from the replication-competent virus 51.2 rMVA was amplified by PCR. Flanking regions were chosen to include all mutations related to vgf (promoter and 3'UTR) and to promote homologous recombination into MVA nucleic acid. A second construct containing the same vgf region from a different replication-competent virus, VACV-WR, was generated to show a second example of this discovery and the usefulness of this procedure. In this example, a 769 bp region containing the vgf gene from VACV-WR was amplified, allowing flanking regions for homologous recombination. To ease the acquisition of these sequences, each PCR product was inserted into a TOPO plasmid and used in a modified infection/transfection procedure. Plasmids containing the exogenous vgf gene are pJM5, pJM8, and pJM11. The nucleic acids inserted into MVA is amplified with forward primer AGCAAAGAA-TATAAGAATGAAGCGGT and reverse primer ACCCACTGTATTCATTTTCAAG-GTA when using 51.2 rMVA nucleic acid as the template; or with forward primer ATCATTTTAAACAGCAACACATTCAATATTG and reverse primer ACCCACTGTA-TTCATTTTCAAGGTA when using VACV-WR nucleic acid as the template. Plasmids

pJM5 and pJM8 include nucleic acid from 51.2 rMVA, while plasmid pJM11 contains the nucleic acid derived from VACV-WR.

A non-permissive cell line for MVA (in this case, VERO cells) was infected with MVA and transfected with each plasmid independently. The construct containing the vgf region was used as a selection marker allowing selective growth of the recombinant mutant. Infected/transfected cells were incubated overnight and harvested. To maximize recovery of recombinant viruses and reduce the amount of the parental strain (MVA), the harvested infected cell preparation (crude viral sample) was used to infect again another monolayer of non-permissive cell lines for MVA (again VERO cells). Half of the crude viral sample was used to infect VERO cells (non-permissive condition for MVA). In this second round, the infection medium was replaced with 0.5% methyl cellulose overlay 2 h post infection. Foci with clumped cells were observed as early as 24 h post infection and served as an indication of the presence of the recombinant virus. It also facilitates the clonal purification process. Longer incubation may be used to allow growth of the foci using adherent plates. Serial infection and harvesting was repeated using non-permissive conditions such as VERO cells to ensure elimination of the replication-incompetent virus. This process may be repeated as desired to reduce the likelihood of contamination with the parental virus. The final viral clone was amplified in BS-C-1 cells and used for DNA extraction and sequencing verification.

Results

Confirmation of rMVA plaque formation ability

All rMVAs were kindly provided by Dr. Linda Wyatt in the form of crude viral preparations. Each virus was purified and amplified to generate new viral stocks (Figure

3). All viruses were tested for their ability to form plaques in one human cell line (HeLa cells) and two African green monkey cell lines (VERO and BS-C-1). Previous plaque formation reports were confirmed, in which 44/47.1 rMVA formed the largest plaques (Figure 22), while the other rMVAs formed intermediate or small plaques in all three mammalian cell lines. The intermediate phenotypes suggest that plaque formation is regulated by the accumulative effect of several genes, and that viruses 51.2, 51.1 and 44.1 rMVA recovered some of those gene involved in plaque formation and replication.

Evaluation of rMVA morphogenesis by EM

MVA is an attenuated virus that lost the ability to replicate efficiently in most mammalian cell lines. Characterization of MVA in non-permissive cells by EM revealed that the block occurs late in the viral cycle manifested by the accumulation of IVs and dense spherical particles [329] [318]. In order to determine if a defect in morphogenesis accounts for the different phenotypes, HeLa cells were infected with each rMVA and evaluated by EM. MVA and Ankara virus were also included as controls. Preparation of infected monolayers for electron microscopy and capture of images was kindly done by Andrea Weisberg. During an infection with wild type VACV, IVs and brick-shaped MVs predominate. However, in cells infected with MVA, there are dense spherical particles instead of MVs. In contrast, all of the rMVAs had a mixture of dense spherical particles and MVs (Fig. 26). The ratios of MVs to spherical particles were directly proportional to the abilities of the rMVAs to produce infectious virus (Table 8). Thus, 44.1/47.1 and 51.2 had the highest ratios, while 47.1 and MVA had the lowest.

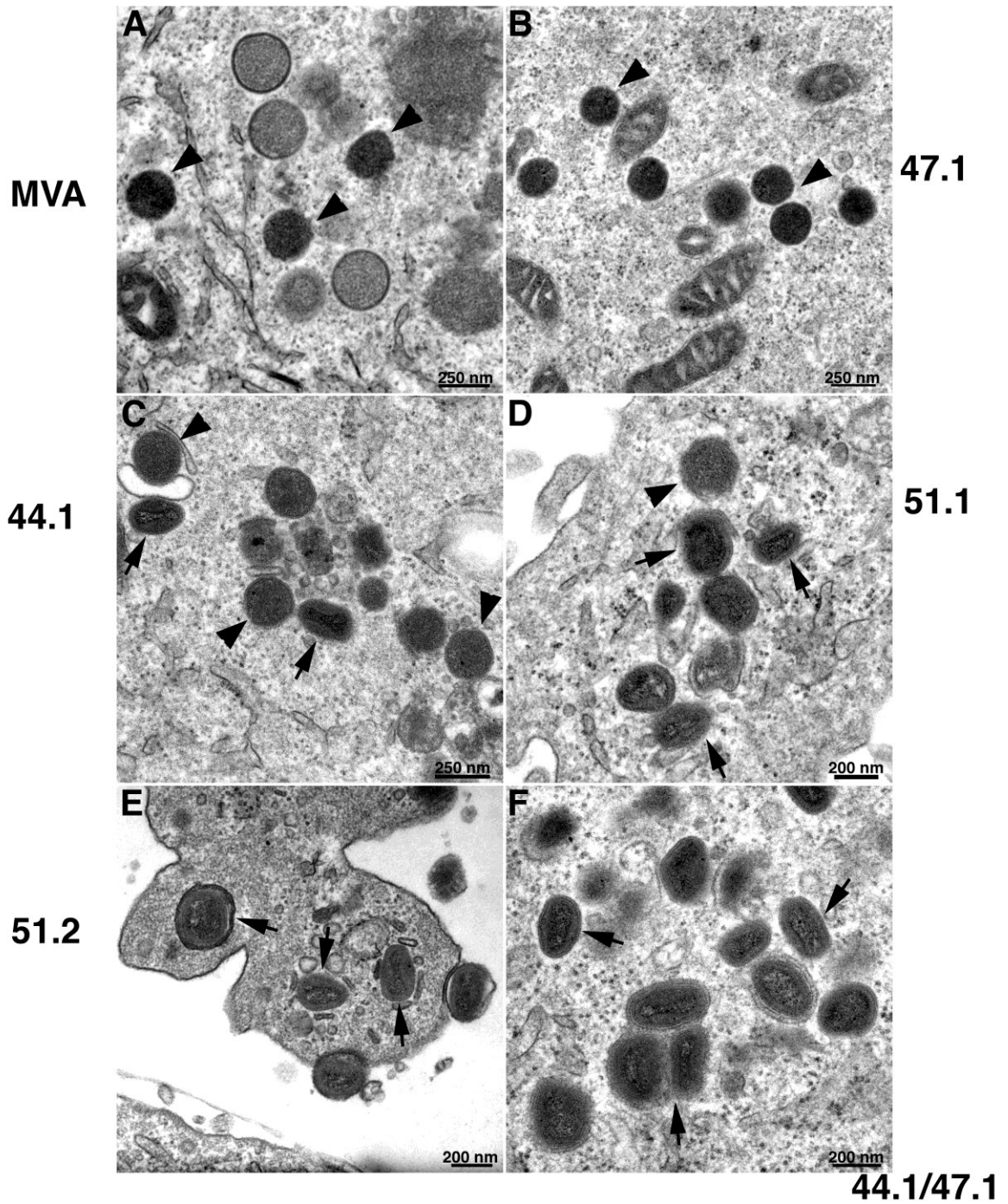


Figure 26. Evaluation of virus morphologies in HeLa cells at 24 hpi. A) MVA, B) 51.2 rMVA, c) 44.1 rMVA, D) 47.1 rMVA E) 51.1 rMVA, F) 44/47.1 rMVA, and G) Ankara virus.

Table 8. Quantification of mature and dense particles for the rMVAs in HeLa cells.

	Dense Particles	Normal Matures
MVA	61 (25/25)	0
47.1	81 (23/25)	26 (8/25)
44.1	167 (24/25)	107 (19/25)
51.1	51 (19/25)	88 (18/25)
51.2	9 (9/25)	174 (24/25)
44.1/47.1	16 (7/25)	420 (24/25)

HeLa cells were infected with an MOI of 5 with each virus and their morphology evaluated by EM. Cells were fixed 24 hpi and cells quantify by the presence of each particle.

Identification of major recombination events on the left portion of the genome

Wyatt and co-workers demonstrated that one or more host-range genes were located on the left terminal portion of the genome when MVA's replication was rescued with long cosmids [204]. Identification of the inserted genes requires solving several challenges. First, mosaic-like recombination occurs with long constructs, making it erroneous to assume the insertion of the whole cosmid. Moreover, since the cosmid contains sequences similar to both ITRs, insertion could also have occurred in the right side of the genome. To confirm the location of the insertions, genomic DNA from each rMVA was digested with restriction enzyme HindIII. Electrophoresis of the digested DNA is shown in Figure 23. The HindIII C band corresponds to the left-most region of the genome, while bands A and B correspond to the right portion of the genomes. Migration of HindIII was slower for 44/47.1 rMVA and 51.1 rMVA, suggesting the acquisition of long sequences. Smaller changes were identified for virus 44.1 and 51.2 rMVA. Finally, the 47.1 rMVA shows the fastest mobility for the HindIII C band demonstrating a smaller size relative to the other rMVAs. Nevertheless, migration of bands "A" and "B" show no changes in any of the 5 viruses. This provided evidence that the recombination events occurred exclusively in the left-most side of the genomes for all rMVAs.

Genome annotation and comparison

In order to compare the gene content of the genomes, a non-biased approach to identify genes was needed. For this, a tool called GATU (Genome Annotation Transfer Utility) was used, which performs *de novo* annotation by protein sequence homology [265]. A second round of annotation was done with a broader scope as described in the method. This time all viruses were re-annotated using Acam2000 that has all genes present in all

the viruses analyzed (Table 11 & Suppl. Table 1). This annotation allowed a better understanding of the evolution of the sequences used, and identification of all genes inserted into the rMVAs (Figure 24). Comparison of the sequences inserted into the rMVAs against other VACV genomes revealed that the inserts were more similar to Acam2000 (Table 11 & Suppl. Table 1). All 5 rMVAs and the MVA genomes were aligned using ClustalW2 ran in NIH's High-Performance Computing Cluster (Figure 24). This provided the definitive evidence that all cosmids were inserted in the left genomic region. It also showed that partial insertions occurred. It is worth noting that the 44/47.1 rMVA acquired the longest insertion affecting up to ~80 kbp, repairing deletion I, V and II, up to the "G" gene cluster. Virus 51.1 rMVA acquired a smaller insert that also repaired deletion as 44/47.1 rMVA plus a small cluster of genes near the end of the genome. Partial insertions were also observed for virus 51.2 rMVA and 47.1 rMVA. The cosmid 51 used to generate 51.2 rMVA only repaired deletion I and a few additional genes including C10 and C11. The virus with the smallest insert was 47.1 rMVA for which cosmid 47 modified the "cowpox host-range" region, causing a deletion instead of an insertion. The multi-genome alignment served as the main tool to identify the repaired genes and selected the host-range candidates.

Replication and spreading are distinguishable phenomena.

In order to integrate the gene constellation of each virus to the phenotype, several observations were made. Wyatt et al. [204], showed that some rMVAs formed small plaques, but produced virus yields similar to the parental strain. This is the case for 44.1, 51.1, 51.2, but not 47.1 rMVA. These observations were first confirmed here (Suppl. Figure 2), and by two other groups showing similar viral yield for 44.1 rMVA, 51.1

rMVA and 51.2 rMVA [251, 252]. 51.2 rMVA represented an interesting virus since it replicates in mammalian cell lines with a relatively small region repaired. These observations highlighted the few repaired genes within 51.2 rMVA's genome as potential host-range genes.

Selection and deletion of candidate genes.

Multi-genome alignment was used to compare rMVA's genomes and for the identification of the repaired genes. Figure 24 shows the left portion of all genomes relative to MVA (Acambis 3000). Four out of six major deletions in MVA were located in this region. Virus 44/47.1 rMVA acquired repairs that spans up to 80 kbp, including three major deletions (I, V, II). In order to simplify our search in this broad region, several genes were selected to be deleted from 44/47.1 rMVA. Seven of these genes were located outside MVA's deleted regions (O1, C17, F11, F5, C11, C10, C9). Additionally, there were three major deletions that were repaired in the 44/47.1 rMVA (dI, dII & dV) that included genes C12, C13, C14, and C15 from deletion I; genes C5, C4, C3, C2, C1, N1, M1, M2, and K1. This adds up to a total of 20 candidate genes to screen. DNA constructs to generate deletion mutants were designed with GFP as the marker (Figure 25). Since there were a total of 20 genes to screen, some genes were deleted in groups. By deleting genes in clusters, the number of mutants to generate was reduced to 13. For practical purposes, the following nomenclature will be used for the deletion mutants: vdO1-gfp is an O1 deletion mutant from 44/47.1 rMVA expressing GFP, and so forth. After selection and clonal purification, all deletion mutants were amplified and virus stocks prepared. All mutated sequences were verified using flanking primers to the insert region.

Testing the screening strategy.

In order to test the screening approach, deletion mutant vdO1-gfp was used to infect eight cell lines, to evaluate its plaque formation ability. Viruses 44/47.1 rMVA and MVA were included as controls. The results showed that vdO1-gfp formed smaller plaques in all cell lines when compared to the parental virus 44/47.1 rMVA (Figure 27). Nevertheless, the plaques were still larger than plaque produced by 51.1 rMVA, 44.1 rMVA and MVA. Statistical analysis of the plaque sizes for all cell lines showed that deletion of O1 significantly reduced plaque size in A-549, VERO, BSC1, MA-104, 3T3 and L929 cells (Figure 28), but not in MRC5 or HeLa cells. Based on this initial assay, the strategy to evaluate the role of each candidate gene on plaque formation proved successful, for which a similar approach was used for all other deletion mutants.

Plaque formation is regulated in a modular and cumulative fashion.

In order to evaluate the role of the selected genes in plaque formation, all deletion mutants were used to infect mammalian cell lines and the plaques sizes were compared to those made by 44/47.1-gfp and MVA-gfp. Plaque sizes were evaluated 36 hpi (Figure 29), and statistical analysis used to determine significance in plaque reduction (Figure 30 and Table 9.1). By simple inspection, plaque sizes for all mutants, except for vdC9-gfp, were reduced in size. As expected, MVA-gfp is barely detectable, demonstrating its inability to efficiently plaque and replicate in mammalian cell lines. On the other hand, 44/47.1 rMVA continues to form large plaques in all cell lines. Interestingly, a different pattern of genes involved in plaque formation for each cell line can be observed. For example, the plaque size of vdO1-gfp in HeLa cells is large, but not in BS-C-1 or VERO.

This cell-dependent variability is repeated with the other mutants. An important common feature is that vdF5-gfp formed small plaque in all three cell lines tested. Since plaque sizes vary within each well, statistical analysis of the plaque was required. For these, plaque sizes were quantified and analyzed digitally. In Figure 30, plaque sizes were plotted and compared among each deletion mutant. In order to present this data in a comprehensive way, the effect in plaque sizes were grouped as follows: a) reduction of 50% or more in plaque size, b) less than 50% reduction, c) increase in plaque size, d) no significant difference detected. All values were calculated relative to the 44/47.1 rMVA plaque size of in the same cell line. The results are summarized in Table 9.1 and 9.2. Since our interest is evaluating the genes that provided that strongest effect, they were classified based on the percentage of reduction of plaque sizes. As described previously, dvF5-gfp showed a significant reduction in all three cell lines. vdO1-gfp, and vdC11C10-gfp showed significant plaque reduction in BS-C-1 and VERO, both African green monkey cell lines. vdC17-gfp showed a significant reduction in VERO and HeLa. These results demonstrated that plaque size is determined in a modular fashion, and that deletion of a gene affects virus plaques in a cell-dependent manner. Moreover, intermediate plaque sizes provide evidence for the cumulative role of each one of the genes. Finally, this modularity requires a functional F5L gene for all cell lines tested.

Measuring virus yield for 44/47.1 rMVA deletion mutants

Virus yields for all deletion mutants in mammalian cell lines were determined using a high-throughput flow-cytometry method (see diagram in Figure 31). Several controls were used to test the validity and sensitivity of this approach (data not shown). Two

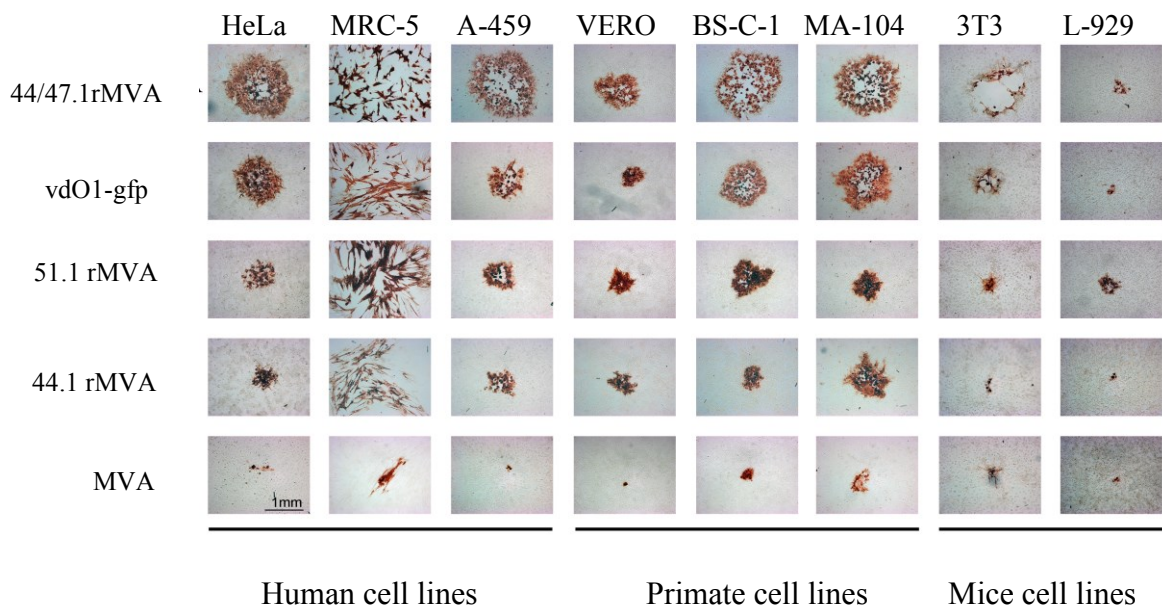


Figure 27. Plaque formation assay using one deletion mutant (vdO1-gfp) to test the strategy. Human, primate and mouse cell lines were infected with vdO1-gfp and plaques compared. Deletion of gene O1 was important for plaque formation in all cell lines tested.

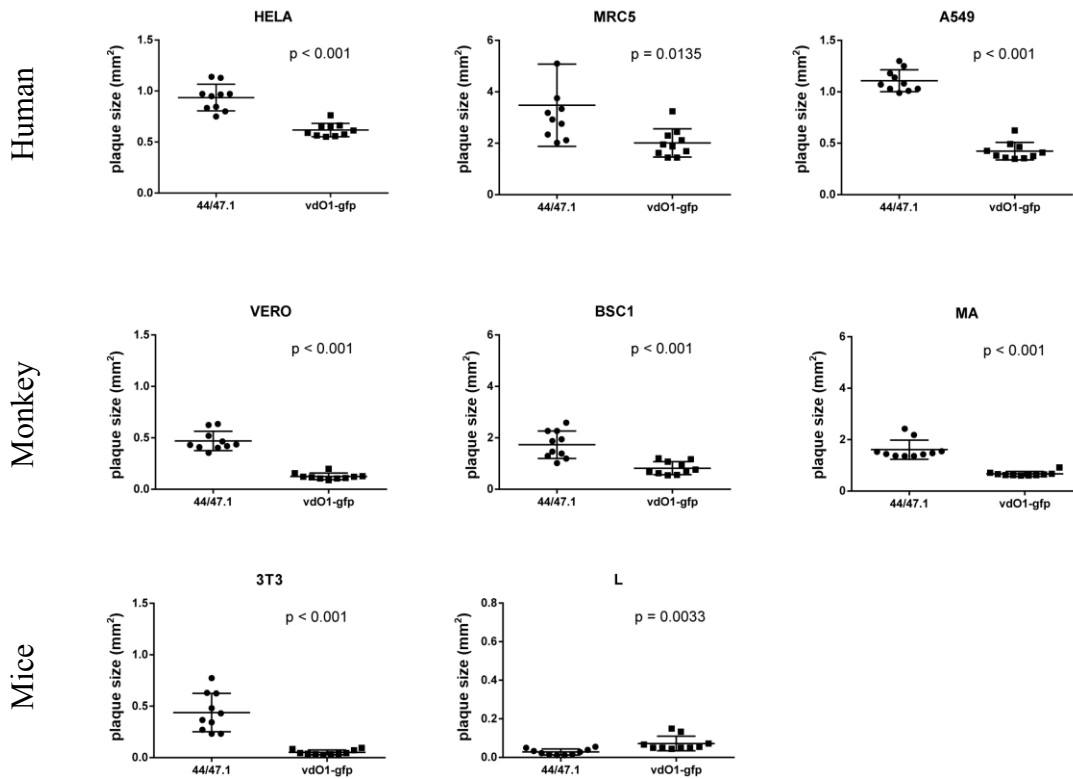


Figure 28. Deletion of gene O1 from 44/47.1 rMVA reduced plaque size significantly in several mammalian cell lines. Since plaque size may not be homogeneous, statistical analysis was done after immunostaining and digital analysis of the plaque sizes. The statistical analysis was done using Student's t-distribution.

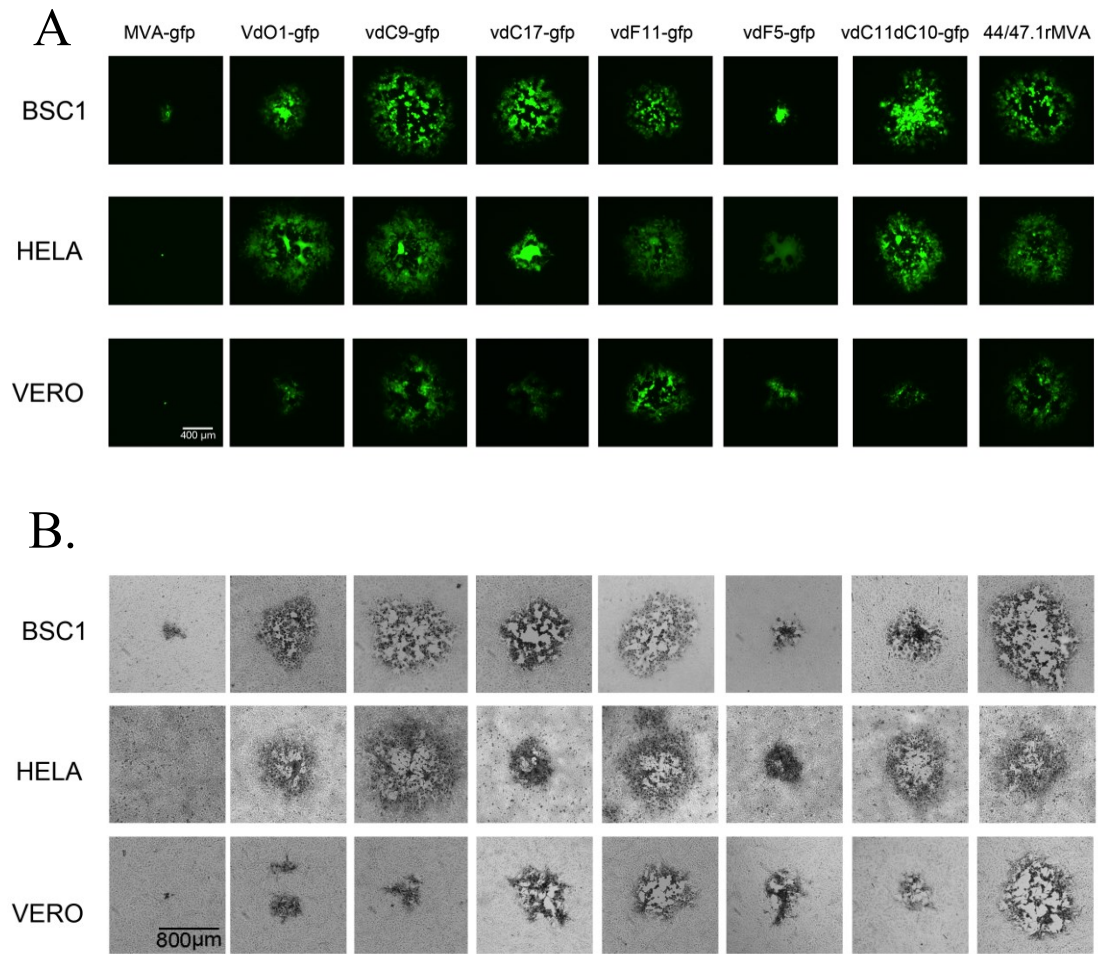


Figure 29. Plaque assay for all 44/47.1 rMVA deletion mutants revealed that plaque size is determined in a modular fashion. Plaque sizes for seven deletion mutants, 44/47.1-gfp and MVA-gfp were compared in one human cell lines (HeLa) and two green African monkey cells (VERO, BS-C-1). Plaque morphologies and sizes are shown (A) under a fluorescent microscope, or (B) after immunostaining. Deletion of F5 affected plaque sizes in all the tested cells lines. The effect of several genes on plaque formation was cell-dependent.

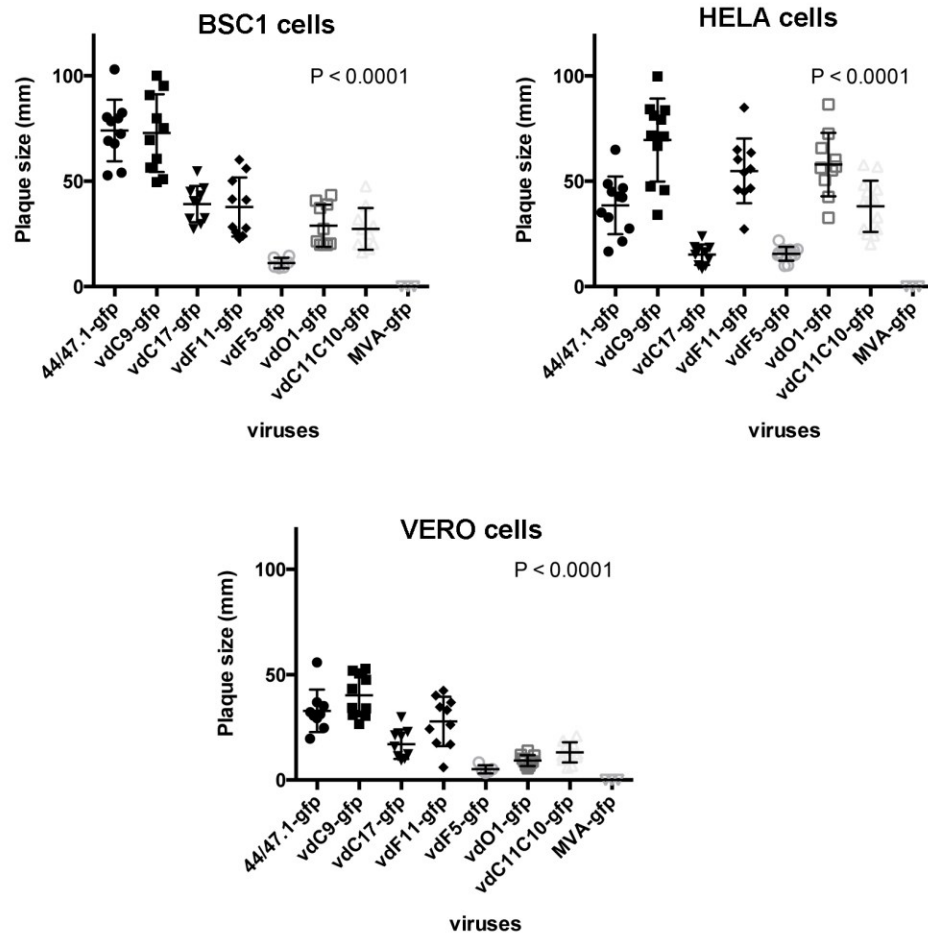


Figure 30. Statistical analysis of plaque sizes for 44/47.1 rMVA deletion mutants. The plaque sizes were analyzed and compared to identify genes involved in plaque formation. Cells were infected with a low MOI and overlaid with methyl cellulose 2 hpi. Cells were fixed at 36 hpi with acetone and methanol (1:1) and immunostained. An ordinary ANOVA test was used to determine the significance among the viruses.

Table 9.1. Results of plaque assay for 44/47.1 deletion mutants.

A		44/47.1-gfp	vdC9-gfp	vdC17-gfp	vdF11-gfp	vdF5-gfp	vdO1-gfp	vdC11C10-gfp
BSC1	Avg. (mm)	74.04	72.82	39.13	37.77	11.19	28.89	27.32
	N	10	10	10	10	6	10	10
	StdDev	14.64	18.46	8.63	13.98	2.48	10.01	9.9
	StdErr	4.63	5.84	2.73	4.42	1.01	3.17	3.13
HeLa	Avg. (mm)	38.58	69.54	15.14	54.87	15.55	57.93	38.13
	N	11	11	10	10	12	10	14
	StdDev	13.71	19.7	4.85	15.35	3.3	15.03	12.16
	StdErr	4.13	5.94	1.53	4.85	0.95	4.75	3.25
VERO	Avg. (mm)	32.86	40.28	17.07	27.85	5.11	9.28	13.17
	N	9	10	9	10	5	10	11
	StdDev	10.06	10.04	7	11.71	1.92	2.62	4.81
	StdErr	3.35	3.17	2.33	3.7	0.86	0.83	1.45

Table 9.2. Results of plaque assay for 44/47.1 deletion mutants organized by the impact in plaque size.

Cell lines	Plaque reduction			
	>50% reduction	<50% reduction	No significant effect	Increase
BS-C-1	O1, F5, C11-C10	C17, F11	C9	-
HeLa	C17, F5	-	C11-C10	O1, C9 F11
VERO	O1, C17, F5, C11-C10	-	C9, F11	-

independent experiments were done and virus yields presented as percentages of the input. The results show that all deletion mutants have a lower yield at 24 hpi relative to 44/47.1 rMVA (Figure 32). The results can be organized in three groups, in which vdO1-gfp, vdf11-gfp and vdC9-gfp have around two-fold reduction in viral yield relative to 44/47.1 rMVA. Replication was around four-fold lower for dC17-gfp; and finally, two deletion mutants, vdf5-gfp and vdC11-C10-gfp, showed virus yields similar to MVA, which was ~10-fold lower than 44/47.1 rMVA. Similar to plaque formation, the contribution of the genes to virus yield seemed to be cumulative. Nevertheless, deletion of F5L, C11R and C10L had a higher impact by reducing virus yield to levels similar to MVA.

C11 is selected to evaluate its role as host-range gene

Plaque size has been used as an indirect measure of attenuation for poxviruses. This is frequently true since a detrimental effect in the production or spread of infectious progeny can be observed as the formation of a small plaque. Nevertheless, our results (Suppl. Figure 2) and recent findings [251, 254] suggest that plaque formation can vary even when viruses replicate to the same extent in a single-step growth cycle and these two processes should be analyzed separately. Since our goal was to identify a gene or genes that explain MVA's host-restriction, this can be better determined by measuring the number of infectious particles rather than plaque morphology.

Up to now, gene F5L, C11L and/or C10R have been associated to plaque formation and viral replication. Going back to our comparative genomics analysis (Figure 24), an interesting correlation appeared. When identifying which viruses have these candidate

genes repaired, a common feature was present among all replicative viruses. Mutations in the C11R and C10L region were all present in the replication-competent viruses (44/47.1 rMVA, 51.1 rMVA, 44.1 rMVA, 51.1 rMVA), but not in the restricted viruses (47.1 rMVA nor MVA). F5L was repaired in all rMVAs with the exception of 51.1 rMVA and 47.1 rMVA. This precludes F5L as required for viral replication in these cells since virus 51.1 rMVA replicates in mammalian cells. This put C11 and C10 at the top of the list to be tested for their ability to rescue MVA's replication. More importantly, review of the literature revealed that C11, also known as vgf, shares amino acid sequence homology and functional properties with cellular growth factors EGF and TGF-[330]. It has been shown that vgf is required for efficient replication *in vivo* and for virulence [330, 331]; and more recently, it has also been associated with an immune evasion mechanism [332].

From now on, gene C11L and vgf (or C11 and VGF) will be used interchangeably in this text. For this reason, vgf was selected for further evaluation as a potential host-range determinant.

C11 expression in trans increases MVA's yield in VERO and BS-C-1 cells

Gene vgf and F11 were both cloned separately into expression plasmids under the control of VACV early/late promoters. Here, the ability of each transfected plasmid to complement MVA was compared in two cell lines. Virus yield was measured at 24 hpi using two different non-permissive cell lines for MVA. Interestingly, transfection with vgf increased MVA's replication up to ~25% in both cell lines, relative to the negative control (Figure 33). In contrast, transfection of F11 showed a ~15% increase in virus yield only in VERO cells. These preliminary results suggested that vgf is capable of

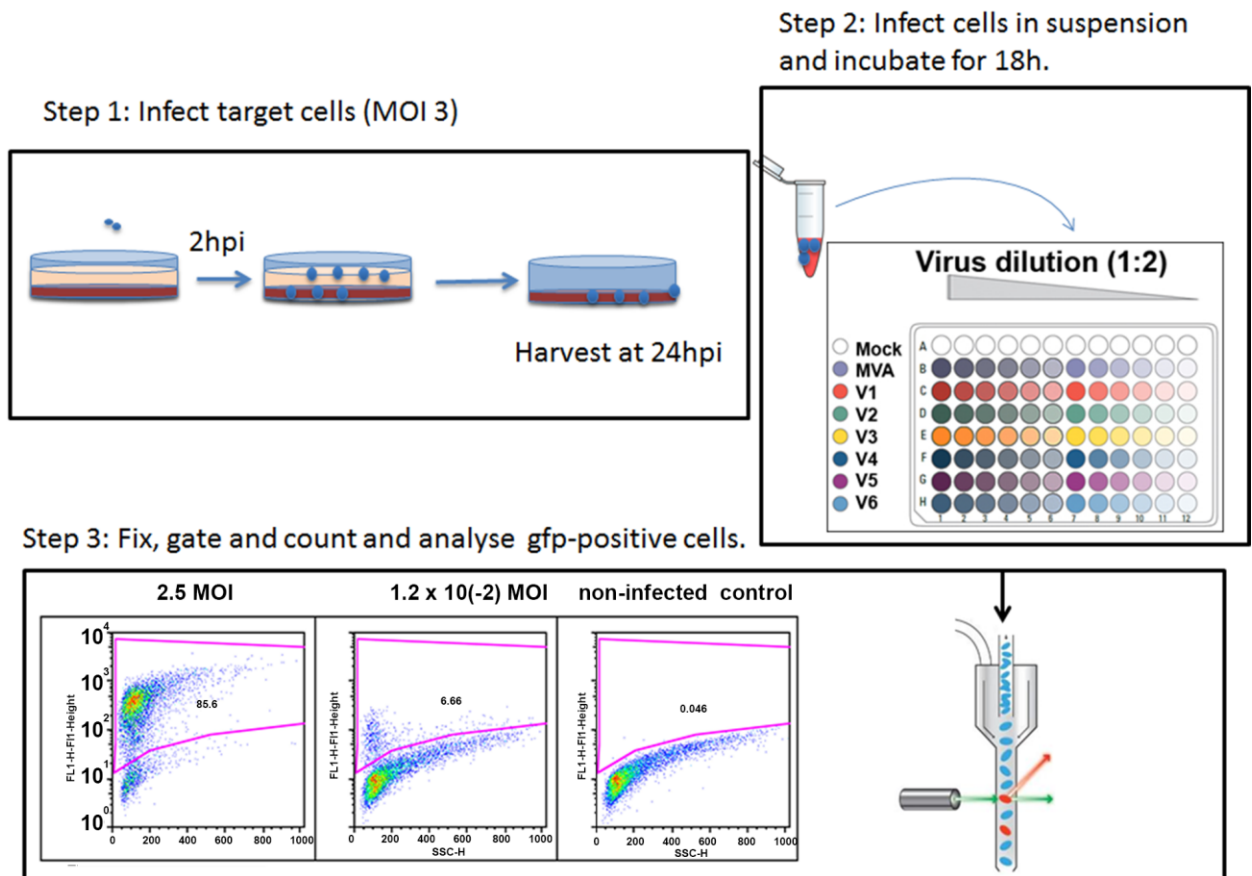


Figure 31. Workflow for high-throughput method to measure virus yield by flow-cytometry. This flow cytometry-based method of quantifying virus progeny allows high-throughput comparison of virus yields by detecting *gfp* expression. Step 1 consists in infection of the target cells, and incubation for 24 hours. In step 2, the infected cells are harvested and used to infect HeLa-S3 cells pre-incubated in AraC which limits the viral cycle to early gene expression. Serial dilutions of the virus are used to detect *gfp* at the linear portion of the curve. In step 3, HeLa cells were fixed and read in a flow-cytometer by counting *gfp* positive events.

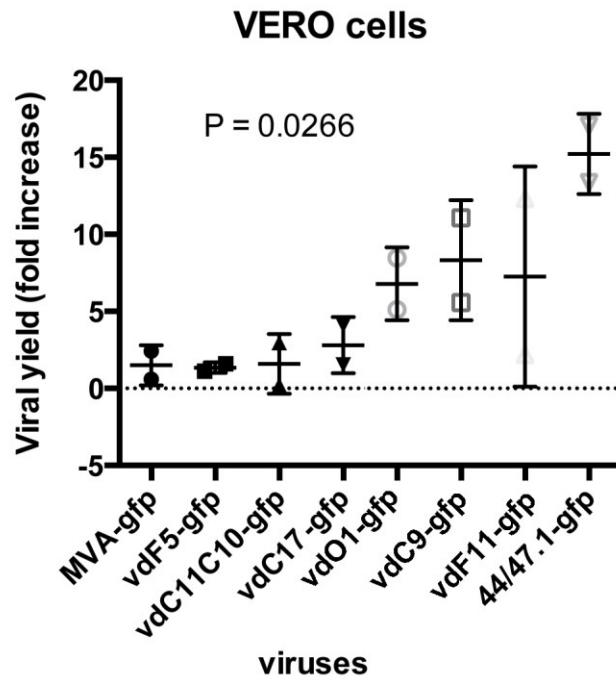


Figure 32. Virus yields were significantly reduced for several 44/47.1 rMVA deletion mutants revealing the contribution of each gene to viral replication. VERO cells were infected and harvested at 3 hpi and 24 hpi . Virus yields were then read using a high-throughput method based on gfp expression and flow cytometry. The numbers of gfp-positive cells at 24 hpi were normalized by the input at (3 hpi) and plotted using Prism. Statistical significance was determined for all groups using an ordinary ANOVA analysis.

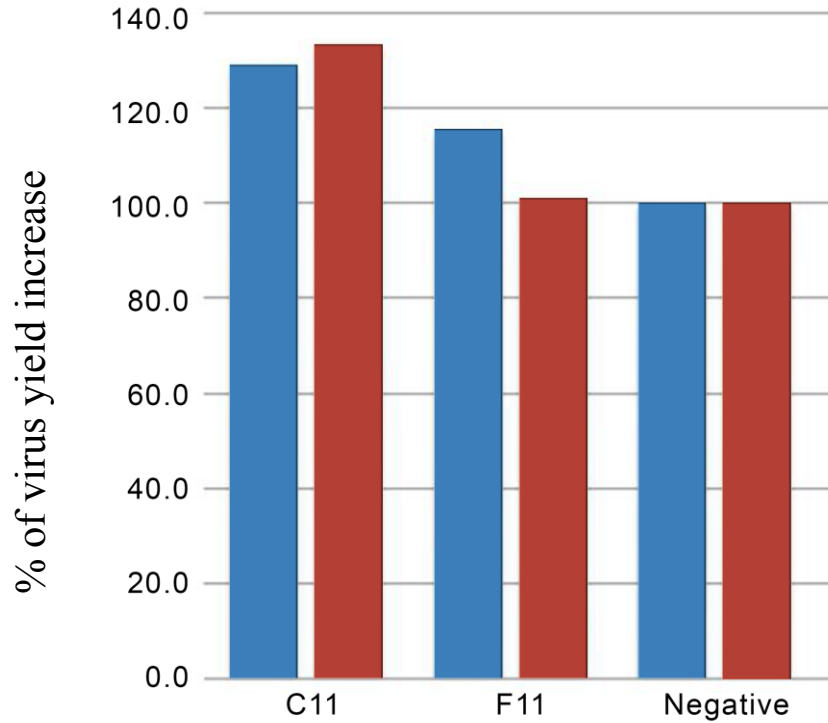


Figure 33. Trans-complementation experiment provides initial evidence for C11 as a host-range determinant. To test the effect of some of the selected genes, C11 and F11 were initially cloned into TOPO vector under the control of an early/late promoter. An additional TOPO plasmid with a deleted promoter was used as a negative control. BSC1 and VERO cells were infected followed by transfection of each plasmid independently. Infected cells were harvested 24 hours post infection and viral titers evaluated by immunostaining in CEF cells.

complementing replication of the defective MVA in these non-permissive cell lines. Although complementation occurred, the effect measured in trans should be confirmed by repairing the endogenous vgf from MVA genome.

Conceptualization and development of a one-tier recombination method and generation of MVA-C11

To confirm the trans-complementation screening experiment and confirmed vgf host-range function, the endogenous vgf from MVA genome needed to be replaced by a homologous sequence derived from a replication competent virus. Recent methods to replace a gene by recombination are frequently done in a two-tier process when the replacement does not cause a change in plaque phenotype, host range or drug resistance. Using this common method, the gene to be removed from the virus needs to be replaced with a DNA construct containing a genetic marker flanked by homologous regions to the target gene. The marker gene (gfp, tk, or any other marker) facilitates selection of this first mutant. The second step requires the use of a second construct that contain the gene to be inserted into the genome, again, flanked by homologous sequences to replace the marker gene previously inserted. The resulting mutant is a virus with the new insert, forming “white plaques” that lacks a marker. The resulting white plaques also represent a challenge to purify especially when the virus does not form plaques that helps in the selection. To solve these challenges, I designed a one-tier method for replacing the endogenous vgf gene from MVA and recover the replication ability provided by the exogenous vgf derived from a replication competent virus. This method provides several advantages over the historical one-tiered and the common two-tiered methods: a) this method generates a MVA mutant in a simplified one-step tier; b) this method

complements MVA by inserting vgf into the genome, c) this method uses vgf as its own selection marker under MVA's non-permissive condition, and e) this method minimizes growth of the parental, non-replicative MVA strain by using a non-permissive condition, f) this method generates an MVA mutant with no traditional marker which is required for its use in humans, and g) this method does not require plaque formation for the virus purification process.

As the initial hypothesis, the role of vgf as a host-range determinant would be revealed by using this method to replace MVA's endogenous vgf under non-permissive condition, allowing selective growth of the recombinant virus. This invention can be applied in many contexts (oncolytic vectors, increase vaccines production, vectors with conditional expression of vgf, selection marker, etc...) for which a vgf-containing sequence derived from a replication-competent virus could extend the host-range of a non-replicative virus into mammalian cell lines in cis or in trans. The protocol was carried out as described in the methods. After purification of the recombinant mutant in VERO cells, all replication-competent viruses were amplified in BS-C-1 cells. Verification of the insert was done by PCR and Sanger sequencing. By generating two viruses, one containing the vgf region derived from 51.2 rMVA, and the other sequence derived from VACV-WR, two examples are provided in which replication-competent viruses can be generated using a one-tier procedure and selection under non-permissive condition, using vgf as its own marker.

MVA-C11 as a novel host-range gene without affecting plaque size

The MVA-C11 produced with the one-tier method was compared to MVA and 44/47.1 rMVA in its ability to form plaques in several mammalian cell lines. Figure 34 compares the plaque formation ability of MVA-C11, MVA and 44/47.1 rMVA. MVA-C11 is able to form plaques, slightly larger than MVA, but much smaller than 44/47.1rMVA. In order to demonstrate the contribution of the newly inserted *vgf* to MVA's growth, a one-step growth curved was used to determine virus replication. An MOI of 3 was used to infect the three mammalian cells lines. Virus yields were then measured by traditional immunostaining methods at 24 hpi. In all cases, MVA-C11 showed ~10 fold increase in virus yield. Nevertheless, it still replicated lower than 44/47.1 rMVA. This suggests the existence of other genes that contribute in some extend to 44/47.1 rMVA replication. In this respect, deletion of both copies of the *vgf* gene from VACV WR did not cause a replication defect [331, 333].

Evaluation of wild-type *vgf* and other poxvirus sequences

The *vgf* construct used to generate the replication-competent MVA contains several polymorphisms when compared with the endogenous *vgf*. The differences are summarized in Table 10 and include mutations in the 5' and 3'UTR of the *vgf* gene. Changes within the coding region for *vgf* also occurred, causing substitutions within the predicted protein. Although there are several mutations in the amino acid sequence, it is worth mentioning a few important observations. The second, third and fourth amino acids that correspond to the amino acid sequence "LIN" were substituted for "SMK" (Figure 35). The sequence is located within a predicted secretion signal. Other substitutions also occurred in the transmembrane domain and in the tyrosine kinase domain. Importantly,

several changes are common to all replication-competent VACVs, including the SMK sequence, but neither for Acam3000 nor VACV-Lister. Other mutations were found in the 5' and 3' UTR that might also contribute to vgf's effect as host-range determinant (Table 10 and Suppl. Figure 4). Further characterization of this vgf gene will be needed to determine the exact mechanism and structural changes responsible for its function.

The similarity of vgf to other sequences was also evaluated. Protein alignment confirmed that the identity of the amino acid sequence is 98.6% similar to VACV-Acam2000, but 96.5% similar to the suggested parental strain (Table 11). Further genome-wide analysis will be useful to have a global view in the matter.

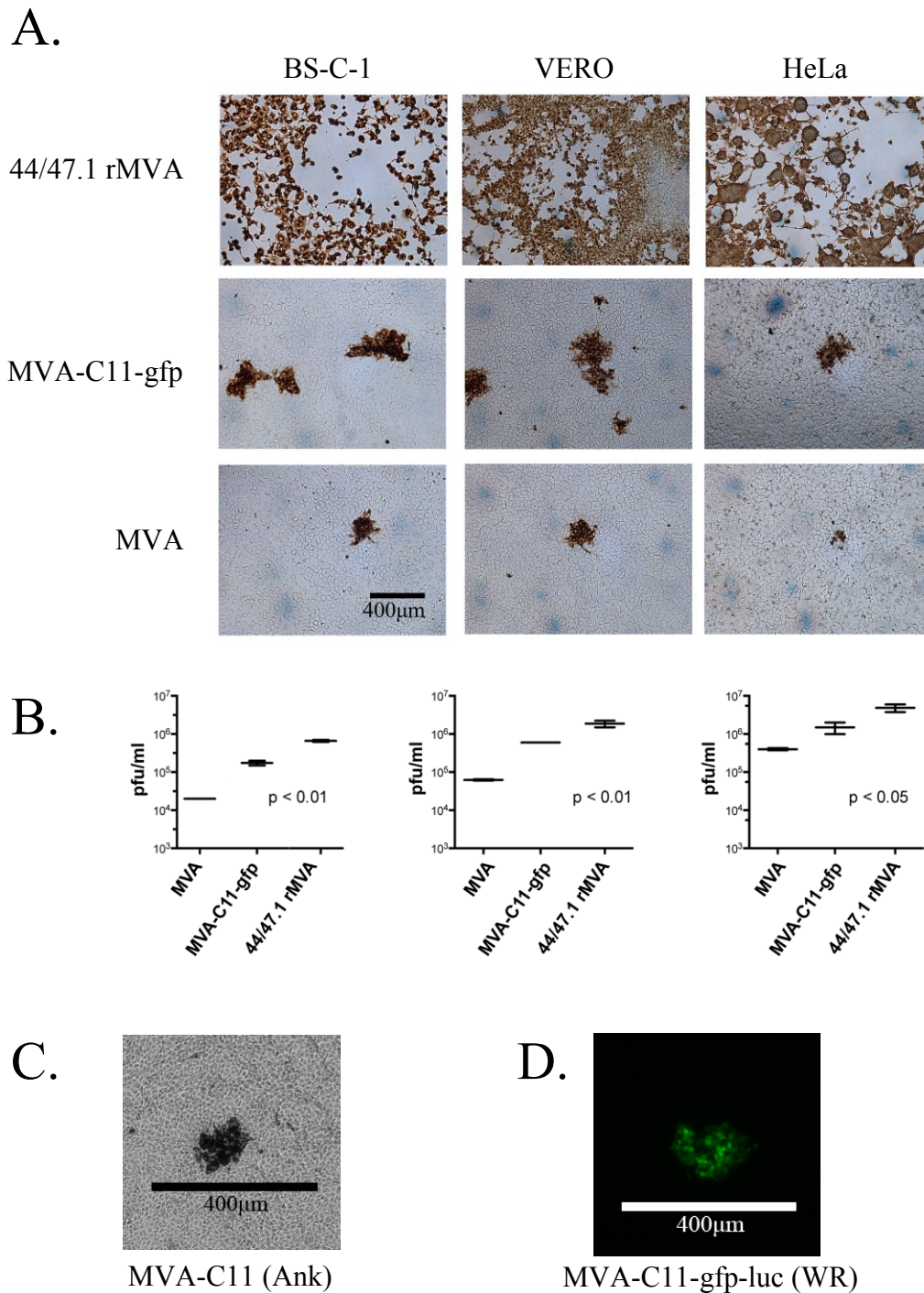


Figure 34. Repair of endogenous vgf with a homologous sequence derived from a replication-competent virus was sufficient to recover MVA's host-range in mammalian cells. Replacement of MVA's endogenous vgf and flanking sequences derived from replication-competent virus 51.2 rMVA did not affect plaque size 3 dpi (A), but increased virus yield at 24 hpi by one log (B). Foci are formed in VERO cells by MVA-C11 24hpi (C) and MVA-C11-luc-gfp 5dpi (D). The statistical analysis used was an ordinary ANOVA test.

Table 10. Sequence differences in vgf gene and flanking sequences between the replication-competent MVA-C11 (Ank) and MVA

Position (bp) ^a	nt change ^b	codon affected ^b	aa change ^b	type
-81	T -> C	-	-	SNP (transition)
-46	C -> T	-	-	SNP (transition)
-41	A -> T	-	-	SNP (transversion)
-13	A -> G	-	-	SNP (transition)
5	T -> C	TTG -> TCG	L -> S	SNP (transition)
9	A -> G	ATA -> ATG	I -> M	SNP (transition)
12	T -> A	AAT -> AAA	N -> K	SNP (transversion)
86	C -> T	TCG -> TTG	S -> L	SNP (transition)
103	G -> A	GCT -> ACT	A -> T	SNP (transition)
348	-TAC	ATT,ACG -> ATG	IT -> M	Deletion
385	C -> A	CGA -> AGA		SNP (transversion)
388	+TAA	ACT -> ACT,AAT	T -> TN	Insertion
400	A -> C	ATA -> CTA	I -> L	SNP (transversion)
503	A -> G	-	-	SNP (transition)
548	C -> T	-	-	SNP (transition)

^aPosition relative to TSS of gene vgf; ^bchanges relative to MVA. bp: base pairs; nt: nucleotide; aa: amino acid; SNP: single nucleotide polymorphism;

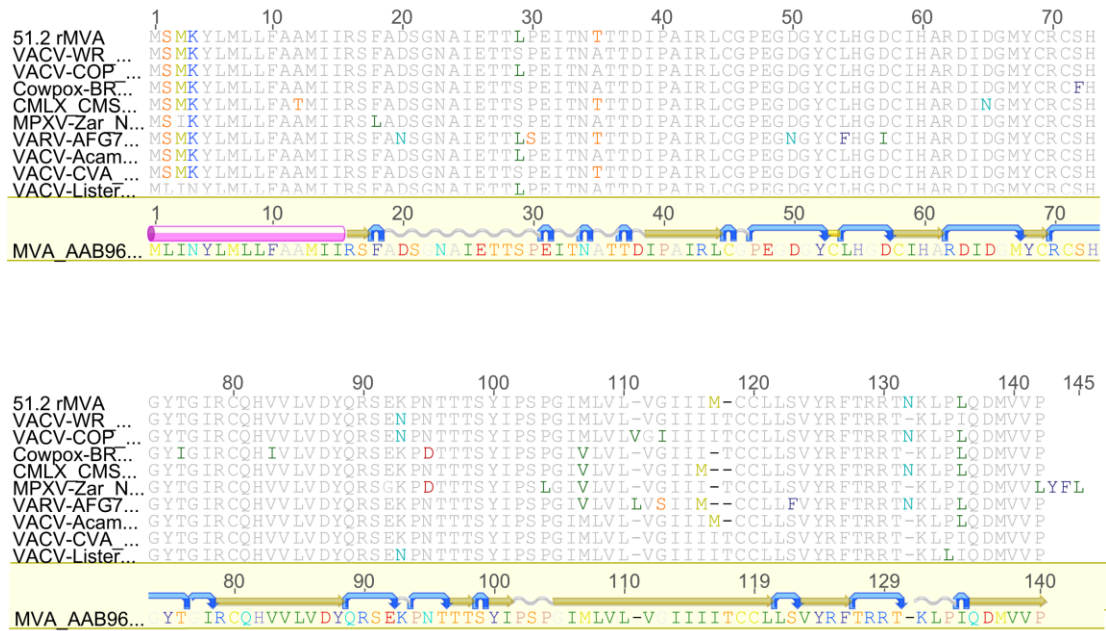


Figure 35. Multi-sequence alignment of C11 for several orthopoxviruses. This multiple-sequence alignment showed several amino acid changes for the replication-competent rMVAs (represented by 51.2 rMVA) relative to other orthopoxviruses. Changes were found through the whole protein, including the SMK sequence in the signal peptide region at the N-terminus. Also changes were found in the predicted transmembrane domain and the kinase domain. Purple bar: single peptide; blue arrows: turns; orange arrows: beta strands; gray: coil;

Discussion

MVA is an attenuated poxvirus that has been used as vaccine against smallpox and other infectious diseases [310]. Its attenuation was achieved by passaging the virus in chicken embryonic cells for over 500 times, causing several deletions and mutations throughout the genome [321]. Attempts to identify the gene or genes responsible for this attenuation have provided partial explanations to such a complex question [204, 251, 254, 322]. Importantly, systematic repair of MVA's deletion were not sufficient to explain its attenuation, suggesting that important host-range genes were located outside the deleted regions [322]. Wyatt and co-workers inserted long cosmids that allowed them to recover MVA mutants by plaque selection in BS-C-1 cells [204]. Some mutants generated with a single cosmid showed intermediate phenotypes, demonstrating that recovery of the full phenotype requires more than one gene. Because of the extensive insertions and the different phenotypes of each rMVA, whole-genome sequencing and comparative genomic approach seemed to be the most efficient technique to address the issue. The multi-genome comparison performed here allowed the identification of the genes repaired in the rMVAs, allowing the selection of candidate host-range genes for further investigation.

Initial characterization of all rMVAs was done to confirm that plaque formation ability was still retained for all rMVAs (Figure 22). The initial clonal purification was also important for sequencing, in order to have a homogenous viral preparation that minimize the presence of quasi-species. For this reason, all mutants were clonally purified, new viral stocks prepared, and the plaque formation phenotypes confirmed. Furthermore, evaluation by EM was also carried out to rule out possible differences in virus

morphogenesis (Figure 26). As expected, MVA showed accumulation of abnormal dense spherical particles and no MVs at late times during the infection. The viruses 44/47.1, 44.1, 51.1 & 51.2 rMVA all showed clear formation of MVs in addition to some dense spherical particles, suggesting that the differences in plaque formation and replication are directly linked to morphogenesis. Indeed, the rMVAs that replicated best had the highest number of MVs compared to dense spherical particles.

Because some cosmids overlapped with the ITRs, recombination could have occurred virtually in either side of the genome. Electrophoresis of the digested genomic DNA showed a clear shift in the C bands, which correspond to the left-most portion of the genome (Figure 23). The bands A and B, which are located in the right part of the genome, are identical in all rMVAs. These results provided further evidence that mutations in all rMVAs were restricted to the left side of the genomes. Additionally, migration of the C band for the 44/47.1 rMVA also confirmed that a longer insertion occurred in this virus, which is compatible with the rescued phenotype.

After sequencing and solving the assembly challenges, all genomes were aligned and annotated (Figure 24). By detecting all mutations relative to MVA, the inserted genes and regions were visually identified. As suggested by gel electrophoresis, the sequence alignment confirmed that all recombination events occurred on the left side of the genome. For 44/47.1 rMVA, the repaired region spanned up to 80 kbp. Moreover, some viruses showed partial repair, which highlights the importance of doing whole-genome sequencing. For example, cosmid 44 did not repair deletion V & II, but it repaired the flanking regions. Also, cosmid 47 was partially inserted in the C region

Table 11. Amino acid identity of the vgf ORF of 51.2 rMVA is closest to that of ACAM2000

Virus	Identity
51.2 rMVA	-
Acam2000	98.60%
VACV-CVA	96.50%
CMLX_CMS	95.70%
VACV-COP	95.10%
VACV-WR	95.00%
Acambis3000	93.60%
Cowpox-BR	92.90%
VACV-Lister	92.90%
VAR-AFG70	92.20%
MPXV-Zar	90.80%

causing deletion of several MVA genes. This occurred because MVA has a segment of genes denominated cowpox host-range genes, which are absent in the virus used to generate the cosmids [334]. Also, this deletion explains the increase in migration of the HindIII C segment in this virus and the replication in any mammalian cells. Nevertheless, deletion of the cowpox host-range cluster does not explain the increase in cytopathogenicity shown for 47.1 rMVA in BS-C-1 cells documented elsewhere [204]. Nevertheless, the report by Wyatt et al. [204] was confirmed by showing that 47.1 rMVA was indeed forming plaques with small clearance. It seems counterintuitive that loss of genes can increase cytopathology, but a report has described similar findings for other regions [322].

Since 44/47.1 rMVA showed a similar plaque phenotype as the parental strain, the repaired genes from this virus were considered as potential host-range genes. The initial strategy to evaluate the gene contribution to the 44/47.1 rMVA phenotype was by deleting each candidate gene at a time, and comparing plaque sizes of the deletion mutants. Our early observations that plaque formation and viral yield may be independent (Suppl. Figure 2) and further confirmations by others [251], made it essential to include the virus replication assay.

A total of 20 genes were selected for screening based on visual evaluation of the mutations throughout all rMVAs. In order to make the numbers of mutants more manageable, some genes were deleted in pairs. In this way, the number of mutants was reduced to a total of 13. Soon after generating all deletion mutants, a new report demonstrated that repair of genes within the six deletions were not sufficient to explain

MVA's phenotype [322]. For this reason, efforts were concentrated in investigating the role of those seven genes outside MVA's deletions. A plaque assay for all 13 deletion mutants initially generated can be found in Supplementary figure 3.

The seven deletion mutants were then used in plaque formation assay in three different mammalian cell lines (VERO, HeLa, and BS-C-1). These cell lines were used in order to compare results to previous reports. Moreover, VERO cells are mammalian cell lines approved for vaccine/vector development and represent an interesting cell line to test [252]. The results from our plaque assay showed that different genes were required for plaque formation in a cell-dependent manner (Figure 29 and 29). It also suggested that plaque formation is determined in a modular fashion in which spreading is affected by the micro environment of that particular cell. For example, deletion of O1, F5 and C11/C10 show significant reduction in plaque size in BSC1 cells. C17 and F5 are both necessary for plaque formation in HeLa cells. And finally, a broader group composed of genes O1, C15, C17, F5, and C11/C10 are required for plaque formation in VERO cells. It was also striking to see that deletion of F5 negatively impacted plaque formation in all cell lines tested. This is compatible with recent findings describing the recovering of plaque formation of 51.2 rMVA by repairing F5 and F11, but not F11 by itself [251]. Nevertheless, the mechanism for which F5 affects plaque formation has not been determined. Whether F5 or F11 are sufficient to increase plaque size for MVA has not been demonstrated neither. Moreover, the rest of the data can be interpreted as if the other genes contribute indirectly or partial to plaque formation.

As explained before, plaque formation may not correlate directly with virus yield. Therefore, the ability to produce progeny in mammalian cells seems to be a better indicator of host-range. In order to screen a large number of mutants, a flow-cytometry based method was first used to determine viral yield of each deletion mutant (Figure 31). An MOI of 3 was used to ensure infection of the whole monolayer and eliminate the effect caused by spreading, which is related to plaque formation. Comparison of virus yields in VERO cells showed different degrees of replication. Arbitrarily grouping of the viral yields simplified the interpretation of the data. For example, deletion of O1, F11, and C9 all showed some negative effect in virus yield; nevertheless statistical significance for F11 and C9 was not determined. This could be explained together with the plaque assay in which plaque sizes for these two viruses included a broad range. It can be speculated that the absence of these two genes could cause a delay in some viral process, causing desynchronized plaque formation. The effect of O1 in plaque formation, but not virus replication is supported in a recent publication. [254]. Deletion of genes such as C17, led to replication five-fold lower than 44/47.1 rMVA, which indicates that they provide an accumulative effect on viral replication. Finally, F5, C11 and/or C10 showed the most significant reduction in virus yield, comparable to that found for MVA. Here, the genes with the strongest contribution to viral replication must have a higher likelihood to have an essential role such as host-range determination. Based on this approach, F5, C11 and C10 were all interesting candidates for further evaluation. Nevertheless, the absence of a repaired F5 from the replication-competent 51.1 rMVA suggested C11 or C10 to be considered first.

Plaque formation and replication data can be coupled with the genome alignments to identify the candidate genes repaired in the rMVAs (Figure 24). C17 is partially repaired in 44/47.1, and completely repaired in 51.1 rMVA. F5, F11 are all repaired in 44/47.1 rMVA and 44.1 rMVA. O1 is only repaired in 44/47.1 rMVA. Now, the most interesting observation that provided the strongest evidence for C11 and C10 was that mutations in that region were all common to the replication-competent viruses (44/47.1 rMVA, 51.1 rMVA, 51.2 rMVA and 44.1 rMVA). This, together with the plaque and replication data, suggests that one or both of these genes are host-range determinant in mammalian cell lines.

A closer look into the literature revealed that C11, also known as *vgf*, codes for a secreted protein that structurally and functionally resembles the mammalian EGF [330, 335]. Deletion of this gene causes significant reduction of virulence and virus growth [331, 333]. One of the mechanisms demonstrated for *vgf* is the ability to prevent apoptosis, and promote cell growth [336]. Since *vgf* showed to be important for plaque formation and replication in our experiments, I decided to test its effect in trans- by cloning *vgf* into a plasmid under the control of an early/late synthetic promoter. Although early promoters are not efficiently expressed by transfection, the experiment showed that expression of *vgf* increases MVA replication by ~25% for both mammalian cell lines tested (Figure 33). Because transfection efficiency could be a concern in this approach, I decided to replace MVA's endogenous *vgf* with the homologous region derived from 51.2 rMVA (replication-competent virus).

The replication-competent MVAs (MVA-C11) lacking any traditional marker (gfp, luc, tk) are potential candidates as smallpox vaccines or vectors. The construction of these viruses has several challenges. In the absence of a selectable marker, a two-tier procedure in which the endogenous sequence is replaced with a construct containing a marker is frequently used. The sequence to be inserted has flanking sequences homologous to the target region. Purification and amplification of this deletion mutant is usually done with the help of the marker. The second step consists of infecting cells with the mutant virus and transfection of a second DNA construct. This second construct contains the gene to be inserted, flanked with regions that allow replacement of the previously inserted marker. One challenge in this method is that the clonal purification is done blindly, with no marker. This is further complicated by the absence of plaque formation in the resulting virus.

To facilitate the generation of the recombinant virus, and at the same time demonstrate the role of vgf, I developed a one-tier procedure, similar to some degree to previous methods [204], but with additional unique features. The unique features of this procedures also include: a) the generation of a recombinant mutant in a one-tier procedure that simplifies and reduces the time to obtain the replication-competent mutant, b) the use of vgf as its own marker in VERO cells, allowing selective growth of the recombinant mutant in an otherwise non-permissive condition, c) the expansion of MVA's host-range into mammalian cell lines as evidence of its host-range determination for mammalian cell lines, d) the negative selection for the replication-incompetent virus (MVA) in the selected non-permissive condition, e) the generation of a product (MVA-C11) with no traditional marker, which is suitable for as vaccine or therapeutics, and g)

this method does not requires plaque formation for the virus purification process and clonal purification can also be done selecting clumps or foci. Other benefits or a replication-competent virus have been previously suggested as capable of enhancing the immunogenicity for the vaccines or vectors against the infectious diseases they were designed for [332].

VERO cells were used because they are non-permissive for MVA, and commonly used for vaccine production. The use of a non-permissive cell line (or condition) reduced the chances of recovering the attenuated parental strain. Also, it provided the proper selection pressure that allows the growth of a replication-competent virus.

The first virus to be generated with this method (MVA-C11) was cloned purified and amplified, and sequence verified. This virus was then characterized, showing formation of small foci comparable to MVA, and the ability to increase virus yield by at least one log in all cell lines tested (Figure 34). The findings that MVA-C11 formed foci similar in size to MVA was not surprising, since virus as 51.2 rMVA showed a similar phenotype. The surprising finding was that a single repair was able to increase virus yield by one log at 24 hpi.

The vgf gene has been associated with immune-evasion roles, by targeting the NF-kB pathway [332]. Since MVA does not grow in other mammalian cell lines (like VERO, BS-C-1, etc.), the role of vgf in the NF-kB pathway has not been determined. Nevertheless, the vgf gene derived from the replicative-competent virus 51.2 rMVA (identical to all other replication-competent rMVAs) and the vgf derived from VACV-WR are sufficient to extend MVA's host range into mammalian cells. In the second

example mentioned previously, the vgf derived from VACV-WR was inserted into an MVA strain that contains LUC and GFP genes (Figure 34-C). This virus was constructed to further evaluate and elucidate the mechanism of action of vgf and its role in host-range determination for mammalian cells.

A recent publication showed an interesting perspective about vgf. It was demonstrated that MVA's endogenous vgf is capable of inhibiting NF-k-beta and ERK activation in two cell lines, 293T cells and Hacat [332]. Although this protein shows some functions in some cell lines, its role as a host-range determinant has not been demonstrated until now.

It is important to point out that the repairs inserted into MVA capable of extending their host-range include several mutations in the 5' & 3' UTR (Table 10). In order to identify a mechanism behind the host-range rescue, further experiments are required. Changes in the RNA sequence may contribute to the stability and role of the vgf transcript. For example, bioinformatics analysis of sequences from MVA and the replication-competent viruses (VACV-WR and 51.2 rMVA) shows a more stable secondary structure (data not shown). From the vaccinology point of view, the role of vgf is important since the current MVA vaccine has the disadvantage in that it induces lower immunogenicity when compared with other VACV vaccines. The use of a replication-competent virus as vaccine or vector has been suggested to induce a better immunogenicity [252, 332]. Additional experiments should be done to determine the impact of this replication-competent MVA to the mechanism and its immunogenicity to measure its value as vectors or vaccines. Moreover, replication of these viruses are important from the production point of view, since the use of chicken cells represents a challenge when

compared to the use of mammalian cell lines such as MRC5 or VERO cells. Although the safety of the rMVAs containing this vgf sequence has been evaluated in mice [252], it will also be important to confirm the safety of these new replication-competent MVA for humans. The potential applications of this discovery are broad and include designing new replicative-competent vectors and vaccines capable of replicating in approved mammalian cell lines such as VERO. This could be potentially applied to other non-Orthopoxviruses. Moreover, similarly to the VACV tyrosine kinase gene, the vgf gene can be effectively used as a selection marker to generate recombinant strains in a non-permissive cell for research.

Conclusions

Here, a comprehensive survey for new poxvirus host-range genes and the discovery of a new host-range determinant gene (vgf) is presented. The results showed that deletion of five genes (O1, F5, C11-C10 and C17) was associated with a significant reduction in plaque formation. Deletion mutants lacking F5, and C11-C10 also showed significant impaired viral replication. Here, we also demonstrated the functional redundancy in plaque formation and the requirement for gene F5 in several mammalian cells. This functional redundancy can be imagined as a cluster of genes that targets similar pathways, but can be counteracted by host factors that are differentially expressed in these cell lines. Those genes associated with plaque formation can be considered redundant in the sense that each one facilitates viral spreading independently.

Moreover, this approach also let us to the identification and demonstration that mutations within the vgf region are sufficient to extend MVAs host-range to mammalian cells.

Moreover, the method describe here teaches a simplify procedure using vgf as a selection marker, and demonstrated the generation of replication-competent viruses that can be used as vaccine or therapeutics for humans and veterinarian purposes. Further characterizations of the mutations related to vgf will be valuable to determine a specific mechanism. This discovery represents the first gene outside MVA's deletion capable of rescuing its replication in mammalian cells; thus providing the bases to further improve Poxvirus-based vaccines and vectors.

Chapter 5: Significance of our findings from a clinical point of view.

The three projects presented here used sequencing technology to address different aspects of Poxvirus host-range and the identification of a viral isolate. Whole-genome sequencing and RNA-Seq have demonstrated to be useful complements to traditional techniques in addressing unresolved questions for the Poxvirology field. The use of deep-sequencing allowed us to simplify the sequencing process from laborious Sanger sequencing of overlapping PCR products to simplified library generation and automated sequencing.

Erythromelalgia-related poxvirus and future research

In the first chapter, the identity of the Erythromelalgia-related poxvirus (ERPV) was revealed 25 years after its isolation [27, 259, 260]. This is one of many examples available in the literature showing that whole-genome sequencing can be used in the discovery and identification of viruses in clinical scenarios [337]. Traditional methods were unable to identify this isolate because of their intrinsic limitations these techniques poses. Although we expected to identify a novel poxvirus, our findings demonstrated that ERPV is closely related to the Ectromelia Naval strain.

ECTV's outbreaks in laboratory mice and the detection of viral DNA in mouse serum used for tissue culturing raise the question of whether ERPV is a human pathogen or a contaminant [338-341]. There is evidence that support both perspectives. First, the elevated neutralizing antibody titers found in patients diagnosed with Erythromelalgia, but not in healthy population, suggests a real human exposure to ERPV [260]. Nevertheless, this can also be explained by cross-reactivity of antibodies induced by the

Smallpox vaccine. It is believed that vaccination in China ended in the early 1980s and these outbreaks were documented in 1987, increasing the likelihood of cross-reactivity as the explanation. Second, the existence of other Orthopoxviruses capable of infecting multiple species also suggests that a human infection is not far-fetched, but a frequent event when humans get in close proximity with their vectors [342, 343]. From an epidemiologic point of view, crowded living conditions can facilitate zoonosis especially with those vectors that cohabit with humans as mice do. Since ERPV is almost identical to ECTV-Nav, further characterization of the virus and host-range genes will require confirmation of ERPV as a human pathogen. Current efforts are underway by another group to evaluate the antibody titers using novel methods not available at the time of its isolation.

Molluscum contagiosum transcriptome and new tools to study the virus.

Molluscum contagiosum is an interesting virus, especially from a research point of view. The virus is unable to grow *in vitro*, and there is no animal model for research [285, 288]. Although it is a human pathogen, the requirements to replicate are more stringent when compared to other Poxviruses. For decades, researchers have tried to understand the genetic and molecular basis of its blockage. The data presented here is a step forward in our understanding of this intriguing virus. Reports showing detection of PR genes in the absence of DNA replication [287] were in conflict with our current knowledge of poxvirus' gene expression. In VACV, PR gene expression only occurs after DNA replication [67], which does not occur *in vitro* experiments for MOCV. Nevertheless, PR transcripts were detected by qPCR in the absence of MOCV DNA replication [287]. By

using RNA-Seq, we demonstrated the absence of PR gene expression *in vitro*. This was further supported by functional assays using reporter genes in trans for which we were not able to detect PR gene expression. We concluded that MOCV's transcriptome from *in vitro* assays is early in nature. This is an important finding for the field since it allows future research to re-focus in the early steps of the viral cycle and to determine the location of the MOCV blockage. Future research should evaluate aspects of the viral cycle such as viral uncoating, early gene translation and DNA replication in order to further address this issue.

From the clinical point of view, the transcriptome generated from infected human tissue provided evidence of the genes expressed in a clinical specimen. We were able to confirm sixty early genes and demonstrate the expression of MOCV genes *in vivo*. The identification of the genes expressed *in vivo* and their temporal classification could be used as a tool for the selection of new viral targets in the designing of new antiviral treatments.

Our knowledge of MOCV has been limited by the inability to grow the virus *in vitro* and the absence of an animal model. Since there is a need for an *in vitro* system to grow the virus, methods and tools to detect events pass the MOCV blockage are required. I have designed and tested a plasmid containing the MOCV promoter MC095, which is compatible with VACV and ERPV transcription machinery. The results showed that expression of *gfp* using this plasmid is inhibited with a DNA replication inhibitor. This property highlights the specificity of this promoter for PR event and makes the plasmid an ideal tool to screen for conditions that allow MOCV to continue in the viral cycle. The

identification of such conditions will facilitate further studies to understand the bases of this blockage and hopefully lead to the development of new drugs against MOCV.

MVA and improvements to current vaccines and vectors.

The story presented here for MVA and rMVAs compiles knowledge of Poxvirus for the past 50 years. MVA is an attenuated virus proven to be safe as a Smallpox vaccine [319, 344, 345]. The need for a safe vaccine came after the global campaigns against Smallpox and the adverse effects of the original vaccine. Currently, MVA represents an interesting candidate not only as a Smallpox vaccine but as a vector against several infectious diseases and for viral oncolysis [13, 15, 199, 346]. The elements evaluated for the use of MVA as a vaccine or vector includes the ease of production, the immunogenicity, and its safety profile. Several groups have been continuously looking for new ways to improve MVA and make it comparable or better than other vaccines (Acam2000, Acam3000, Lister, etc.) [204, 252, 347]. The work presented here confirms genes recently associated with plaque formation (O1, F5, F11, C17) and has the potential to be used to improve MVA and expands our knowledge of the viral-host interaction. A potential application of these findings is the repair of these genes in MVA to allow better spread during production. Nevertheless, an increase in spreading might be a concern in terms of safety from a clinical or veterinarian point of view.

The exact mechanism by which these genes are able to increase plaque formation is not clear. For example, O1 is known to activate the ERK2 pathway, which is similar to what has been shown for the vgf gene [254]. This suggests that both O1 and vgf modulate the same pathway at different levels. C17 is an ankyrin-like protein [26]. This family of

domains is conserved throughout mammals and plays an important role in the cell's cytoskeleton [348-350]. Although a specific mechanism hasn't been elucidated for most of these viral proteins, we can speculate that they might be involved in actin filaments formation to some degree. For example, VACV F11 protein is known to increase plaque formation in cells by its ability to modulate the host's actin filaments, especially those filaments within the cell's cortex [256, 257]. Experiments using a poxvirus that does not form plaques (Myxoma virus) showed that insertion of VACV F11 into its genome allows plaque formation by modulating the formation and the speed at which the actin filaments form [351]. The final outcome is an increased ability of the virus in cell to cell spreading. Importantly, we also showed that a non-truncated F5 is required for plaque formation in all cell lines tested demonstrating a central role.

Interestingly, our data also shows that the role of these genes is cell-line dependent, for which a different subset of genes are required on each cell type. This requirement for different subset of genes may be explained if these genes are functionally redundant but with different targets. This functional redundancy provides the means for the virus to spread in different tissues or cells. This property makes more sense in a real infection for which a dynamic microenvironment is the norm. During a real infection, the virus goes through several tissues and different cells that have different gene expression [352, 353]. The virus is equipped with these functionally redundant genes that possibly target the same pathway at different levels [178]. In this regard, the cell-dependence effect observed in our assays could be explained by the presence or absence of cell factors that interact with the viral proteins on each cell line.

Evidence of modularity was also observed as we dissected replication and spreading phenotypes. Some genes specifically contribute to the ability of the virus to spread (eg. O1), while other genes specifically increase viral replication (vgf/C11). One interesting example is the previously identified K1L host-range gene, which extends viral replication of MVA into RK-13 cells, but not to other mammalian cell lines [204, 256]. The function of K1L is dependent on its antagonizing effect of IFN. Nevertheless, this host-range specificity is not seen with every viral IFN antagonists. Taken together, replication and plaque formation genes depend on the presence or absence of particular host-factors to counteract viral proteins in a cell-type or tissue- dependent manner; this is a property that can be better appreciated when imagining a real infection.

Throughout MVA's attenuation process, the virus not only lost the ability to spread but also lost its ability to replicate in mammalian cell lines [317, 354, 355]. The identification of the genes responsible for this replication defect has been a major topic of research for the past four decades. Several authors have envisioned repairs to the MVA genome to allow the virus to replicate in mammalian cell lines without compromising its safeness [252, 322, 355]. Fortunately, we have been able to identify the vgf gene and its flanking sequences (3' UTR and 5' UTR) as sufficient to extend MVA's host-range into HeLa, Vero, and BS-C-1 cells. Two vgf encoding plasmids from different replication-competent viruses were used to demonstrate our findings. vgf's role in morphogenesis is inferred by its ability to restore MVA's replication has not been elucidated. Nevertheless, it has been suggested that vgf has an anti-apoptotic effect [204] by activating the EGF pathway [333] and allowing the viral cycle to proceed. Activation of the EGF pathway allows the cell to grow and transform, providing additional metabolites that facilitate viral DNA

replication. This finding represents a major breakthrough not only for the Poxvirology field, but also from a vaccinology and therapeutics perspective. The method described here provides sufficient details to reproduce the recovery of replication for other poxviruses and vaccine strains. These enhancements might contribute significantly to virus production, and possibly enhance immunogenicity when used as a vaccine. The growth of MVA-based vaccine and vectors is a challenging and tedious process when using CEF cells, and the use of other mammalian cell lines are preferred [356]. As primary cells, CEF cells need to be constantly screened for contamination which raises the cost of vaccine production. Also, traces of avian peptides are a concern for the possibility of anaphylactic reactions in the vaccinees. A virus capable of replicating in FDA-approved mammalian cells has been envisioned and desired for decades. The use of recombinant viruses such as those generated here fulfills all these desired properties. Safety of the virus containing these sequences has been demonstrated elsewhere [252]. Moreover, it has been hypothesized that by repairing MVA with such a gene, the immunogenicity of the vaccines will also be enhanced while retaining the safety profile [252, 332]. Other applications can also be envisioned for different clinical situations. It includes the selective expression of vgf enhancing growth of the virus only in cancer cells; or the generation of cell lines that conditionally express vgf, and allow the growth of vgf deletion mutants. Finally, the gene and the method described here can be readily used to re-engineer the viruses currently used in clinical and veterinary applications providing several advantages of using a replication-competent virus.

Final words

The available technology is continuously shaping our future. Sequencing technology is serving its purpose in expanding our knowledge and increasing our ability to address unanswered questions. It also has accelerated our ability to translate basic research into clinical applications. Nevertheless, we are still in infant times for sequencing for which we envisioned significant changes in the way we do research and do clinical diagnostic. We have already seen a dramatic increase in knowledge in all fields, including virology, and expect these technologies to be prevalent in our daily life.

This unique experience has allowed me to understand research in an interesting way. It is the desire of most researchers to have a positive impact on human health. This includes providing benefits to those in undeveloped countries that do not have the infrastructure or resources to generate solutions by themselves. Developed countries have the resources, while the undeveloped countries suffer from the viral diversity and emerging diseases that constantly threaten their population. Scientific cooperation and partnership between institutions of these two worlds should be more intensively promoted. By co-developing and patenting in partnership, developed countries could directly contributing economically, academically and logistically with these undeveloped countries. Done properly, science and research might contribute to re-balance a world in need for the greater good of humanity.

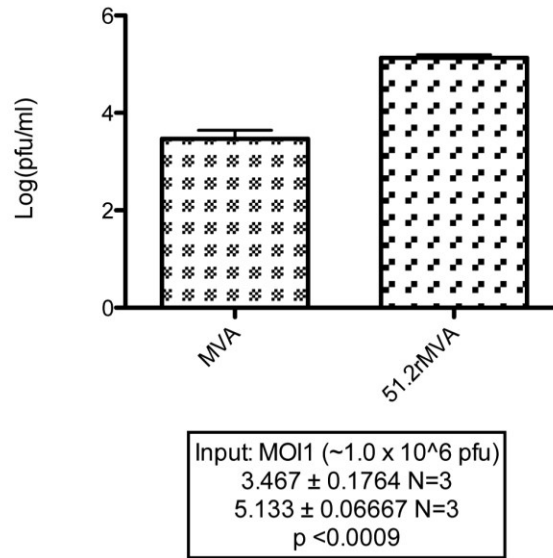
Appendices

Supplementary table 1. Comparative table of all predicted proteins on the left side of the genome for all rMVAs and other relevant Vaccinia viruses.

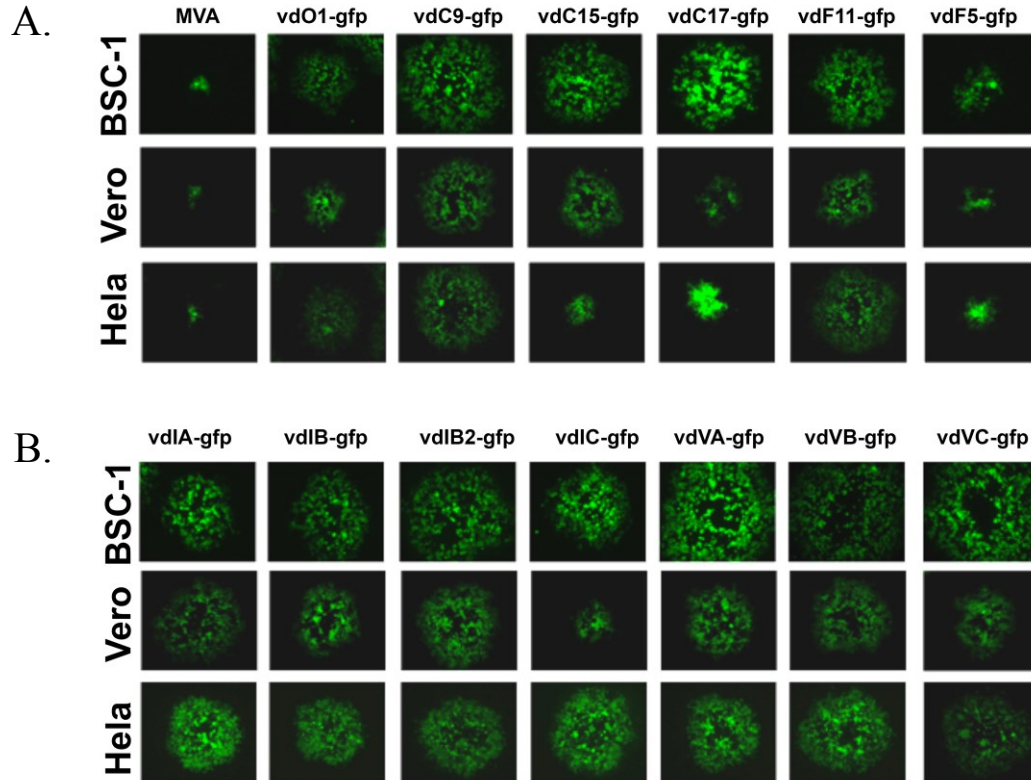
Acam2000 ORF	VACV-Cop	Acambis2000	44/47 rMVA	44.1 rMVA	51.1 rMVA	51.2 rMVA	47.1 rMVA	VACV-COP	VACV-CVA	Lister-VACV107	Acam3000
		Size (AA)									
1	C23L	241	37	37	37	37	136	244	241	258	136
2	-	146	176	176	42	176	176	63	126	63	176
3	C22L	122	-	-	122	-	-	122	-	122	-
4	C21L	111	-	-	113	-	-	113	-	64	-
5	-	128	-	-	109	-	-	103	-	128	-
6	-	137	-	-	128	-	-	259	75	144	-
7	-	198	45	54	198	37	45	38	97	145	45
8	C17L	382	251	251	375	382	233	386	81	424	102
9	C16L	181	181	181	181	181	57	181	200	147	57
10	C15L	89	89	89	-	89	-	91	63	89	-
11	-	51	51	51	51	51	-	51	-	-	-
12	-	190	190	190	190	190	-	114	80	190	-
13	C12L	357	357	357	357	357	-	357	357	357	-
14	C11R	139	140	140	140	140	140	142	140	140	140
15	C10L	331	331	331	331	331	326	331	326	331	326
16	-	44	-	-	-	-	-	-	44	-	-
17	-	83	-	-	-	91	-	-	83	180	91
18	-	62	-	-	-	60	-	-	62	62	60
19	-	124	-	-	-	120	-	-	120	126	120
20	-	90	-	-	-	93	-	-	93	93	93
21	-	142	-	-	-	142	100	-	142	142	142
22	-	135	-	-	-	197	197	-	197	199	197
23	-	77	-	-	-	90	90	-	90	77	90
24	-	71	-	-	-	85	85	-	85	85	85
25	-	55	-	-	-	69	69	-	59	69	69
26	C9L	634	634	634	634	179	113	634	297	634	297

27	C8L	177	184	184	184	177	177	184	177	177	177
28	C7L	150	150	150	150	150	150	150	150	158	150
29	C6L	151	151	155	151	155	155	151	151	151	157
30	C5L	204	224	36	224	36	36	224	224	224	36
31	-	62	-	-	-	-	-	-	-	-	-
32	-	136	222	-	222	-	-	316	189	316	-
33	-	59	39	-	39	-	-	-	39	-	-
34	C3L	263	263	-	263	-	-	263	263	263	-
35	C2L	506	512	-	512	-	-	512	495	512	-
36	C1L	224	227	-	227	-	-	227	227	227	-
37	N1L	117	117	113	117	113	113	117	117	117	113
38	N2L	175	175	170	175	170	170	175	175	175	170
39	-	-	-	-	-	-	-	-	-	-	-
40	-	-	-	-	-	-	-	-	-	-	-
41	M1L	469	472	-	472	-	-	472	299	470	-
42	M2L	220	227	-	227	-	-	227	227	227	-
43	K1L	284	284	98	284	98	98	284	284	284	98
44	K2L	369	369	369	369	369	369	369	369	369	369
45	K3L	88	88	88	88	88	88	88	88	88	88
46	K4L	424	424	424	424	424	424	424	424	424	424
47	K5L	136	175	174	174	174	174	140	174	175	174
48	K6L	81	81	81	64	64	64	81	81	81	64
49	K7R	149	149	149	149	149	149	149	149	149	149
50	F1L	226	226	226	222	222	222	226	226	226	222
51	F2L	147	147	147	147	147	147	147	147	147	147
52	F3L	480	480	480	476	476	476	480	480	480	476
53	F4L	319	319	319	319	319	319	319	319	319	319
54	F5L	321	332	332	97	229	97	332	330	332	97
55	F6L	74	74	74	74	74	74	74	74	74	74
56	F7L	80	80	80	80	80	80	92	80	80	80
57	F8L	65	65	65	65	65	65	65	65	65	65
58	F9L	212	212	212	212	212	212	212	212	212	212
59	F10L	439	439	439	439	439	439	439	439	439	439
60	F11L	348	354	354	100	100	168	354	354	354	100
61	F12L	635	635	635	635	635	635	635	635	635	635
62	-	372	372	372	372	372	372	372	372	372	372

63	F14L	73	87	87	87	87	87	87	87	87	87
64	F15L	158	158	158	158	158	158	158	158	158	158
65	F16L	231	231	231	231	231	231	231	231	231	231
66	F17R	101	101	101	101	101	101	101	101	101	101
67	E1L	479	479	479	346	479	479	479	479	479	479
68	E2L	737	737	737	737	737	737	737	737	737	737
69	E3L	190	190	190	190	190	190	190	190	190	190
70	E4L	259	259	259	259	259	259	259	259	259	259
71	-	189	331	331	331	331	331	331	331	331	331
72	-	149	-	-	-	-	-	-	-	-	-
73	E6R	567	567	567	501	567	567	567	567	567	567
74	E7R	166	166	166	166	166	166	166	166	166	166
75	E8R	273	273	273	273	273	273	273	273	273	273
76	E9L	1005	1006	1006	1006	1006	1006	1006	1006	1006	1006
77	E10R	95	95	95	95	95	95	95	95	95	95
78	E11L	129	129	129	129	129	129	129	129	129	129
79	O1L	666	684	204	50	50	204	684	684	684	204
80	O2L	108	108	108	108	108	108	108	108	108	108
81	I1L	312	312	312	312	312	312	312	312	312	312
82	I2L	73	73	56	56	73	73	73	73	73	73
83	I3L	269	269	269	269	269	269	269	269	269	269
84	I4L	771	771	771	771	771	771	771	771	771	771
85	I5L	79	79	79	79	79	79	79	79	79	79
86	I6L	382	393	393	393	393	393	382	382	382	382
87	I7L	423	423	423	423	423	423	423	423	423	423
88	I8R	676	683	683	683	683	683	683	683	683	683
89	G1L	591	591	591	591	591	591	591	591	591	591
90	G3L	111	111	111	111	111	111	111	111	111	111
91	G2R	220	220	220	220	220	220	220	220	220	220
92	G4L	124	124	124	124	124	124	124	124	124	124
93	G5R	434	434	434	434	434	434	434	434	434	434
94	G5.5R	63	63	63	63	63	63	63	63	63	63
95	G6R	165	165	165	165	165	165	165	165	165	165
96	G7L	371	371	371	371	371	371	371	371	371	371
97	G8R	260	275	275	275	275	275	275	275	275	275
98	G9R	340	340	340	340	340	340	340	340	340	340



Supplementary figure 2. Replication of MVA and 51.2 rMVA in BS-C-1 cells 24 hpi. Initial observations that the virus yield from 51.2 rMVA was 2 logs higher than MVA served as the start point to further evaluate replication, especially in genes acquired by this virus. Statistical significance was determined using Student's t-test.



Supplementary figure 3. Additional deletion mutants generated. 13 deletion mutants were initially generated for this screening. Either single genes or clusters of genes were deleted in 44/47.1 rMVA. The plaques were visualized by fluorescent microscopy 48 hours post infection. Panel A are viruses in which deleted genes are located outside MVA's deleted region. Panel B are viruses with deleted genes located within MVA's deletions.

```

1      10      20      30      40      50      60      70
TACTGAATTAATAATAAAAAATCCCAATCTTGTCAATAAACACACACTGAGAAACAGCATAAACACAAAAATCCATC
80      90      100     110     120     130     140     150
AAAAATGTTGATAAAATATCTGATGTTGTTGTTGCTGCTATGATAAATCAGATCATTCGCCGATAGTGGTAACGCT
160     170     180     190     200     210     220
ATCGAAACGACATCGCCAGAAATACAAACGCTACAACAGATAATCCAGCTATCAGATTA TGCGGTCCAGAGGGAG
230     240     250     260     270     280     290     300
ATGGATATTGTTTACACGGTGA CTGTA TCCACGCTAGAGATA TCGACGGTATG TATTGTAGATGCTCTCATGGTTA
310     320     330     340     350     360     370     380
TACAGGCATTAGATGTCAGCATGTAGTATTAGTAGACTATCAACGTT CAGAAAAACCAAACTACAACGTCATAT
390     400     410     420     430     440     450
ATCCCATCTCCCGGTA TTAGCTTGTA TTAGTAGGCATTATTTATTA TTAACGTGTTGCTATTA TCTGTTTATAGGT
460     470     480     490     500     510     520     530
TCACTCGACGAAC TAAACTACCTATACAAGATA TGGTTGTGCCA TAA TTTTTATAAA TTTTTTTTATGAGTATTTT
540     550     560     570     580     590     600
TACAAAAATGTA TAAAGTGATGTCTTATGTA TATTTATAAAAA TGCTAAATATGCGATGTA TCTATGTTATTTGT
610     620     630     640     647
ATTTATCTAAACAA TACCTCTACCTCTAGATA TTTATACA

```

Supplementary figure 4. Sequence inserted into MVA responsible for the host-range extension. The sequence identified as responsible for MVA's host-range extension consist of the *vgf* ORF and its 3' & 5' UTR presented above. This sequence corresponds to the insert derived from 51.2 rMVA.

Bibliography

1. Zhao, G., et al., *The genome of Yoka poxvirus*. J Virol, 2011. **85**(19): p. 10230-8.
2. McLysaght, A., P.F. Baldi, and B.S. Gaut, *Extensive gene gain associated with adaptive evolution of poxviruses*. Proc Natl Acad Sci U S A, 2003. **100**(26): p. 15655-60.
3. Gubser, C., et al., *Poxvirus genomes: a phylogenetic analysis*. J Gen Virol, 2004. **85**(Pt 1): p. 105-17.
4. Eyler, J.M., *Smallpox in history: the birth, death, and impact of a dread disease*. J Lab Clin Med, 2003. **142**(4): p. 216-20.
5. Stewart, A.J. and P.M. Devlin, *The history of the smallpox vaccine*. J Infect, 2006. **52**(5): p. 329-34.
6. Behbehani, A.M., *The smallpox story: life and death of an old disease*. Microbiol Rev, 1983. **47**(4): p. 455-509.
7. Strohl, E.L., *The Fascinating Lady Mary Wortley Montagu, 1689-1762*. Arch Surg, 1964. **89**: p. 554-8.
8. *WHO Expert Committee on Smallpox Eradication. Second report*. World Health Organ Tech Rep Ser, 1972. **493**: p. 1-64.
9. Fenner, F., *A successful eradication campaign. Global eradication of smallpox*. Rev Infect Dis, 1982. **4**(5): p. 916-30.
10. Jacobs, B.L., et al., *Vaccinia virus vaccines: past, present and future*. Antiviral Res, 2009. **84**(1): p. 1-13.
11. Mayr, A. and E. Munz, *[Changes in the vaccinia virus through continuing passages in chick embryo fibroblast cultures]*. Zentralbl Bakteriol Orig, 1964. **195**(1): p. 24-35.
12. Howles, S., et al., *Vaccination with a modified vaccinia virus Ankara (MVA)-vectored HIV-1 immunogen induces modest vector-specific T cell responses in human subjects*. Vaccine, 2010. **28**(45): p. 7306-12.
13. Kolibab, K., et al., *Highly persistent and effective prime/boost regimens against tuberculosis that use a multivalent modified vaccine virus Ankara-based tuberculosis vaccine with interleukin-15 as a molecular adjuvant*. Clin Vaccine Immunol, 2010. **17**(5): p. 793-801.
14. Song, F., et al., *Middle East respiratory syndrome coronavirus spike protein delivered by modified vaccinia virus Ankara efficiently induces virus-neutralizing antibodies*. J Virol, 2013. **87**(21): p. 11950-4.

15. Remy-Ziller, C., et al., *Immunological characterization of a modified vaccinia virus ankara vector expressing the human papillomavirus 16 e1 protein*. Clin Vaccine Immunol, 2014. **21**(2): p. 147-55.
16. Laxmisha, C., D.M. Thappa, and T.J. Jaisankar, *Clinical profile of molluscum contagiosum in children versus adults*. Dermatol Online J, 2003. **9**(5): p. 1.
17. Senkevich, T.G., et al., *The genome of molluscum contagiosum virus: analysis and comparison with other poxviruses*. Virology, 1997. **233**(1): p. 19-42.
18. Nguyen, H.P., et al., *Treatment of molluscum contagiosum in adult, pediatric, and immunodeficient populations*. J Cutan Med Surg, 2014. **18**: p. 1-8.
19. Rimoin, A.W., et al., *Endemic human monkeypox, Democratic Republic of Congo, 2001-2004*. Emerg Infect Dis, 2007. **13**(6): p. 934-7.
20. Breman, J.G. and D.A. Henderson, *Poxvirus dilemmas--monkeypox, smallpox, and biologic terrorism*. N Engl J Med, 1998. **339**(8): p. 556-9.
21. Sodeik, B., et al., *Assembly of vaccinia virus: incorporation of p14 and p32 into the membrane of the intracellular mature virus*. J Virol, 1995. **69**(6): p. 3560-74.
22. Morgan, C., et al., *Structure and development of viruses observed in the electron microscope. II. Vaccinia and fowl pox viruses*. J Exp Med, 1954. **100**(3): p. 301-10.
23. Dubochet, J., et al., *Structure of intracellular mature vaccinia virus observed by cryoelectron microscopy*. J Virol, 1994. **68**(3): p. 1935-41.
24. Zwartouw, H.T., *The Chemical Composition of Vaccinia Virus*. J Gen Microbiol, 1964. **34**: p. 115-23.
25. Geshelin, P. and K.I. Berns, *Characterization and localization of the naturally occurring cross-links in vaccinia virus DNA*. J Mol Biol, 1974. **88**(4): p. 785-96.
26. Goebel, S.J., et al., *The complete DNA sequence of vaccinia virus*. Virology, 1990. **179**(1): p. 247-66, 517-63.
27. Mendez-Rios, J.D., et al., *Genome sequence of erythromelalgia-related poxvirus identifies it as an ectromelia virus strain*. PLoS One, 2012. **7**(4): p. e34604.
28. Tulman, E.R., et al., *The genome of canarypox virus*. J Virol, 2004. **78**(1): p. 353-66.
29. Meisinger-Henschel, C., et al., *Genomic sequence of chorioallantois vaccinia virus Ankara, the ancestor of modified vaccinia virus Ankara*. J Gen Virol, 2007. **88**(Pt 12): p. 3249-59.
30. Upton, C., et al., *Poxvirus orthologous clusters: toward defining the minimum essential poxvirus genome*. J Virol, 2003. **77**(13): p. 7590-600.

31. Ehlers, A., et al., *Poxvirus Orthologous Clusters (POCs)*. Bioinformatics, 2002. **18**(11): p. 1544-5.
32. Merchlinsky, M., C.F. Garon, and B. Moss, *Molecular cloning and sequence of the concatemer junction from vaccinia virus replicative DNA. Viral nuclease cleavage sites in cruciform structures*. J Mol Biol, 1988. **199**(3): p. 399-413.
33. Wittek, R., et al., *Inverted terminal repeats in rabbit poxvirus and vaccinia virus DNA*. J Virol, 1978. **28**(1): p. 171-81.
34. Wittek, R. and B. Moss, *Tandem repeats within the inverted terminal repetition of vaccinia virus DNA*. Cell, 1980. **21**(1): p. 277-84.
35. Baroudy, B.M. and B. Moss, *Sequence homologies of diverse length tandem repetitions near ends of vaccinia virus genome suggest unequal crossing over*. Nucleic Acids Res, 1982. **10**(18): p. 5673-9.
36. Winters, E., B.M. Baroudy, and B. Moss, *Molecular cloning of the terminal hairpin of vaccinia virus DNA as an imperfect palindrome in an Escherichia coli plasmid*. Gene, 1985. **37**(1-3): p. 221-8.
37. Baroudy, B.M., S. Venkatesan, and B. Moss, *Incompletely base-paired flip-flop terminal loops link the two DNA strands of the vaccinia virus genome into one uninterrupted polynucleotide chain*. Cell, 1982. **28**(2): p. 315-24.
38. Chernomordik, L.V. and M.M. Kozlov, *Membrane hemifusion: crossing a chasm in two leaps*. Cell, 2005. **123**(3): p. 375-82.
39. Laliberte, J.P., A.S. Weisberg, and B. Moss, *The membrane fusion step of vaccinia virus entry is cooperatively mediated by multiple viral proteins and host cell components*. PLoS Pathog, 2011. **7**(12): p. e1002446.
40. Bisht, H., A.S. Weisberg, and B. Moss, *Vaccinia virus I1 protein is required for cell entry and membrane fusion*. J Virol, 2008. **82**(17): p. 8687-94.
41. Brown, E., T.G. Senkevich, and B. Moss, *Vaccinia virus F9 virion membrane protein is required for entry but not virus assembly, in contrast to the related I1 protein*. J Virol, 2006. **80**(19): p. 9455-64.
42. Hiller, G. and K. Weber, *Golgi-derived membranes that contain an acylated viral polypeptide are used for vaccinia virus envelopment*. J Virol, 1985. **55**(3): p. 651-9.
43. Izmailyan, R.A., et al., *The envelope G3L protein is essential for entry of vaccinia virus into host cells*. J Virol, 2006. **80**(17): p. 8402-10.
44. Nichols, R.J., et al., *The vaccinia virus gene I2L encodes a membrane protein with an essential role in virion entry*. J Virol, 2008. **82**(20): p. 10247-61.

45. Ojeda, S., T.G. Senkevich, and B. Moss, *Entry of vaccinia virus and cell-cell fusion require a highly conserved cysteine-rich membrane protein encoded by the A16L gene*. J Virol, 2006. **80**(1): p. 51-61.
46. Satheshkumar, P.S. and B. Moss, *Characterization of a newly identified 35-amino-acid component of the vaccinia virus entry/fusion complex conserved in all chordopoxviruses*. J Virol, 2009. **83**(24): p. 12822-32.
47. Schmelz, M., et al., *Assembly of vaccinia virus: the second wrapping cisterna is derived from the trans Golgi network*. J Virol, 1994. **68**(1): p. 130-47.
48. Senkevich, T.G. and B. Moss, *Vaccinia virus H2 protein is an essential component of a complex involved in virus entry and cell-cell fusion*. J Virol, 2005. **79**(8): p. 4744-54.
49. Senkevich, T.G., et al., *Poxvirus multiprotein entry-fusion complex*. Proc Natl Acad Sci U S A, 2005. **102**(51): p. 18572-7.
50. Senkevich, T.G., B.M. Ward, and B. Moss, *Vaccinia virus A28L gene encodes an essential protein component of the virion membrane with intramolecular disulfide bonds formed by the viral cytoplasmic redox pathway*. J Virol, 2004. **78**(5): p. 2348-56.
51. Townsley, A.C., T.G. Senkevich, and B. Moss, *The product of the vaccinia virus L5R gene is a fourth membrane protein encoded by all poxviruses that is required for cell entry and cell-cell fusion*. J Virol, 2005. **79**(17): p. 10988-98.
52. Townsley, A.C., T.G. Senkevich, and B. Moss, *Vaccinia virus A21 virion membrane protein is required for cell entry and fusion*. J Virol, 2005. **79**(15): p. 9458-69.
53. Wolfe, C.L., S. Ojeda, and B. Moss, *Transcriptional repression and RNA silencing act synergistically to demonstrate the function of the eleventh component of the vaccinia virus entry-fusion complex*. J Virol, 2012. **86**(1): p. 293-301.
54. Huang, C.Y., et al., *A novel cellular protein, VPEF, facilitates vaccinia virus penetration into HeLa cells through fluid phase endocytosis*. J Virol, 2008. **82**(16): p. 7988-99.
55. Mercer, J. and A. Helenius, *Vaccinia virus uses macropinocytosis and apoptotic mimicry to enter host cells*. Science, 2008. **320**(5875): p. 531-5.
56. Mercer, J., et al., *Vaccinia virus strains use distinct forms of macropinocytosis for host-cell entry*. Proc Natl Acad Sci U S A, 2010. **107**(20): p. 9346-51.
57. Moser, T.S., et al., *A kinome RNAi screen identified AMPK as promoting poxvirus entry through the control of actin dynamics*. PLoS Pathog, 2010. **6**(6): p. e1000954.
58. Moss, B., *Poxvirus entry and membrane fusion*. Virology, 2006. **344**(1): p. 48-54.
59. Sandgren, K.J., et al., *A differential role for macropinocytosis in mediating entry of the two forms of vaccinia virus into dendritic cells*. PLoS Pathog, 2010. **6**(4): p. e1000866.

60. Villa, N.Y., et al., *Myxoma and vaccinia viruses exploit different mechanisms to enter and infect human cancer cells*. Virology, 2010. **401**(2): p. 266-79.
61. Baldick, C.J., Jr., J.G. Keck, and B. Moss, *Mutational analysis of the core, spacer, and initiator regions of vaccinia virus intermediate-class promoters*. J Virol, 1992. **66**(8): p. 4710-9.
62. Davison, A.J. and B. Moss, *Structure of vaccinia virus early promoters*. J Mol Biol, 1989. **210**(4): p. 749-69.
63. Davison, A.J. and B. Moss, *Structure of vaccinia virus late promoters*. J Mol Biol, 1989. **210**(4): p. 771-84.
64. Ahn, B.Y., P.D. Gershon, and B. Moss, *RNA polymerase-associated protein Rap94 confers promoter specificity for initiating transcription of vaccinia virus early stage genes*. J Biol Chem, 1994. **269**(10): p. 7552-7.
65. Baroudy, B.M. and B. Moss, *Purification and characterization of a DNA-dependent RNA polymerase from vaccinia virions*. J Biol Chem, 1980. **255**(9): p. 4372-80.
66. Broyles, S.S., et al., *Purification of a factor required for transcription of vaccinia virus early genes*. J Biol Chem, 1988. **263**(22): p. 10754-60.
67. Keck, J.G., C.J. Baldick, Jr., and B. Moss, *Role of DNA replication in vaccinia virus gene expression: a naked template is required for transcription of three late trans-activator genes*. Cell, 1990. **61**(5): p. 801-9.
68. Sanz, P. and B. Moss, *Identification of a transcription factor, encoded by two vaccinia virus early genes, that regulates the intermediate stage of viral gene expression*. Proc Natl Acad Sci U S A, 1999. **96**(6): p. 2692-7.
69. Baldick, C.J., Jr. and B. Moss, *Characterization and temporal regulation of mRNAs encoded by vaccinia virus intermediate-stage genes*. J Virol, 1993. **67**(6): p. 3515-27.
70. Yang, Z., et al., *Expression profiling of the intermediate and late stages of poxvirus replication*. J Virol, 2011. **85**(19): p. 9899-908.
71. Gershowitz, A., R.F. Boone, and B. Moss, *Multiple roles for ATP in the synthesis and processing of mRNA by vaccinia virus: specific inhibitory effects of adenosine (beta,gamma-imido) triphosphate*. J Virol, 1978. **27**(2): p. 399-408.
72. Golini, F. and J.R. Kates, *A soluble transcription system derived from purified vaccinia virions*. J Virol, 1985. **53**(1): p. 205-13.
73. Kates, J.R. and B.R. McAuslan, *Poxvirus DNA-dependent RNA polymerase*. Proc Natl Acad Sci U S A, 1967. **58**(1): p. 134-41.
74. Rohrmann, G. and B. Moss, *Transcription of vaccinia virus early genes by a template-dependent soluble extract of purified virions*. J Virol, 1985. **56**(2): p. 349-55.

75. Ahn, B.Y. and B. Moss, *RNA polymerase-associated transcription specificity factor encoded by vaccinia virus*. Proc Natl Acad Sci U S A, 1992. **89**(8): p. 3536-40.
76. Deng, L. and S. Shuman, *A role for the H4 subunit of vaccinia RNA polymerase in transcription initiation at a viral early promoter*. J Biol Chem, 1994. **269**(19): p. 14323-8.
77. Kane, E.M. and S. Shuman, *Temperature-sensitive mutations in the vaccinia virus H4 gene encoding a component of the virion RNA polymerase*. J Virol, 1992. **66**(10): p. 5752-62.
78. Gershon, P.D., et al., *Poly(A) polymerase and a dissociable polyadenylation stimulatory factor encoded by vaccinia virus*. Cell, 1991. **66**(6): p. 1269-78.
79. Szymczak, A.L. and D.A. Vignali, *Development of 2A peptide-based strategies in the design of multicistronic vectors*. Expert Opin Biol Ther, 2005. **5**(5): p. 627-38.
80. Latner, D.R., et al., *The vaccinia virus bifunctional gene J3 (nucleoside-2'-O)-methyltransferase and poly(A) polymerase stimulatory factor is implicated as a positive transcription elongation factor by two genetic approaches*. Virology, 2000. **269**(2): p. 345-55.
81. Zhang, Y., B.Y. Ahn, and B. Moss, *Targeting of a multicomponent transcription apparatus into assembling vaccinia virus particles requires RAP94, an RNA polymerase-associated protein*. J Virol, 1994. **68**(3): p. 1360-70.
82. Mohamed, M.R., et al., *Interaction between the J3R subunit of vaccinia virus poly(A) polymerase and the H4L subunit of the viral RNA polymerase*. Virology, 2001. **280**(1): p. 143-52.
83. Mohamed, M.R. and E.G. Niles, *The viral RNA polymerase H4L subunit is required for Vaccinia virus early gene transcription termination*. J Biol Chem, 2001. **276**(23): p. 20758-65.
84. Yang, Z. and B. Moss, *Interaction of the vaccinia virus RNA polymerase-associated 94-kilodalton protein with the early transcription factor*. J Virol, 2009. **83**(23): p. 12018-26.
85. Broyles, S.S., *Vaccinia virus transcription*. J Gen Virol, 2003. **84**(Pt 9): p. 2293-303.
86. Vos, J.C., M. Saker, and H.G. Stunnenberg, *Promoter melting by a stage-specific vaccinia virus transcription factor is independent of the presence of RNA polymerase*. Cell, 1991. **65**(1): p. 105-13.
87. Vos, J.C., M. Saker, and H.G. Stunnenberg, *Vaccinia virus capping enzyme is a transcription initiation factor*. EMBO J, 1991. **10**(9): p. 2553-8.
88. Rosales, R., G. Sutter, and B. Moss, *A cellular factor is required for transcription of vaccinia viral intermediate-stage genes*. Proc Natl Acad Sci U S A, 1994. **91**(9): p. 3794-8.

89. Rosales, R., et al., *Purification and identification of a vaccinia virus-encoded intermediate stage promoter-specific transcription factor that has homology to eukaryotic transcription factor SII (TFIIS) and an additional role as a viral RNA polymerase subunit.* J Biol Chem, 1994. **269**(19): p. 14260-7.
90. Schnierle, B.S., P.D. Gershon, and B. Moss, *Cap-specific mRNA (nucleoside-O2')-methyltransferase and poly(A) polymerase stimulatory activities of vaccinia virus are mediated by a single protein.* Proc Natl Acad Sci U S A, 1992. **89**(7): p. 2897-901.
91. Sanz, P. and B. Moss, *A new vaccinia virus intermediate transcription factor.* J Virol, 1998. **72**(8): p. 6880-3.
92. Lin, S., W. Chen, and S.S. Broyles, *The vaccinia virus BIR gene product is a serine/threonine protein kinase.* J Virol, 1992. **66**(5): p. 2717-23.
93. Banham, A.H. and G.L. Smith, *Vaccinia virus gene BIR encodes a 34-kDa serine/threonine protein kinase that localizes in cytoplasmic factories and is packaged into virions.* Virology, 1992. **191**(2): p. 803-12.
94. Kovacs, G.R., N. Vasilakis, and B. Moss, *Regulation of viral intermediate gene expression by the vaccinia virus B1 protein kinase.* J Virol, 2001. **75**(9): p. 4048-55.
95. Wiebe, M.S. and P. Traktman, *Poxviral B1 kinase overcomes barrier to autointegration factor, a host defense against virus replication.* Cell Host Microbe, 2007. **1**(3): p. 187-97.
96. Zhang, Y., J.G. Keck, and B. Moss, *Transcription of viral late genes is dependent on expression of the viral intermediate gene G8R in cells infected with an inducible conditional-lethal mutant vaccinia virus.* J Virol, 1992. **66**(11): p. 6470-9.
97. Keck, J.G., G.R. Kovacs, and B. Moss, *Overexpression, purification, and late transcription factor activity of the 17-kilodalton protein encoded by the vaccinia virus ALL gene.* J Virol, 1993. **67**(10): p. 5740-8.
98. Keck, J.G., F. Feigenbaum, and B. Moss, *Mutational analysis of a predicted zinc-binding motif in the 26-kilodalton protein encoded by the vaccinia virus A2L gene: correlation of zinc binding with late transcriptional transactivation activity.* J Virol, 1993. **67**(10): p. 5749-53.
99. Knutson, B.A., J. Oh, and S.S. Broyles, *Downregulation of vaccinia virus intermediate and late promoters by host transcription factor YY1.* J Gen Virol, 2009. **90**(Pt 7): p. 1592-9.
100. Broyles, S.S., et al., *Transcription factor YY1 is a vaccinia virus late promoter activator.* J Biol Chem, 1999. **274**(50): p. 35662-7.
101. Wright, C.F., B.W. Oswald, and S. Dellis, *Vaccinia virus late transcription is activated in vitro by cellular heterogeneous nuclear ribonucleoproteins.* J Biol Chem, 2001. **276**(44): p. 40680-6.

102. Dellis, S., et al., *Protein interactions among the vaccinia virus late transcription factors*. Virology, 2004. **329**(2): p. 328-36.
103. D'Costa, S.M., et al., *Vaccinia H5 is a multifunctional protein involved in viral DNA replication, postreplicative gene transcription, and virion morphogenesis*. Virology, 2010. **401**(1): p. 49-60.
104. Deng, L. and S. Shuman, *Vaccinia NPH-I, a DExH-box ATPase, is the energy coupling factor for mRNA transcription termination*. Genes Dev, 1998. **12**(4): p. 538-46.
105. Latner, D.R., et al., *The positive transcription elongation factor activity of the vaccinia virus J3 protein is independent from its (nucleoside-2'-O-) methyltransferase and poly(A) polymerase stimulatory functions*. Virology, 2002. **301**(1): p. 64-80.
106. Black, E.P. and R.C. Condit, *Phenotypic characterization of mutants in vaccinia virus gene G2R, a putative transcription elongation factor*. J Virol, 1996. **70**(1): p. 47-54.
107. Yuen, L., A.J. Davison, and B. Moss, *Early promoter-binding factor from vaccinia virions*. Proc Natl Acad Sci U S A, 1987. **84**(17): p. 6069-73.
108. Yang, Z., et al., *Genome-wide analysis of the 5' and 3' ends of vaccinia virus early mRNAs delineates regulatory sequences of annotated and anomalous transcripts*. J Virol, 2011. **85**(12): p. 5897-909.
109. Boone, R.F. and B. Moss, *Methylated 5'-terminal sequences of vaccinia virus mRNA species made in vivo at early and late times after infection*. Virology, 1977. **79**(1): p. 67-80.
110. Wei, C.M. and B. Moss, *Methylated nucleotides block 5'-terminus of vaccinia virus messenger RNA*. Proc Natl Acad Sci U S A, 1975. **72**(1): p. 318-22.
111. Martin, S.A. and B. Moss, *Modification of RNA by mRNA guanylyltransferase and mRNA (guanine-7-)methyltransferase from vaccinia virions*. J Biol Chem, 1975. **250**(24): p. 9330-5.
112. Venkatesan, S., A. Gershowitz, and B. Moss, *Modification of the 5' end of mRNA. Association of RNA triphosphatase with the RNA guanylyltransferase-RNA (guanine-7-)methyltransferase complex from vaccinia virus*. J Biol Chem, 1980. **255**(3): p. 903-8.
113. Venkatesan, S., A. Gershowitz, and B. Moss, *Purification and characterization of mRNA guanylyltransferase from HeLa cell nuclei*. J Biol Chem, 1980. **255**(7): p. 2829-34.
114. Kates, J. and J. Beeson, *Ribonucleic acid synthesis in vaccinia virus. I. The mechanism of synthesis and release of RNA in vaccinia cores*. J Mol Biol, 1970. **50**(1): p. 1-18.
115. Kates, J. and J. Beeson, *Ribonucleic acid synthesis in vaccinia virus. II. Synthesis of polyriboadenylic acid*. J Mol Biol, 1970. **50**(1): p. 19-33.
116. Gershon, P.D. and B. Moss, *Stimulation of poly(A) tail elongation by the VP39 subunit of the vaccinia virus-encoded poly(A) polymerase*. J Biol Chem, 1993. **268**(3): p. 2203-10.

117. Yuen, L. and B. Moss, *Oligonucleotide sequence signaling transcriptional termination of vaccinia virus early genes*. Proc Natl Acad Sci U S A, 1987. **84**(18): p. 6417-21.
118. Yang, Z., et al., *Pervasive initiation and 3'-end formation of poxvirus postreplicative RNAs*. J Biol Chem, 2012. **287**(37): p. 31050-60.
119. Ahn, B.Y., E.V. Jones, and B. Moss, *Identification of the vaccinia virus gene encoding an 18-kilodalton subunit of RNA polymerase and demonstration of a 5' poly(A) leader on its early transcript*. J Virol, 1990. **64**(6): p. 3019-24.
120. Ink, B.S. and D.J. Pickup, *Vaccinia virus directs the synthesis of early mRNAs containing 5' poly(A) sequences*. Proc Natl Acad Sci U S A, 1990. **87**(4): p. 1536-40.
121. Patel, D.D. and D.J. Pickup, *Messenger RNAs of a strongly-expressed late gene of cowpox virus contain 5'-terminal poly(A) sequences*. EMBO J, 1987. **6**(12): p. 3787-94.
122. Schwer, B., et al., *Discontinuous transcription or RNA processing of vaccinia virus late messengers results in a 5' poly(A) leader*. Cell, 1987. **50**(2): p. 163-9.
123. Katsafanas, G.C. and B. Moss, *Colocalization of transcription and translation within cytoplasmic poxvirus factories coordinates viral expression and subjugates host functions*. Cell Host Microbe, 2007. **2**(4): p. 221-8.
124. Cairns, J., *The initiation of vaccinia infection*. Virology, 1960. **11**: p. 603-23.
125. Harford, C.G., A. Hamlin, and E. Rieders, *Electron microscopic autoradiography of DNA synthesis in cells infected with vaccinia virus*. Exp Cell Res, 1966. **42**(1): p. 50-7.
126. Dales, S. and L. Siminovitch, *The development of vaccinia virus in Earle's L strain cells as examined by electron microscopy*. J Biophys Biochem Cytol, 1961. **10**: p. 475-503.
127. Moss, B., *Poxvirus DNA replication*. Cold Spring Harb Perspect Biol, 2013. **5**(9).
128. Jones, E.V. and B. Moss, *Mapping of the vaccinia virus DNA polymerase gene by marker rescue and cell-free translation of selected RNA*. J Virol, 1984. **49**(1): p. 72-7.
129. Traktman, P., et al., *Transcriptional mapping of the DNA polymerase gene of vaccinia virus*. J Virol, 1984. **49**(1): p. 125-31.
130. Challberg, M.D. and P.T. Englund, *Purification and properties of the deoxyribonucleic acid polymerase induced by vaccinia virus*. J Biol Chem, 1979. **254**(16): p. 7812-9.
131. Willer, D.O., et al., *In vitro concatemer formation catalyzed by vaccinia virus DNA polymerase*. Virology, 2000. **278**(2): p. 562-9.
132. Willer, D.O., et al., *Vaccinia virus DNA polymerase promotes DNA pairing and strand-transfer reactions*. Virology, 1999. **257**(2): p. 511-23.

133. Hamilton, M.D. and D.H. Evans, *Enzymatic processing of replication and recombination intermediates by the vaccinia virus DNA polymerase*. Nucleic Acids Res, 2005. **33**(7): p. 2259-68.
134. Evans, E., et al., *The vaccinia virus D5 protein, which is required for DNA replication, is a nucleic acid-independent nucleoside triphosphatase*. J Virol, 1995. **69**(9): p. 5353-61.
135. Boyle, K.A., L. Arps, and P. Traktman, *Biochemical and genetic analysis of the vaccinia virus d5 protein: Multimerization-dependent ATPase activity is required to support viral DNA replication*. J Virol, 2007. **81**(2): p. 844-59.
136. De Silva, F.S., N. Paran, and B. Moss, *Products and substrate/template usage of vaccinia virus DNA primase*. Virology, 2009. **383**(1): p. 136-41.
137. Upton, C., D.T. Stuart, and G. McFadden, *Identification of a poxvirus gene encoding a uracil DNA glycosylase*. Proc Natl Acad Sci U S A, 1993. **90**(10): p. 4518-22.
138. Stuart, D.T., et al., *A poxvirus-encoded uracil DNA glycosylase is essential for virus viability*. J Virol, 1993. **67**(5): p. 2503-12.
139. Holzer, G.W. and F.G. Falkner, *Construction of a vaccinia virus deficient in the essential DNA repair enzyme uracil DNA glycosylase by a complementing cell line*. J Virol, 1997. **71**(7): p. 4997-5002.
140. De Silva, F.S. and B. Moss, *Vaccinia virus uracil DNA glycosylase has an essential role in DNA synthesis that is independent of its glycosylase activity: catalytic site mutations reduce virulence but not virus replication in cultured cells*. J Virol, 2003. **77**(1): p. 159-66.
141. McCraith, S., et al., *Genome-wide analysis of vaccinia virus protein-protein interactions*. Proc Natl Acad Sci U S A, 2000. **97**(9): p. 4879-84.
142. Punjabi, A., et al., *Clustered charge-to-alanine mutagenesis of the vaccinia virus A20 gene: temperature-sensitive mutants have a DNA-minus phenotype and are defective in the production of processive DNA polymerase activity*. J Virol, 2001. **75**(24): p. 12308-18.
143. Rempel, R.E. and P. Traktman, *Vaccinia virus B1 kinase: phenotypic analysis of temperature-sensitive mutants and enzymatic characterization of recombinant proteins*. J Virol, 1992. **66**(7): p. 4413-26.
144. Nichols, R.J., M.S. Wiebe, and P. Traktman, *The vaccinia-related kinases phosphorylate the N' terminus of BAF, regulating its interaction with DNA and its retention in the nucleus*. Mol Biol Cell, 2006. **17**(5): p. 2451-64.
145. Ibrahim, N., A. Wicklund, and M.S. Wiebe, *Molecular characterization of the host defense activity of the barrier to autointegration factor against vaccinia virus*. J Virol, 2011. **85**(22): p. 11588-600.

146. Brown, N.G., et al., *Identification of sites phosphorylated by the vaccinia virus B1R kinase in viral protein H5R*. BMC Biochem, 2000. **1**: p. 2.
147. Beaud, G., et al., *Ribosomal protein S2/Sa kinase purified from HeLa cells infected with vaccinia virus corresponds to the B1R protein kinase and phosphorylates in vitro the viral ssDNA-binding protein*. J Gen Virol, 1994. **75 (Pt 2)**: p. 283-93.
148. Beaud, G., et al., *Identification of induced protein kinase activities specific for the ribosomal proteins uniquely phosphorylated during infection of HeLa cells with vaccinia virus*. FEBS Lett, 1989. **259(1)**: p. 10-4.
149. Beaud, G., R. Beaud, and D.P. Leader, *Vaccinia virus gene H5R encodes a protein that is phosphorylated by the multisubstrate vaccinia virus B1R protein kinase*. J Virol, 1995. **69(3)**: p. 1819-26.
150. Kerr, S.M. and G.L. Smith, *Vaccinia virus encodes a polypeptide with DNA ligase activity*. Nucleic Acids Res, 1989. **17(22)**: p. 9039-50.
151. Shuman, S., *Vaccinia virus DNA ligase: specificity, fidelity, and inhibition*. Biochemistry, 1995. **34(49)**: p. 16138-47.
152. Merchlinsky, M. and B. Moss, *Resolution of linear minichromosomes with hairpin ends from circular plasmids containing vaccinia virus concatemer junctions*. Cell, 1986. **45(6)**: p. 879-84.
153. Merchlinsky, M. and B. Moss, *Nucleotide sequence required for resolution of the concatemer junction of vaccinia virus DNA*. J Virol, 1989. **63(10)**: p. 4354-61.
154. Merchlinsky, M. and B. Moss, *Resolution of vaccinia virus DNA concatemer junctions requires late-gene expression*. J Virol, 1989. **63(4)**: p. 1595-603.
155. Culyba, M.J., et al., *DNA branch nuclease activity of vaccinia A22 resolvase*. J Biol Chem, 2007. **282(48)**: p. 34644-52.
156. Culyba, M.J., et al., *DNA cleavage by the A22R resolvase of vaccinia virus*. Virology, 2006. **352(2)**: p. 466-76.
157. Garcia, A.D. and B. Moss, *Repression of vaccinia virus Holliday junction resolvase inhibits processing of viral DNA into unit-length genomes*. J Virol, 2001. **75(14)**: p. 6460-71.
158. Shuman, S. and B. Moss, *Identification of a vaccinia virus gene encoding a type I DNA topoisomerase*. Proc Natl Acad Sci U S A, 1987. **84(21)**: p. 7478-82.
159. Shuman, S., M. Golder, and B. Moss, *Characterization of vaccinia virus DNA topoisomerase I expressed in Escherichia coli*. J Biol Chem, 1988. **263(31)**: p. 16401-7.
160. Muzyczka, N., et al., *The genetics of adeno-associated virus*. Adv Exp Med Biol, 1984. **179**: p. 151-61.

161. Moyer, R.W. and R.L. Graves, *The mechanism of cytoplasmic orthopoxvirus DNA replication*. Cell, 1981. **27**(2 Pt 1): p. 391-401.
162. Olgiati, D.D., B.G. Pogo, and S. Dales, *Evidence for RNA linked to nascent DNA in HeLa cells*. J Cell Biol, 1976. **68**(3): p. 557-66.
163. Esteban, M., L. Flores, and J.A. Holowczak, *Model for vaccinia virus DNA replication*. Virology, 1977. **83**(2): p. 467-73.
164. Paran, N., et al., *Cellular DNA ligase I is recruited to cytoplasmic vaccinia virus factories and masks the role of the vaccinia ligase in viral DNA replication*. Cell Host Microbe, 2009. **6**(6): p. 563-9.
165. DeLange, A.M. and G. McFadden, *Sequence-nonspecific replication of transfected plasmid DNA in poxvirus-infected cells*. Proc Natl Acad Sci U S A, 1986. **83**(3): p. 614-8.
166. Du, S. and P. Traktman, *Vaccinia virus DNA replication: two hundred base pairs of telomeric sequence confer optimal replication efficiency on minichromosome templates*. Proc Natl Acad Sci U S A, 1996. **93**(18): p. 9693-8.
167. Pogo, B.G., E.M. Berkowitz, and S. Dales, *Investigation of vaccinia virus DNA replication employing a conditional lethal mutant defective in DNA*. Virology, 1984. **132**(2): p. 436-44.
168. Bahar, M.W., et al., *Insights into the evolution of a complex virus from the crystal structure of vaccinia virus D13*. Structure, 2011. **19**(7): p. 1011-20.
169. Sodeik, B., et al., *Assembly of vaccinia virus: role of the intermediate compartment between the endoplasmic reticulum and the Golgi stacks*. J Cell Biol, 1993. **121**(3): p. 521-41.
170. Maruri-Avidal, L., A.S. Weisberg, and B. Moss, *Direct formation of vaccinia virus membranes from the endoplasmic reticulum in the absence of the newly characterized L2-interacting protein A30.5*. J Virol, 2013. **87**(22): p. 12313-26.
171. Maruri-Avidal, L., A.S. Weisberg, and B. Moss, *Association of the vaccinia virus A11 protein with the endoplasmic reticulum and crescent precursors of immature virions*. J Virol, 2013. **87**(18): p. 10195-206.
172. Moss, B. and E.N. Rosenblum, *Letter: Protein cleavage and poxvirus morphogenesis: tryptic peptide analysis of core precursors accumulated by blocking assembly with rifampicin*. J Mol Biol, 1973. **81**(2): p. 267-9.
173. Dales, S. and B.G. Pogo, *Biology of poxviruses*. Virol Monogr, 1981. **18**: p. 1-109.
174. Payne, L.G. and K. Kristenson, *Mechanism of vaccinia virus release and its specific inhibition by NI-isonicotinoyl-N2-3-methyl-4-chlorobenzoylhydrazine*. J Virol, 1979. **32**(2): p. 614-22.

175. Parrish, S., W. Resch, and B. Moss, *Vaccinia virus D10 protein has mRNA decapping activity, providing a mechanism for control of host and viral gene expression*. Proc Natl Acad Sci U S A, 2007. **104**(7): p. 2139-44.
176. Parrish, S. and B. Moss, *Characterization of a second vaccinia virus mRNA-decapping enzyme conserved in poxviruses*. J Virol, 2007. **81**(23): p. 12973-8.
177. Mazzon, M., et al., *A mechanism for induction of a hypoxic response by vaccinia virus*. Proc Natl Acad Sci U S A, 2013. **110**(30): p. 12444-9.
178. Smith, G.L., et al., *Vaccinia virus immune evasion: mechanisms, virulence and immunogenicity*. J Gen Virol, 2013. **94**(Pt 11): p. 2367-92.
179. Isaacs, A. and J. Lindenmann, *Virus interference. I. The interferon*. Proc R Soc Lond B Biol Sci, 1957. **147**(927): p. 258-67.
180. Lindenmann, J. and A. Isaacs, [*Research on viral interference*]. Schweiz Z Pathol Bakteriologie, 1957. **20**(5): p. 640-6.
181. Isaacs, A. and J. Lindenmann, *Virus interference. I. The interferon. By A. Isaacs and J. Lindenmann, 1957*. J Interferon Res, 1987. **7**(5): p. 429-38.
182. Levy, H.B., *Studies on the Mechanism of Interferon Action. Ii. The Effect of Interferon on Some Early Events in Mengo Virus Infection in L Cells*. Virology, 1964. **22**: p. 575-9.
183. Joklik, W.K. and T.C. Merigan, *Concerning the mechanism of action of interferon*. Proc Natl Acad Sci U S A, 1966. **56**(2): p. 558-65.
184. Symons, J.A., A. Alcami, and G.L. Smith, *Vaccinia virus encodes a soluble type I interferon receptor of novel structure and broad species specificity*. Cell, 1995. **81**(4): p. 551-60.
185. Waibler, Z., et al., *Vaccinia virus-mediated inhibition of type I interferon responses is a multifactorial process involving the soluble type I interferon receptor B18 and intracellular components*. J Virol, 2009. **83**(4): p. 1563-71.
186. Alcami, A. and G.L. Smith, *The vaccinia virus soluble interferon-gamma receptor is a homodimer*. J Gen Virol, 2002. **83**(Pt 3): p. 545-9.
187. Schneider, W.M., M.D. Chevillotte, and C.M. Rice, *Interferon-Stimulated Genes: A Complex Web of Host Defenses*. Annu Rev Immunol, 2014.
188. Mann, B.A., et al., *Vaccinia virus blocks Stat1-dependent and Stat1-independent gene expression induced by type I and type II interferons*. J Interferon Cytokine Res, 2008. **28**(6): p. 367-80.
189. Najjarro, P., P. Traktman, and J.A. Lewis, *Vaccinia virus blocks gamma interferon signal transduction: viral Vh1 phosphatase reverses Stat1 activation*. J Virol, 2001. **75**(7): p. 3185-96.

190. Symons, J.A., et al., *The vaccinia virus C12L protein inhibits mouse IL-18 and promotes virus virulence in the murine intranasal model*. J Gen Virol, 2002. **83**(Pt 11): p. 2833-44.
191. Suresh, R. and D.M. Mosser, *Pattern recognition receptors in innate immunity, host defense, and immunopathology*. Adv Physiol Educ, 2013. **37**(4): p. 284-91.
192. Der, S.D. and A.S. Lau, *Involvement of the double-stranded-RNA-dependent kinase PKR in interferon expression and interferon-mediated antiviral activity*. Proc Natl Acad Sci U S A, 1995. **92**(19): p. 8841-5.
193. Francois, C., et al., *Expression of hepatitis C virus proteins interferes with the antiviral action of interferon independently of PKR-mediated control of protein synthesis*. J Virol, 2000. **74**(12): p. 5587-96.
194. Kalali, B.N., et al., *Double-stranded RNA induces an antiviral defense status in epidermal keratinocytes through TLR3-, PKR-, and MDA5/RIG-I-mediated differential signaling*. J Immunol, 2008. **181**(4): p. 2694-704.
195. Williams, B.R., *PKR; a sentinel kinase for cellular stress*. Oncogene, 1999. **18**(45): p. 6112-20.
196. Ludwig, H., et al., *Double-stranded RNA-binding protein E3 controls translation of viral intermediate RNA, marking an essential step in the life cycle of modified vaccinia virus Ankara*. J Gen Virol, 2006. **87**(Pt 5): p. 1145-55.
197. Ludwig, H., et al., *Role of viral factor E3L in modified vaccinia virus ankara infection of human HeLa Cells: regulation of the virus life cycle and identification of differentially expressed host genes*. J Virol, 2005. **79**(4): p. 2584-96.
198. Chang, H.W., J.C. Watson, and B.L. Jacobs, *The E3L gene of vaccinia virus encodes an inhibitor of the interferon-induced, double-stranded RNA-dependent protein kinase*. Proc Natl Acad Sci U S A, 1992. **89**(11): p. 4825-9.
199. Whitaker-Dowling, P. and J.S. Youngner, *Vaccinia rescue of VSV from interferon-induced resistance: reversal of translation block and inhibition of protein kinase activity*. Virology, 1983. **131**(1): p. 128-36.
200. Paez, E. and M. Esteban, *Resistance of vaccinia virus to interferon is related to an interference phenomenon between the virus and the interferon system*. Virology, 1984. **134**(1): p. 12-28.
201. Guerra, S., et al., *Vaccinia virus E3 protein prevents the antiviral action of ISG15*. PLoS Pathog, 2008. **4**(7): p. e1000096.
202. Beattie, E., J. Tartaglia, and E. Paoletti, *Vaccinia virus-encoded eIF-2 alpha homolog abrogates the antiviral effect of interferon*. Virology, 1991. **183**(1): p. 419-22.
203. Delaloye, J., et al., *Innate immune sensing of modified vaccinia virus Ankara (MVA) is mediated by TLR2-TLR6, MDA-5 and the NALP3 inflammasome*. PLoS Pathog, 2009. **5**(6): p. e1000480.

204. Wyatt, L.S., et al., *Marker rescue of the host range restriction defects of modified vaccinia virus Ankara*. Virology, 1998. **251**(2): p. 334-42.
205. Meng, X., et al., *Vaccinia virus K1L and C7L inhibit antiviral activities induced by type I interferons*. J Virol, 2009. **83**(20): p. 10627-36.
206. Willis, K.L., et al., *The effect of the vaccinia K1 protein on the PKR-eIF2alpha pathway in RK13 and HeLa cells*. Virology, 2009. **394**(1): p. 73-81.
207. Backes, S., et al., *Viral host-range factor C7 or K1 is essential for modified vaccinia virus Ankara late gene expression in human and murine cells, irrespective of their capacity to inhibit protein kinase R-mediated phosphorylation of eukaryotic translation initiation factor 2alpha*. J Gen Virol, 2010. **91**(Pt 2): p. 470-82.
208. Paul Howley, C.M.-H., *Vaccinia virus host range genes to increase the titer of Avipoxviruses*. 2010.
209. Dinarello, C.A., *Interleukin 1 and interleukin 18 as mediators of inflammation and the aging process*. Am J Clin Nutr, 2006. **83**(2): p. 447S-455S.
210. Gerlic, M., et al., *Vaccinia virus F1L protein promotes virulence by inhibiting inflammasome activation*. Proc Natl Acad Sci U S A, 2013. **110**(19): p. 7808-13.
211. Ray, C.A., et al., *Viral inhibition of inflammation: cowpox virus encodes an inhibitor of the interleukin-1 beta converting enzyme*. Cell, 1992. **69**(4): p. 597-604.
212. Dobbelstein, M. and T. Shenk, *Protection against apoptosis by the vaccinia virus SPI-2 (B13R) gene product*. J Virol, 1996. **70**(9): p. 6479-85.
213. Kettle, S., et al., *Vaccinia virus serpin B13R (SPI-2) inhibits interleukin-1beta-converting enzyme and protects virus-infected cells from TNF- and Fas-mediated apoptosis, but does not prevent IL-1beta-induced fever*. J Gen Virol, 1997. **78** (Pt 3): p. 677-85.
214. Tschärke, D.C., P.C. Reading, and G.L. Smith, *Dermal infection with vaccinia virus reveals roles for virus proteins not seen using other inoculation routes*. J Gen Virol, 2002. **83**(Pt 8): p. 1977-86.
215. Spriggs, M.K., et al., *Vaccinia and cowpox viruses encode a novel secreted interleukin-1-binding protein*. Cell, 1992. **71**(1): p. 145-52.
216. Alcami, A. and G.L. Smith, *A mechanism for the inhibition of fever by a virus*. Proc Natl Acad Sci U S A, 1996. **93**(20): p. 11029-34.
217. Stack, J., et al., *Vaccinia virus protein A46R targets multiple Toll-like-interleukin-1 receptor adaptors and contributes to virulence*. J Exp Med, 2005. **201**(6): p. 1007-18.
218. Mansur, D.S., et al., *Poxvirus targeting of E3 ligase beta-TrCP by molecular mimicry: a mechanism to inhibit NF-kappaB activation and promote immune evasion and virulence*. PLoS Pathog, 2013. **9**(2): p. e1003183.

219. Harte, M.T., et al., *The poxvirus protein A52R targets Toll-like receptor signaling complexes to suppress host defense*. J Exp Med, 2003. **197**(3): p. 343-51.
220. Ember, S.W., et al., *Vaccinia virus protein C4 inhibits NF-kappaB activation and promotes virus virulence*. J Gen Virol, 2012. **93**(Pt 10): p. 2098-108.
221. Chen, R.A., N. Jacobs, and G.L. Smith, *Vaccinia virus strain Western Reserve protein B14 is an intracellular virulence factor*. J Gen Virol, 2006. **87**(Pt 6): p. 1451-8.
222. Bartlett, N., et al., *The vaccinia virus NIL protein is an intracellular homodimer that promotes virulence*. J Gen Virol, 2002. **83**(Pt 8): p. 1965-76.
223. Garlanda, C., C.A. Dinarello, and A. Mantovani, *The interleukin-1 family: back to the future*. Immunity, 2013. **39**(6): p. 1003-18.
224. Smith, G.L., *Virus strategies for evasion of the host response to infection*. Trends Microbiol, 1994. **2**(3): p. 81-8.
225. Alcami, A., et al., *Vaccinia virus strains Lister, USSR and Evans express soluble and cell-surface tumour necrosis factor receptors*. J Gen Virol, 1999. **80** (Pt 4): p. 949-59.
226. Reading, P.C., A. Khanna, and G.L. Smith, *Vaccinia virus CrmE encodes a soluble and cell surface tumor necrosis factor receptor that contributes to virus virulence*. Virology, 2002. **292**(2): p. 285-98.
227. Graham, K.A., et al., *The T1/35kDa family of poxvirus-secreted proteins bind chemokines and modulate leukocyte influx into virus-infected tissues*. Virology, 1997. **229**(1): p. 12-24.
228. Smith, C.A., et al., *Poxvirus genomes encode a secreted, soluble protein that preferentially inhibits beta chemokine activity yet lacks sequence homology to known chemokine receptors*. Virology, 1997. **236**(2): p. 316-27.
229. Alejo, A., et al., *A chemokine-binding domain in the tumor necrosis factor receptor from variola (smallpox) virus*. Proc Natl Acad Sci U S A, 2006. **103**(15): p. 5995-6000.
230. Alcami, A., et al., *Blockade of chemokine activity by a soluble chemokine binding protein from vaccinia virus*. J Immunol, 1998. **160**(2): p. 624-33.
231. Ng, A., et al., *The vaccinia virus A41L protein is a soluble 30 kDa glycoprotein that affects virus virulence*. J Gen Virol, 2001. **82**(Pt 9): p. 2095-105.
232. Bahar, M.W., et al., *Structure and function of A41, a vaccinia virus chemokine binding protein*. PLoS Pathog, 2008. **4**(1): p. e5.
233. Wasilenko, S.T., et al., *Vaccinia virus encodes a previously uncharacterized mitochondrial-associated inhibitor of apoptosis*. Proc Natl Acad Sci U S A, 2003. **100**(24): p. 14345-50.

234. Kvensakul, M., et al., *Vaccinia virus anti-apoptotic FIL is a novel Bcl-2-like domain-swapped dimer that binds a highly selective subset of BH3-containing death ligands*. Cell Death Differ, 2008. **15**(10): p. 1564-71.
235. Postigo, A., et al., *Interaction of FIL with the BH3 domain of Bak is responsible for inhibiting vaccinia-induced apoptosis*. Cell Death Differ, 2006. **13**(10): p. 1651-62.
236. Wasilenko, S.T., et al., *The vaccinia virus FIL protein interacts with the proapoptotic protein Bak and inhibits Bak activation*. J Virol, 2005. **79**(22): p. 14031-43.
237. Maluquer de Motes, C., et al., *Inhibition of apoptosis and NF-kappaB activation by vaccinia protein N1 occur via distinct binding surfaces and make different contributions to virulence*. PLoS Pathog, 2011. **7**(12): p. e1002430.
238. Cooray, S., et al., *Functional and structural studies of the vaccinia virus virulence factor N1 reveal a Bcl-2-like anti-apoptotic protein*. J Gen Virol, 2007. **88**(Pt 6): p. 1656-66.
239. Aoyagi, M., et al., *Vaccinia virus NIL protein resembles a B cell lymphoma-2 (Bcl-2) family protein*. Protein Sci, 2007. **16**(1): p. 118-24.
240. Smith, G.L., S.T. Howard, and Y.S. Chan, *Vaccinia virus encodes a family of genes with homology to serine proteinase inhibitors*. J Gen Virol, 1989. **70** (Pt 9): p. 2333-43.
241. Kettle, S., et al., *Vaccinia virus serpins B13R (SPI-2) and B22R (SPI-1) encode M(r) 38.5 and 40K, intracellular polypeptides that do not affect virus virulence in a murine intranasal model*. Virology, 1995. **206**(1): p. 136-47.
242. Kibler, K.V., et al., *Double-stranded RNA is a trigger for apoptosis in vaccinia virus-infected cells*. J Virol, 1997. **71**(3): p. 1992-2003.
243. Garcia, M.A., et al., *Anti-apoptotic and oncogenic properties of the dsRNA-binding protein of vaccinia virus, E3L*. Oncogene, 2002. **21**(55): p. 8379-87.
244. Galasso, G.J. and D.G. Sharp, *Relative Plaque-Forming, Cell-Infecting, and Interfering Qualities of Vaccinia Virus*. J Bacteriol, 1964. **88**: p. 433-9.
245. Takahashi-Nishimaki, F., et al., *Regulation of plaque size and host range by a vaccinia virus gene related to complement system proteins*. Virology, 1991. **181**(1): p. 158-64.
246. Dallo, S., et al., *Humoral immune response elicited by highly attenuated variants of vaccinia virus and by an attenuated recombinant expressing HIV-1 envelope protein*. Virology, 1989. **173**(1): p. 323-9.
247. Rodriguez, J.F. and M. Esteban, *Plaque size phenotype as a selectable marker to generate vaccinia virus recombinants*. J Virol, 1989. **63**(2): p. 997-1001.
248. Blasco, R. and B. Moss, *Selection of recombinant vaccinia viruses on the basis of plaque formation*. Gene, 1995. **158**(2): p. 157-62.

249. Zhang, W.H., D. Wilcock, and G.L. Smith, *Vaccinia virus F12L protein is required for actin tail formation, normal plaque size, and virulence*. J Virol, 2000. **74**(24): p. 11654-62.
250. Mathew, E., et al., *The extracellular domain of vaccinia virus protein B5R affects plaque phenotype, extracellular enveloped virus release, and intracellular actin tail formation*. J Virol, 1998. **72**(3): p. 2429-38.
251. Dobson, B.M. and D.C. Tschärke, *Truncation of gene F5L partially masks rescue of vaccinia virus strain MVA growth on mammalian cells by restricting plaque size*. J Gen Virol, 2014. **95**(Pt 2): p. 466-71.
252. Melamed, S., et al., *Attenuation and immunogenicity of host-range extended modified vaccinia virus Ankara recombinants*. Vaccine, 2013. **31**(41): p. 4569-77.
253. Borges, M.B., et al., *Accuracy and repeatability of a micro plaque reduction neutralization test for vaccinia antibodies*. Biologicals, 2008. **36**(2): p. 105-10.
254. Schweneker, M., et al., *The vaccinia virus O1 protein is required for sustained activation of extracellular signal-regulated kinase 1/2 and promotes viral virulence*. J Virol, 2012. **86**(4): p. 2323-36.
255. Cordeiro, J.V., et al., *F11-mediated inhibition of RhoA signalling enhances the spread of vaccinia virus in vitro and in vivo in an intranasal mouse model of infection*. PLoS One, 2009. **4**(12): p. e8506.
256. Zwillig, J., et al., *Functional F11L and K1L genes in modified vaccinia virus Ankara restore virus-induced cell motility but not growth in human and murine cells*. Virology, 2010. **404**(2): p. 231-9.
257. Morales, I., et al., *The vaccinia virus F11L gene product facilitates cell detachment and promotes migration*. Traffic, 2008. **9**(8): p. 1283-98.
258. Pires de Miranda, M., et al., *The vaccinia virus kelch-like protein C2L affects calcium-independent adhesion to the extracellular matrix and inflammation in a murine intradermal model*. J Gen Virol, 2003. **84**(Pt 9): p. 2459-71.
259. Zheng, Z.M., et al., *Poxviruses isolated from epidemic erythromelalgia in China*. Lancet, 1988. **1**(8580): p. 296.
260. Zheng, Z.M., et al., *Further characterization of the biological and pathogenic properties of erythromelalgia-related poxviruses*. J Gen Virol, 1992. **73** (Pt 8): p. 2011-9.
261. Earl, P.L., et al., *Generation of recombinant vaccinia viruses*, in *Current Protocols in Molecular Biology*, F.M. Ausubel, et al., Editors. 1998, Greene Publishing Associates & Wiley Interscience: New York. p. 16.17.1-16.17.19.
262. Sambrook, J., E.F. Fritsch, and T. Maniatis, *Molecular cloning: A Laboratory Manual/second edition*. Cold Spring Harbor Laboratory Press. Cold Spring Harbor, NY., 1989.

263. Kurtz, S., et al., *Versatile and open software for comparing large genomes*. Genome Biol., 2004. **5**(2): p. R12.
264. Kearse, M., et al., *Geneious Basic: an integrated and extendable desktop software platform for the organization and analysis of sequence data*. Bioinformatics, 2012. **28**(12): p. 1647-9.
265. Tcherepanov, V., A. Ehlers, and C. Upton, *Genome Annotation Transfer Utility (GATU): rapid annotation of viral genomes using a closely related reference genome*. BMC Genomics, 2006. **7**: p. 150.
266. Larkin, M.A., et al., *Clustal W and Clustal X version 2.0*. Bioinformatics, 2007. **23**(21): p. 2947-2948.
267. Goujon, M., et al., *A new bioinformatics analysis tools framework at EMBL=EBI*. Nucleic acids res., 2010. **38 suppl.**: p. W695-699.
268. Tamura, K., et al., *MEGA5: molecular evolutionary genetics analysis using maximum likelihood, evolutionary distance, and maximum parsimony methods*. Mol. Biol. Evol., 2011. **28**(10): p. 2731-2739.
269. Chen, N., et al., *The genomic sequence of ectromelia virus, the causative agent of mousepox*. Virology, 2003. **317**(1): p. 165-86.
270. Lefkowitz, E.J., et al., *Poxvirus Bioinformatics Resource Center: a comprehensive Poxviridae informational and analytical resource*. Nucleic Acids Res, 2005. **33**(Database issue): p. D311-6.
271. Carroll, D.S., et al., *Chasing Jenner's vaccine: revisiting cowpox virus classification*. PLoS One, 2011. **6**(8): p. e23086.
272. Marchal, J., *Infectious ectromelia. A hitherto undescribed virus disease of mice*. The Journal of Pathology and Bacteriology, 1930. **33**(3): p. 713-728.
273. Fenner, F., *Mousepox (infectious ectromelia): past, present, and future*. Lab Anim Sci, 1981. **31**(5 Pt 2): p. 553-9.
274. Esteban, D.J. and R.M. Buller, *Ectromelia virus: the causative agent of mousepox*. J Gen Virol, 2005. **86**(Pt 10): p. 2645-59.
275. Groppe, K.-H., *The occurrence of ectromelia (mousepox) in wild mice*. Arch. Exp. Veterinaermed, 1962. **16**(2): p. 243-278.
276. Dick, E.J., Jr., et al., *Mousepox outbreak in a laboratory mouse colony*. Lab Anim Sci, 1996. **46**(6): p. 602-11.
277. Lipman, N.S., et al., *Mousepox resulting from use of ectromelia virus-contaminated, imported mouse serum*. Comp Med, 2000. **50**(4): p. 426-35.

278. Lipman, N.S., H. Nguyen, and S. Perkins, *Mousepox: a threat to U.S. mouse colonies*. *Lab Anim Sci*, 1999. **49**(3): p. 229.
279. Labelle, P., et al., *Mousepox detected in a research facility: case report and failure of mouse antibody production testing to identify Ectromelia virus in contaminated mouse serum*. *Comp Med*, 2009. **59**(2): p. 180-6.
280. Kitamoto, N., et al., *Cross-reactivity among cowpox, ectromelia and vaccinia viruses with monoclonal antibodies recognizing distinct antigenic determinants in A-type inclusion bodies*. *Arch Virol*, 1986. **91**(3-4): p. 357-66.
281. Davies, D.H., et al., *Proteome-wide analysis of the serological response to vaccinia and smallpox*. *Proteomics*, 2007. **7**(10): p. 1678-86.
282. Seize, M.B., M. Ianhez, and C. Cestari Sda, *A study of the correlation between molluscum contagiosum and atopic dermatitis in children*. *An Bras Dermatol*, 2011. **86**(4): p. 663-8.
283. Solomon, L.M. and P. Telner, *Eruptive molluscum contagiosum in atopic dermatitis*. *Can Med Assoc J*, 1966. **95**(19): p. 978-9.
284. Ficarra, G. and D. Gaglioti, *Facial molluscum contagiosum in HIV-infected patients*. *Int J Oral Maxillofac Surg*, 1989. **18**(4): p. 200-1.
285. Pierard-Franchimont, C., A. Legrain, and G.E. Pierard, *Growth and regression of molluscum contagiosum*. *J Am Acad Dermatol*, 1983. **9**(5): p. 669-72.
286. Bugert, J.J., C. Lohmuller, and G. Darai, *Characterization of early gene transcripts of molluscum contagiosum virus*. *Virology*, 1999. **257**(1): p. 119-29.
287. Bugert, J.J., N. Melquiot, and R. Kehm, *Molluscum contagiosum virus expresses late genes in primary human fibroblasts but does not produce infectious progeny*. *Virus Genes*, 2001. **22**(1): p. 27-33.
288. Fife, K.H., et al., *Growth of molluscum contagiosum virus in a human foreskin xenograft model*. *Virology*, 1996. **226**(1): p. 95-101.
289. McFadden, G., et al., *Biogenesis of poxviruses: transitory expression of Molluscum contagiosum early functions*. *Virology*, 1979. **94**(2): p. 297-313.
290. Dawson, E., *Rapid, Direct Quantification of Viruses in Solution Using the ViroCyt Virus Counter*. *J Biomol Tech*, 2012. **23**(Supl.).
291. Homann, O.R. and A.D. Johnson, *MochiView: versatile software for genome browsing and DNA motif analysis*. *BMC Biol*, 2010. **8**: p. 49.
292. Melquiot, N.V. and J.J. Bugert, *Preparation and use of molluscum contagiosum virus from human tissue biopsy specimens*. *Methods Mol Biol*, 2004. **269**: p. 371-84.

293. Melnick, J.L., et al., *Electron microscopy of viruses of human papilloma, molluscum contagiosum, and vaccinia, including observations on the formation of virus within the cell.* Ann N Y Acad Sci, 1952. **54**(6): p. 1214-25.
294. Burnett, J.W. and J.S. Sutton, *Molluscum contagiosum cytotoxicity for primary human amnion cells in vitro as studied by electron microscopy.* J Invest Dermatol, 1968. **50**(1): p. 67-84.
295. Almeida Jr, H.L., et al., *Scanning electron microscopy of molluscum contagiosum.* An Bras Dermatol, 2013. **88**(1): p. 90-3.
296. Desmyter, J., J.L. Melnick, and W.E. Rawls, *Defectiveness of interferon production and of rubella virus interference in a line of African green monkey kidney cells (Vero).* J Virol, 1968. **2**(10): p. 955-61.
297. Yang, Z., et al., *Simultaneous high-resolution analysis of vaccinia virus and host cell transcriptomes by deep RNA sequencing.* Proc Natl Acad Sci U S A, 2010. **107**(25): p. 11513-8.
298. Tsung, K., et al., *Gene expression and cytopathic effect of vaccinia virus inactivated by psoralen and long-wave UV light.* J Virol, 1996. **70**(1): p. 165-71.
299. Mss, B. and R. Filler, *Irreversible effects of cycloheximide during the early period of vaccinia virus replicaon.* J Virol, 1970. **5**(2): p. 99-108.
300. Espmark, J.A., *Time Relationships in the Development of Cytopathic Response to Vaccinia Virus in Tissue Culture Tubes.* Arch Gesamte Virusforsch, 1965. **15**: p. 123-36.
301. Bablanian, R., et al., *Studies on the mechanisms of vaccinia virus cytopathic effects. II. Early cell rounding is associated with virus polypeptide synthesis.* J Gen Virol, 1978. **39**(3): p. 403-13.
302. Bablanian, R., *Studies on the mechanism of vaccinia virus cytopathic effects: effect of inhibitors of RNA and protein synthesis on early virus-induced cell damage.* J Gen Virol, 1970. **6**(2): p. 221-30.
303. Neva, F.A., *Studies on molluscum contagiosum. Observations on the cytopathic effect of molluscum suspensions in vitro.* Arch Intern Med, 1962. **110**: p. 720-5.
304. Cavicchioli, R. and K. Watson, *The involvement of transcriptional read-through from internal promoters in the expression of a novel endoglucanase gene FSendA, from Fibrobacter succinogenes ARI.* Nucleic Acids Res, 1991. **19**(7): p. 1661-9.
305. Nacu, S., et al., *Deep RNA sequencing analysis of readthrough gene fusions in human prostate adenocarcinoma and reference samples.* BMC Med Genomics, 2011. **4**: p. 11.
306. Feng, Y.X., et al., *Translational readthrough of the murine leukemia virus gag gene amber codon does not require virus-induced alteration of tRNA.* J Virol, 1989. **63**(5): p. 2405-10.

307. Sherwani, S., et al., *New method for the assessment of molluscum contagiosum virus infectivity*. *Methods Mol Biol*, 2012. **890**: p. 135-46.
308. Zaslavsky, V., *Uncoating of vaccinia virus*. *J Virol*, 1985. **55**(2): p. 352-6.
309. Vos, J.C. and H.G. Stunnenberg, *Derepression of a novel class of vaccinia virus genes upon DNA replication*. *EMBO J*, 1988. **7**(11): p. 3487-92.
310. Gilbert, S.C., *Clinical development of Modified Vaccinia virus Ankara vaccines*. *Vaccine*, 2013. **31**(39): p. 4241-6.
311. Vilarinho, S. and T.H. Taddei, *New frontier in liver cancer treatment: oncolytic viral therapy*. *Hepatology*, 2014. **59**(1): p. 343-6.
312. Hou, W., et al., *Oncolytic vaccinia virus demonstrates antiangiogenic effects mediated by targeting of VEGF*. *Int J Cancer*, 2014.
313. Tykodi, S.S. and J.A. Thompson, *Development of modified vaccinia Ankara-5T4 as specific immunotherapy for advanced human cancer*. *Expert Opin Biol Ther*, 2008. **8**(12): p. 1947-53.
314. Krupa, M., et al., *Immunization with recombinant DNA and modified vaccinia virus Ankara (MVA) vectors delivering PSCA and STEAPI antigens inhibits prostate cancer progression*. *Vaccine*, 2011. **29**(7): p. 1504-13.
315. Harrop, R., et al., *Vaccination of colorectal cancer patients with modified vaccinia Ankara delivering the tumor antigen 5T4 (TroVax) induces immune responses which correlate with disease control: a phase I/II trial*. *Clin Cancer Res*, 2006. **12**(11 Pt 1): p. 3416-24.
316. Amato, R.J., et al., *Vaccination of renal cell cancer patients with modified vaccinia Ankara delivering the tumor antigen 5T4 (TroVax) alone or administered in combination with interferon-alpha (IFN-alpha): a phase 2 trial*. *J Immunother*, 2009. **32**(7): p. 765-72.
317. Blanchard, T.J., et al., *Modified vaccinia virus Ankara undergoes limited replication in human cells and lacks several immunomodulatory proteins: implications for use as a human vaccine*. *J Gen Virol*, 1998. **79** (Pt 5): p. 1159-67.
318. Sutter, G. and B. Moss, *Nonreplicating vaccinia vector efficiently expresses recombinant genes*. *Proc Natl Acad Sci U S A*, 1992. **89**(22): p. 10847-51.
319. Stickl, H., et al., *[MVA vaccination against smallpox: clinical tests with an attenuated live vaccinia virus strain (MVA) (author's transl)]*. *Dtsch Med Wochenschr*, 1974. **99**(47): p. 2386-92.
320. Verheust, C., et al., *Biosafety aspects of modified vaccinia virus Ankara (MVA)-based vectors used for gene therapy or vaccination*. *Vaccine*, 2012. **30**(16): p. 2623-32.

321. Meyer, H., G. Sutter, and A. Mayr, *Mapping of deletions in the genome of the highly attenuated vaccinia virus MVA and their influence on virulence*. J Gen Virol, 1991. **72** (Pt 5): p. 1031-8.
322. Meisinger-Henschel, C., et al., *Introduction of the six major genomic deletions of modified vaccinia virus Ankara (MVA) into the parental vaccinia virus is not sufficient to reproduce an MVA-like phenotype in cell culture and in mice*. J Virol, 2010. **84**(19): p. 9907-19.
323. Earl, P.L., et al., *Generation of recombinant vaccinia viruses*. Curr Protoc Mol Biol, 2001. **Chapter 16**: p. Unit16 17.
324. DeFilippes, F.M., *Restriction enzyme mapping of vaccinia virus DNA*. J Virol, 1982. **43**(1): p. 136-49.
325. Delcher, A.L., S.L. Salzberg, and A.M. Phillippy, *Using MUMmer to identify similar regions in large sequence sets*. Curr Protoc Bioinformatics, 2003. **Chapter 10**: p. Unit 10 3.
326. Thompson, J.D., T.J. Gibson, and D.G. Higgins, *Multiple sequence alignment using ClustalW and ClustalX*. Curr Protoc Bioinformatics, 2002. **Chapter 2**: p. Unit 2 3.
327. Chakrabarti, S., J.R. Sisler, and B. Moss, *Compact, synthetic, vaccinia virus early/late promoter for protein expression*. Biotechniques, 1997. **23**(6): p. 1094-7.
328. Earl, P.L., J.L. Americo, and B. Moss, *Development and use of a vaccinia virus neutralization assay based on flow cytometric detection of green fluorescent protein*. J Virol, 2003. **77**(19): p. 10684-8.
329. Sancho, M.C., et al., *The block in assembly of modified vaccinia virus Ankara in HeLa cells reveals new insights into vaccinia virus morphogenesis*. J Virol, 2002. **76**(16): p. 8318-34.
330. Twardzik, D.R., et al., *Vaccinia virus-infected cells release a novel polypeptide functionally related to transforming and epidermal growth factors*. Proc Natl Acad Sci U S A, 1985. **82**(16): p. 5300-4.
331. Buller, R.M., et al., *Deletion of the vaccinia virus growth factor gene reduces virus virulence*. J Virol, 1988. **62**(3): p. 866-74.
332. Martin, S., D.T. Harris, and J. Shisler, *The CIIR gene, which encodes the vaccinia virus growth factor, is partially responsible for MVA-induced NF-kappaB and ERK2 activation*. J Virol, 2012. **86**(18): p. 9629-39.
333. Buller, R.M., et al., *Cell proliferative response to vaccinia virus is mediated by VGF*. Virology, 1988. **164**(1): p. 182-92.
334. Shchelkunov, S.N., et al., *The genomic sequence analysis of the left and right species-specific terminal region of a cowpox virus strain reveals unique sequences and a cluster*

- of intact ORFs for immunomodulatory and host range proteins. Virology, 1998. 243(2): p. 432-60.*
335. Eppstein, D.A., et al., *Epidermal growth factor receptor occupancy inhibits vaccinia virus infection. Nature, 1985. 318(6047): p. 663-5.*
336. Postigo, A., et al., *Vaccinia-induced epidermal growth factor receptor-MEK signalling and the anti-apoptotic protein FIL synergize to suppress cell death during infection. Cell Microbiol, 2009. 11(8): p. 1208-18.*
337. Singh, K., R. Kaur, and W. Qiu, *New virus discovery by deep sequencing of small RNAs. Methods Mol Biol, 2012. 883: p. 177-91.*
338. Whitney, R.A., Jr., J.D. Small, and A.E. New, *Mousepox-National Institutes of Health experiences. Lab Anim Sci, 1981. 31(5 Pt 2): p. 570-3.*
339. Wallace, G.D., et al., *Epizootiology of an outbreak of mousepox at the National Institutes of Health. Lab Anim Sci, 1981. 31(5 Pt 2): p. 609-15.*
340. Wagner, J.E. and R.A. Daynes, *Observations of an outbreak of mousepox in laboratory mice in 1979 at the University of Utah Medical Center, USA. Lab Anim Sci, 1981. 31(5 Pt 2): p. 565-9.*
341. Trentin, J.J., *An outbreak of mousepox (infectious ectromelia) in the United States. I. Presumptive diagnosis. Science, 1953. 117(3035): p. 226-7.*
342. Di Giulio, D.B. and P.B. Eckburg, *Human monkeypox: an emerging zoonosis. Lancet Infect Dis, 2004. 4(1): p. 15-25.*
343. Anderson, M.G., et al., *A case of severe monkeypox virus disease in an American child: emerging infections and changing professional values. Pediatr Infect Dis J, 2003. 22(12): p. 1093-6; discussion 1096-8.*
344. Mayr, A., *[TC marker of the attenuated vaccinia vaccide strain "MVA" in human cell cultures and protective immunization against orthopox diseases in animals]. Zentralbl Veterinarmed B, 1976. 23(5-6): p. 417-30.*
345. Sutter, G. and B. Moss, *Novel vaccinia vector derived from the host range restricted and highly attenuated MVA strain of vaccinia virus. Dev Biol Stand, 1995. 84: p. 195-200.*
346. McCart, J.A., et al., *Systemic cancer therapy with a tumor-selective vaccinia virus mutant lacking thymidine kinase and vaccinia growth factor genes. Cancer Res, 2001. 61(24): p. 8751-7.*
347. Drexler, I., et al., *Highly attenuated modified vaccinia virus Ankara replicates in baby hamster kidney cells, a potential host for virus propagation, but not in various human transformed and primary cells. J Gen Virol, 1998. 79 (Pt 2): p. 347-52.*

348. Hermann, J., M. Barel, and R. Frade, *Human erythrocyte ankyrin, a cytoskeleton component, generates the p57 membrane proteinase which cleaves C3, the third component of complement*. *Biochem Biophys Res Commun*, 1994. **204**(2): p. 453-60.
349. Das, A., et al., *Spectrin functions upstream of ankyrin in a spectrin cytoskeleton assembly pathway*. *J Cell Biol*, 2006. **175**(2): p. 325-35.
350. Cairo, C.W., et al., *Dynamic regulation of CD45 lateral mobility by the spectrin-ankyrin cytoskeleton of T cells*. *J Biol Chem*, 2010. **285**(15): p. 11392-401.
351. Irwin, C.R. and D.H. Evans, *Modulation of the myxoma virus plaque phenotype by vaccinia virus protein F11*. *J Virol*, 2012. **86**(13): p. 7167-79.
352. Sharon, D., et al., *Profile of the genes expressed in the human peripheral retina, macula, and retinal pigment epithelium determined through serial analysis of gene expression (SAGE)*. *Proc Natl Acad Sci U S A*, 2002. **99**(1): p. 315-20.
353. Brendel, C., et al., *Distinct gene expression profile of human mesenchymal stem cells in comparison to skin fibroblasts employing cDNA microarray analysis of 9600 genes*. *Gene Expr*, 2005. **12**(4-6): p. 245-57.
354. Altenburger, W., C.P. Suter, and J. Altenburger, *Partial deletion of the human host range gene in the attenuated vaccinia virus MVA*. *Arch Virol*, 1989. **105**(1-2): p. 15-27.
355. Antoine, G., et al., *The complete genomic sequence of the modified vaccinia Ankara strain: comparison with other orthopoxviruses*. *Virology*, 1998. **244**(2): p. 365-96.
356. Barrett, P.N., et al., *Vero cell platform in vaccine production: moving towards cell culture-based viral vaccines*. *Expert Rev Vaccines*, 2009. **8**(5): p. 607-18.